GEM TN-93-266

Cathode Strip Chambers Group Meeting - SSCL

January 8, 1993

Abstract:

Agenda, attendees, and presentations of the GEM CSC Group Meeting held at the SSC Laboratory on January 8, 1993

AGENDA OF JANUARY 8 CSC MEETING, 9 AM - 5:30 PM

SSC Laboratory

(1) Test results:

- BNL prototypes - V.Chernyatin
- Dubna prototype - Yu.Kiryushin/P.Murat
- UH prototype - B.Mayes

(2) CSC Baseline parameters optimization:

- Optimization of barrel layout and channel count - Yu.Kiryushin

- CSC parameters optimization - V.Polichronakos

- Requirements for pattern recognition - simulation results - P.Murat

- Momentum reconstruction and effect of double-hit - C.Yanagisawa

- Optimization of endcap layout and channel count - F.Nimblett
- Rectangular vs. trapezoidal chambers in endcaps
  - simulation - V.Chernyatin
  - trigger issues - A.Korytov
  - general consideration - S.Whitaker

- discussion, decision, task assignments - group

(3) CSC Electronics update - D.Marlow

(4) Discussion of Jan.18-19 technology review and CSC document update
- task assignments - group

CSC Meeting, SSCL, January 8

1.	Gena Mitselmakher	SSCL	(214)-708-6001	SSCVX1::Mitsel
2.	Roy Weinstein	Houston	(713) 743-3600	weinstein
3.	Bill W. Mayes II	Houston	(713) 743-3548	mayes@UH.E
4.	LARRY PINSKY	HOUSTON	(713) 743-3552	PINSKY@UH.E
5.	Andrey Korytov	MIT	(617) 253-7587	Korytov@mit
6.	VLADIMIR GLEBOV	SSCL	(214)-708-6321	SSCVX1::GLEBO
7.	Yu. Kiryushin	SSCL	-30-64	SSCVX1::YUKI
8.	Andrey Ostapchuk	SSCL	(214)-708-3007	SSCVX1::OSTAPCH
9.	Vinnie Polychronakos	BNL	(516) 282-3982	BNLDAG::POLYCH
10.	Frank Taylor	MIT	617 253-7245	FET@MITLN
11.	Rick Sawicki	LLNL	510 423 0943	SAWICKI@LLNL.G
12.	Frank Nimblett	Duke	617-254-1343	Nimblett@duke.edu
13.	COLEMAN JOHNSON	SSCL	214 708 1188	JOHNCOLE@SSCL
14.	MIKE GAMBLE	SSCL	(214) 708-6050	gamble@SSCVX1
15.	Yanan GUO	SSCL	(214) 708-4457	GUO@SSCVX1
16.	Bondar Nikolai	BNL	(516) 282-5336	Bonder@BNLCL6.B
17.	Paul Murat	SSCL	(214) 708-3066	MURAT@SSC
18.	Dmitri Smoline	BNL	(214) 708-3064	Smolne.
19.	Vadim Gratchev	LNPI	708-3220	GRATCH@BNL
20.	Rick Shypit	SSCL	708-4465	SHYPIT@SSC
21.	Yuri Bonushkin	SSCL	708-3078	BONUSHKIN@SSCL
22.	Barry Barish	CALTECH	818-356-6684	BARISH@SSCVX
23.	Chiaki Yanagisawa	Stony Brook	516-632-8105	SBHEP::CHIAKI
24.	George P. Yost	SSCL	(214) 708-6028	YOST@SSCVX
25.	Daniel Marlow	Princeton	609 258 4383	PUPHEP::MARLO
26.	Dick Edelstein	Carnegie Mellon	412 268 2760	EDELSTEIN@CMPH
27.	Mark [illegible]	SSC	6188	MARK@SSCV.
28.	Cas Milner	SSC	6216	milner@SSCV.

gem

γeμ

Presentation by:

V. Chernyatin

93/01/07 01.05

run 28 phi

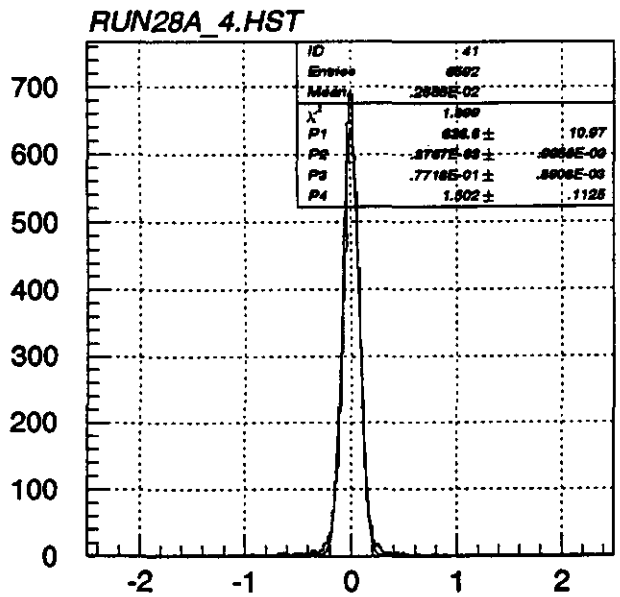

1st layer residuals +/- 6 deg

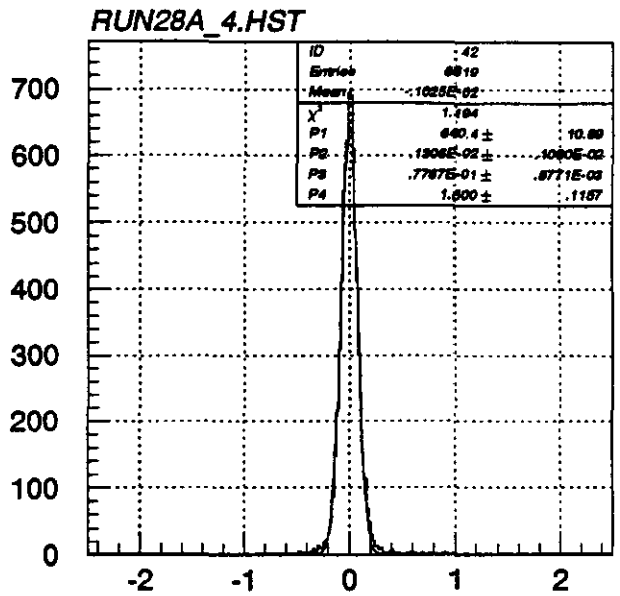

2nd layer residuals +/- 6 deg

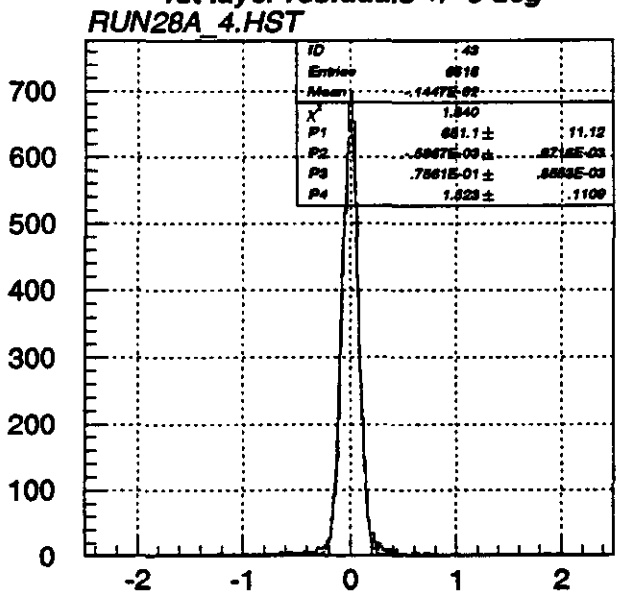

3rd layer residuals +/- 6 deg

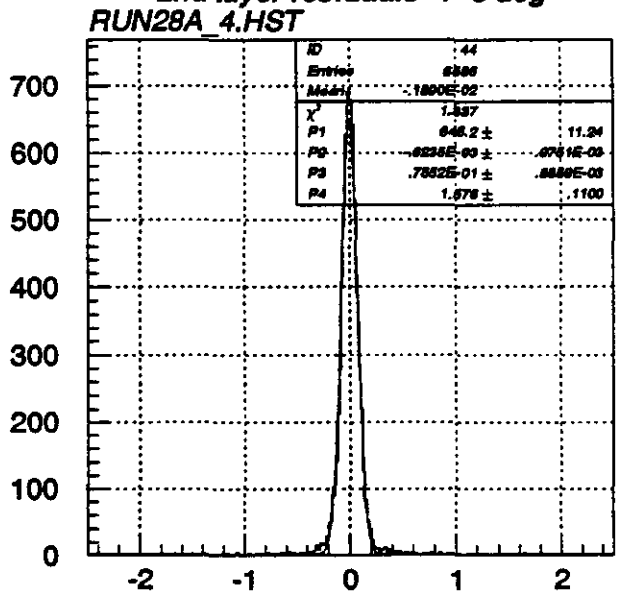

4th layer residuals +/- 6 deg

93/01/07 01.05

run 28 phi

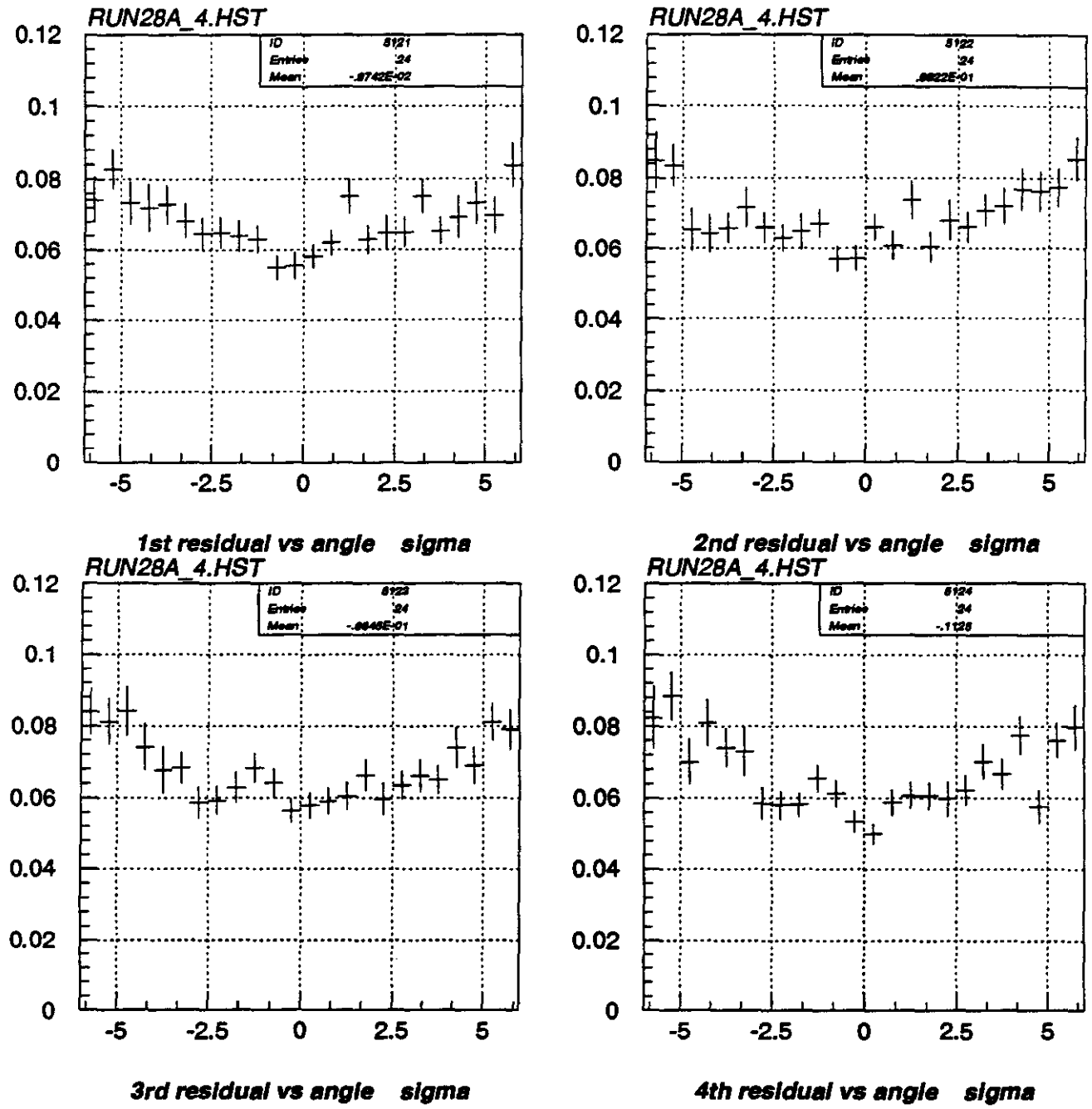

93/01/07 01.16

run 29

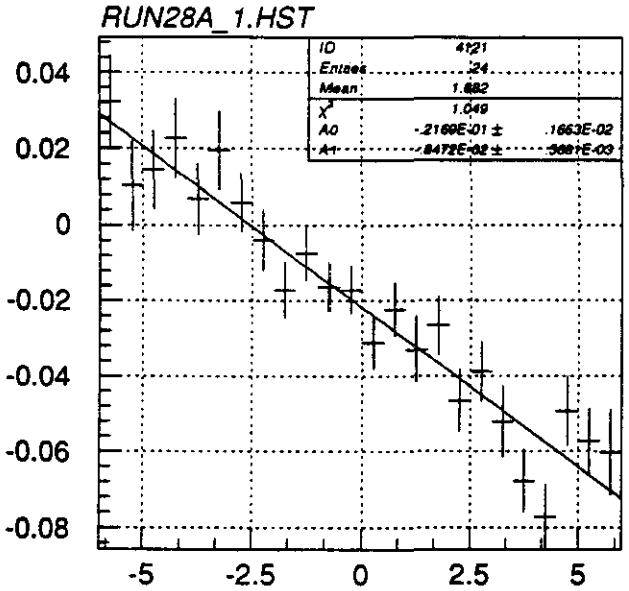

1st residual vs angle mean

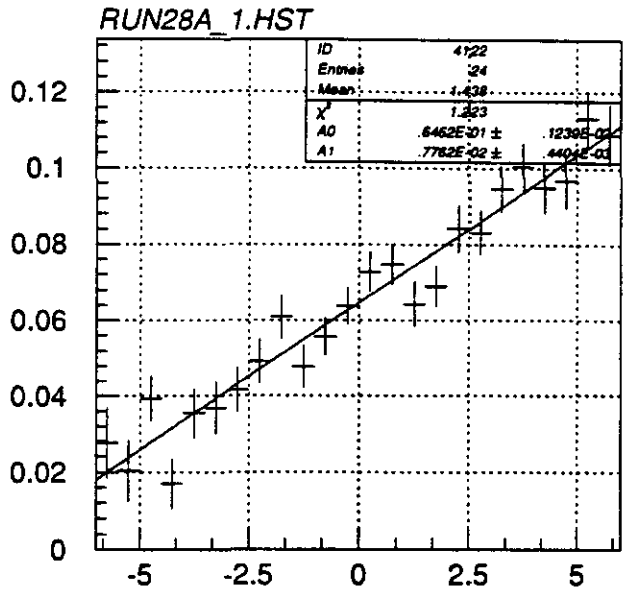

2nd residual vs angle mean

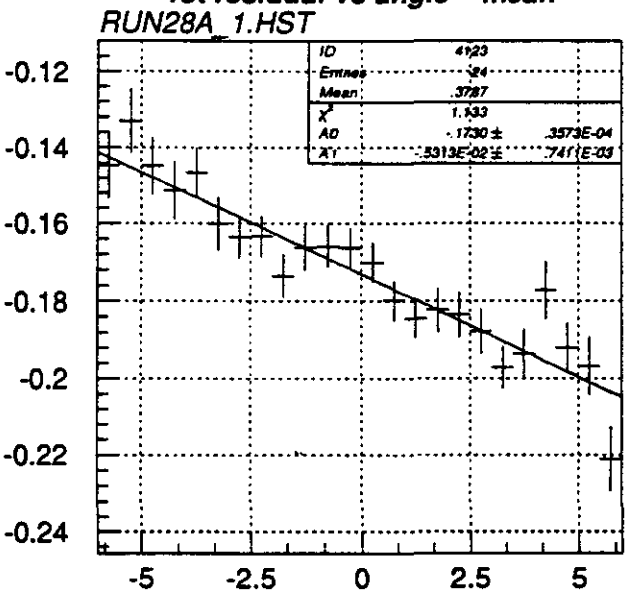

3rd residual vs angle mean

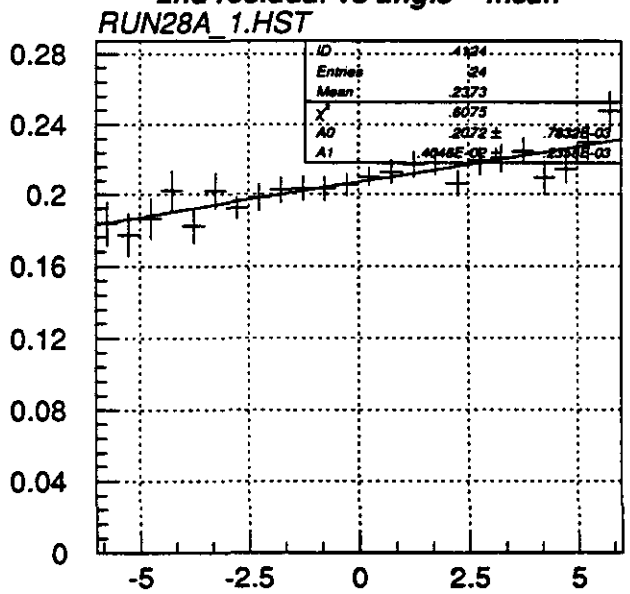

4th residual vs angle mean

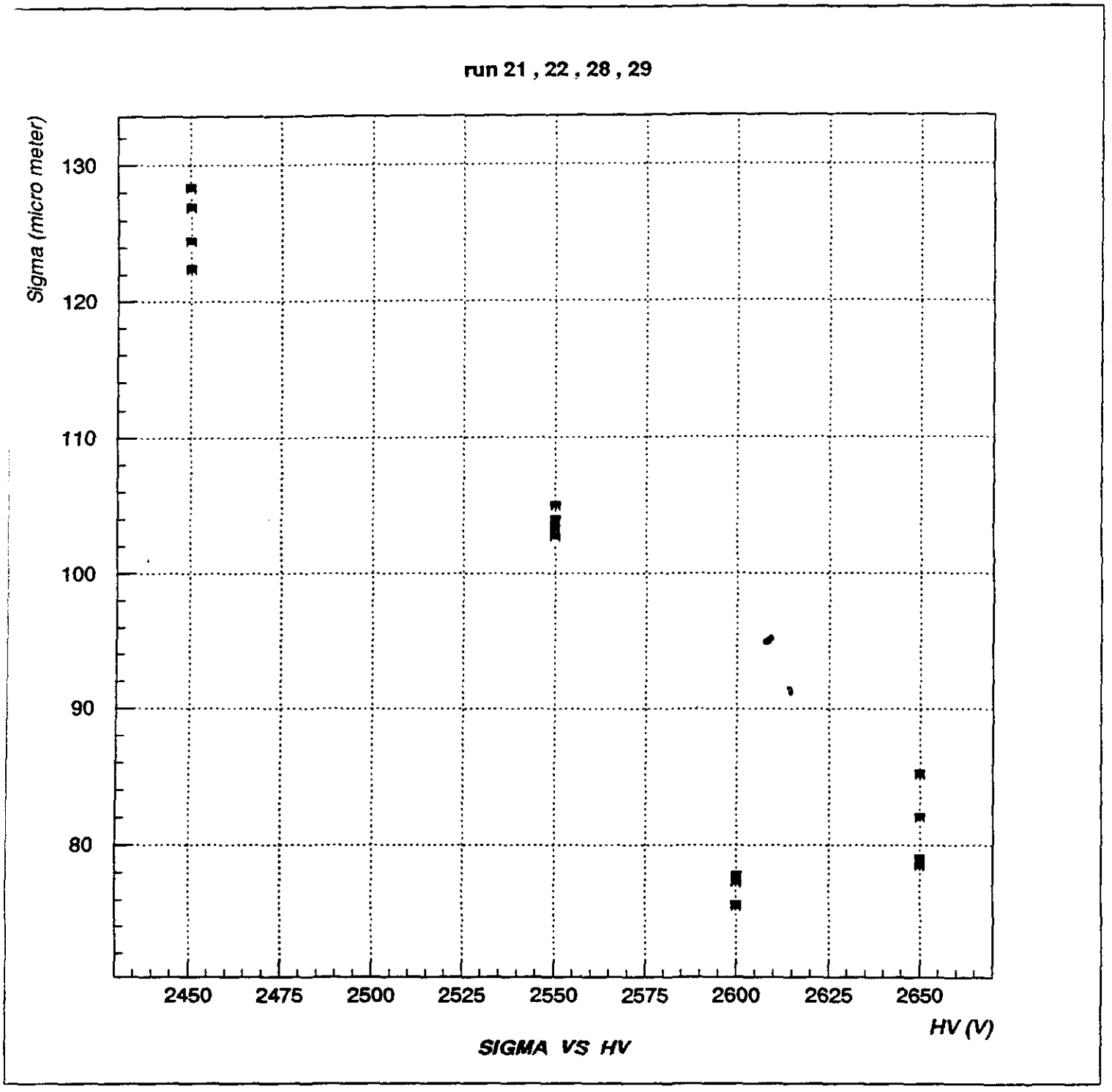
run 21 , 22 , 28 , 29
Sigma (micro meter)
130
120
110
100
90
80
2450
2475
2500
2525
2550
2575
2600
2625
2650
HV (V)
SIGMA VS HV

gem

γeμ

Presentation by:

Yu. Kiryushin

Dubna CSC status

1. Installation in TTR- 19/21/92
2. Calibration procedure

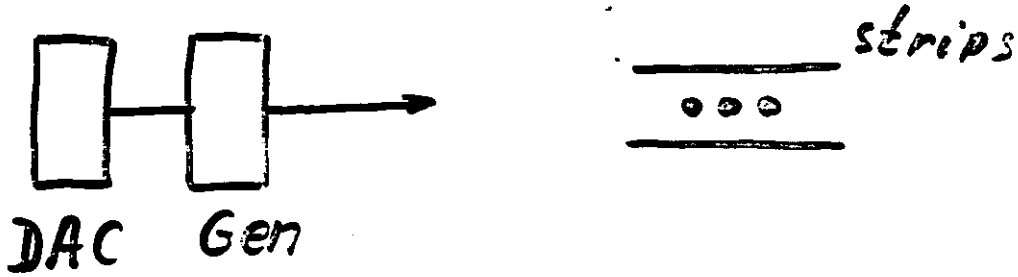

3. Gas mixture

Ar - 30%	Ar - 30%
CF_4 - 60%	CF_4 - 20%
C_4H_{10} - 10%	CO_2 - 50%

4. Recalibration - 10 hours
5. Range of ADC - ~10 bits
6. Sensitivity of electronics - 44 v/pc
7. Gas amplification ~ $3 \cdot 10^4$
8. Change of sensitivity - 22 v/pc
9. Gas amplification - $5 \cdot 10^4$

Data processing in progress

TIME MEASUREMENTS

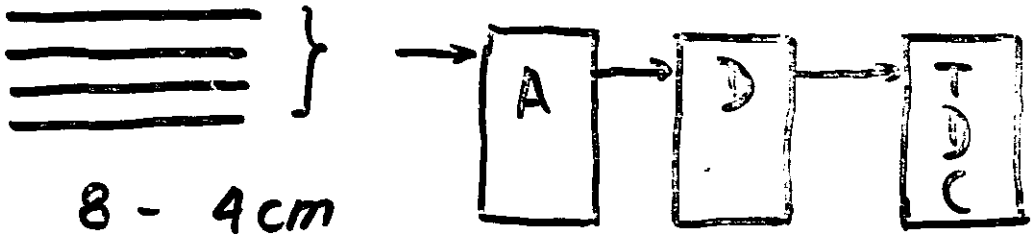

8 - 4cm
4 - 2cm
3 - 1.5cm

KORYTOV ampl.

Sensitivity of Ampl. ~ $260 \cdot 10^{-3}$ V/μA

Data processing in progress

Presentation by:

P. Muzat

Dubna CSC
data analysis
(progress report)

Presented by P. Murat

01/08/93
SSCL

* The main question about CSC performance: do they provide high resolution and high efficiency SIMULTANEOUSLY? (FROM THE POINT OF VIEW OF TRACKING)

* Data analysis scheme:

DUBNA CSC

CLUSTER: 3 STRIPS

$q_{max} > 100$

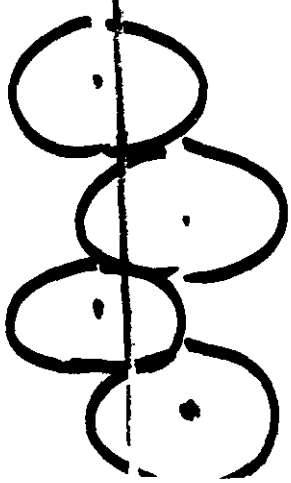

DUBNA RDT

channel # 16

92/12/20 18.50

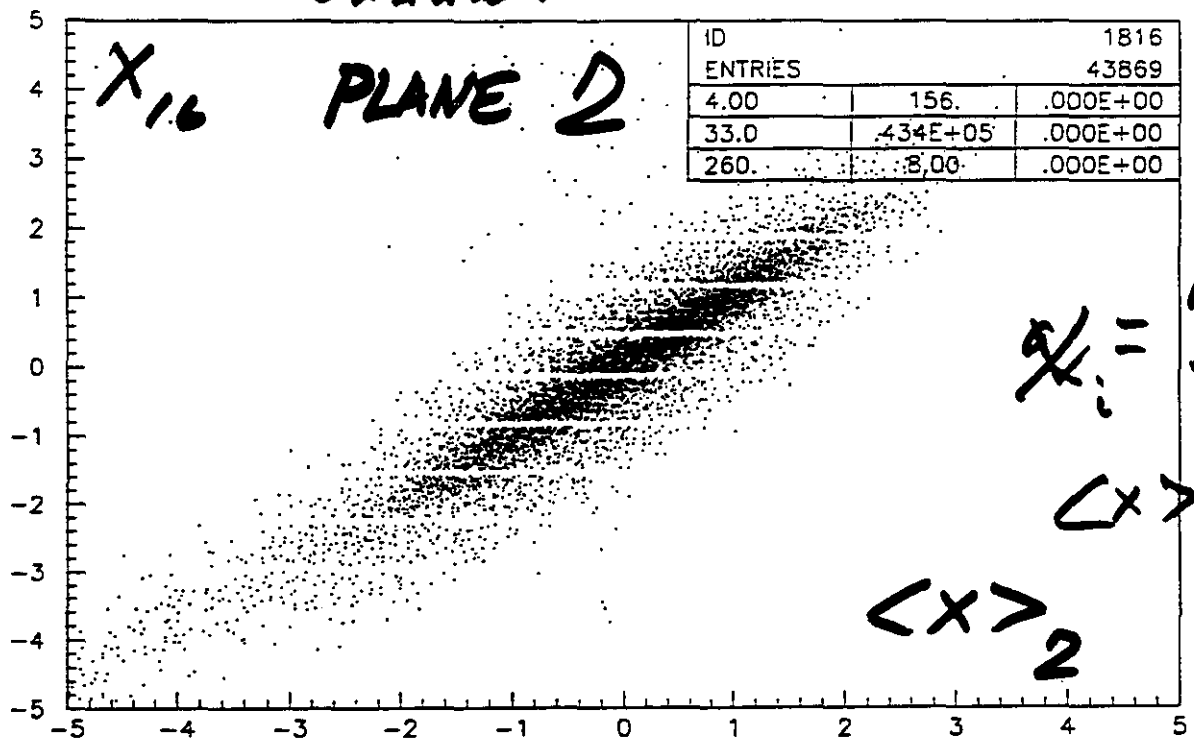

$$x_i = \frac{q_i - q_{i0}}{\sigma_i}$$

$\langle x \rangle$

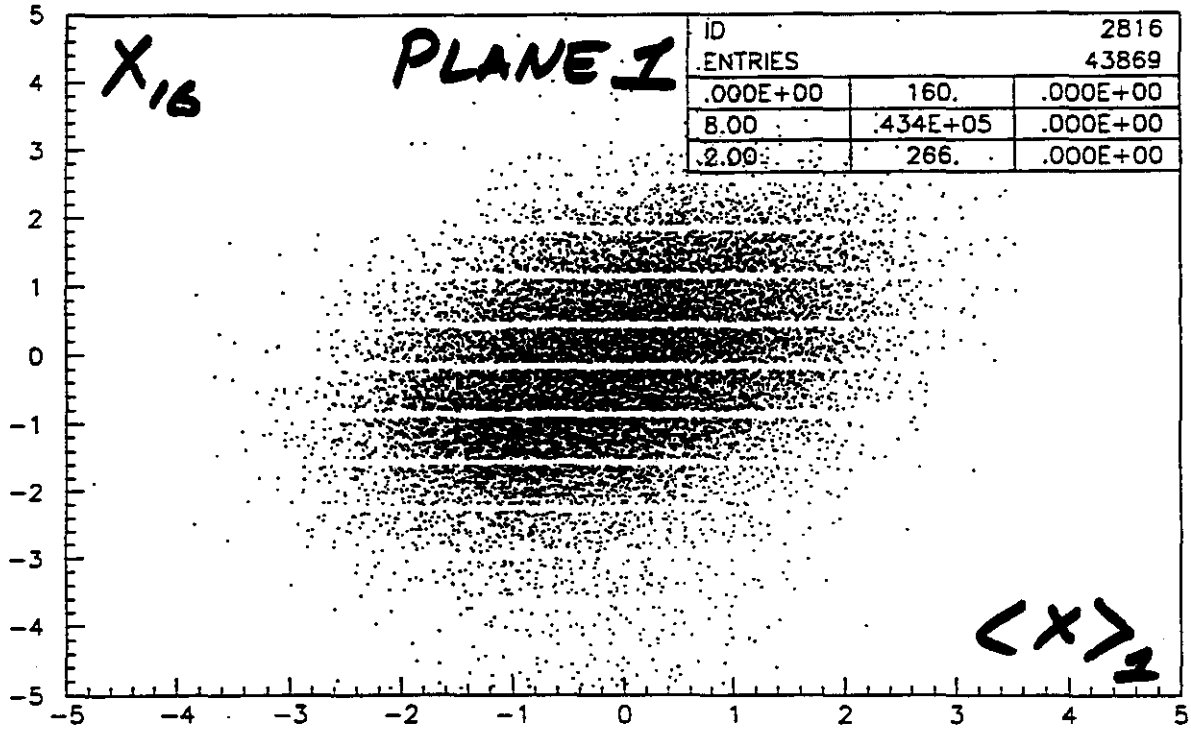

channel # 16 is in plane 2

PEDESTAL WIDTH

93/01/04 13.06

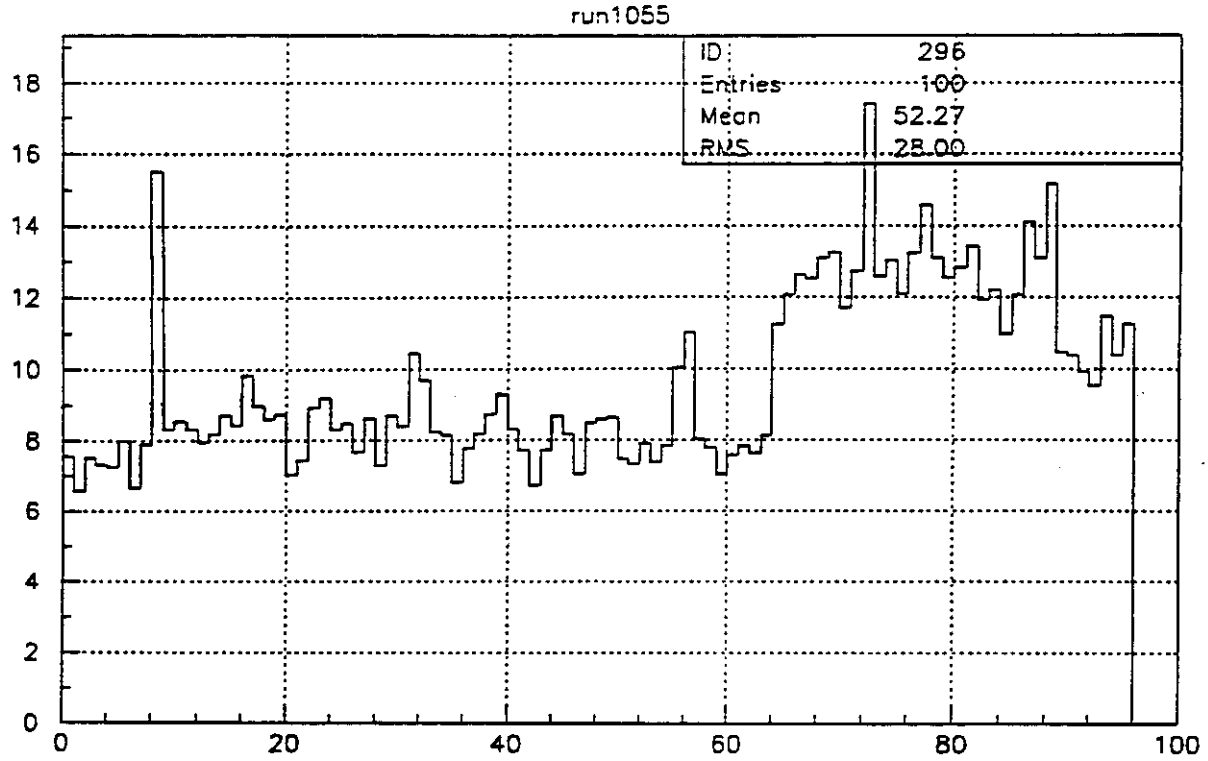

pedestals without subtraction of correlated noise

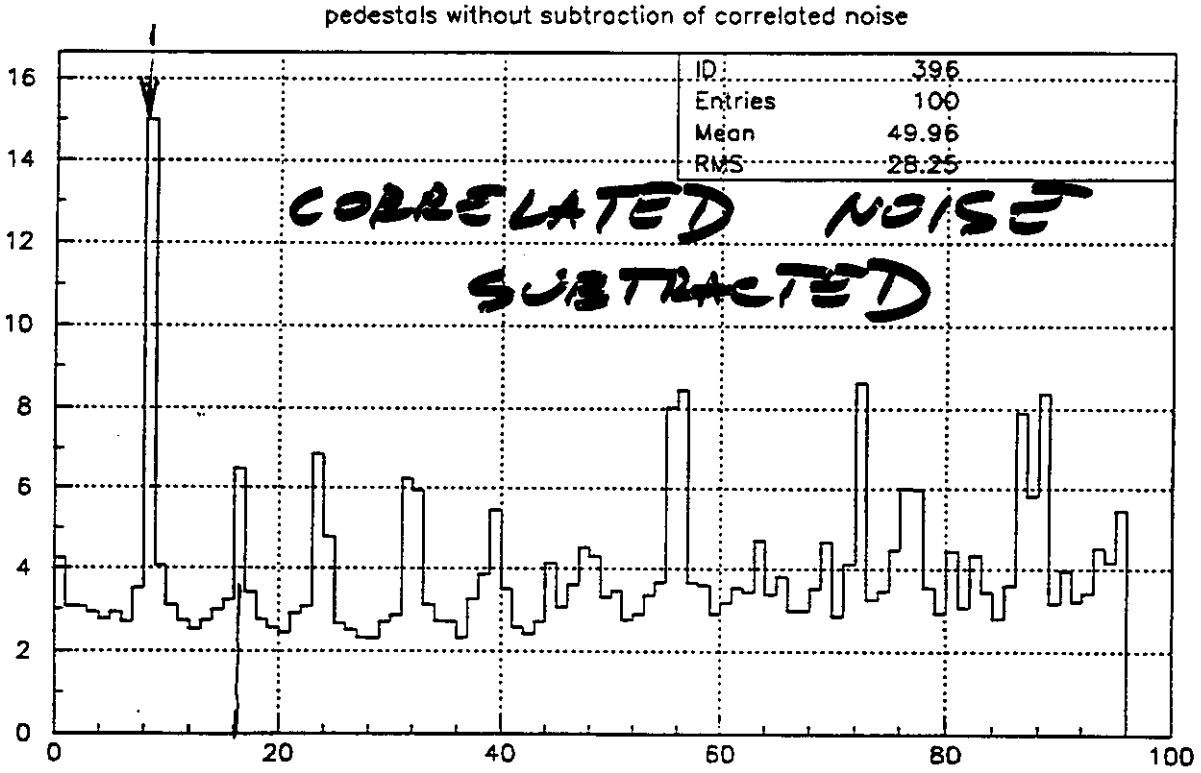

pedestals correlated noise subtracted

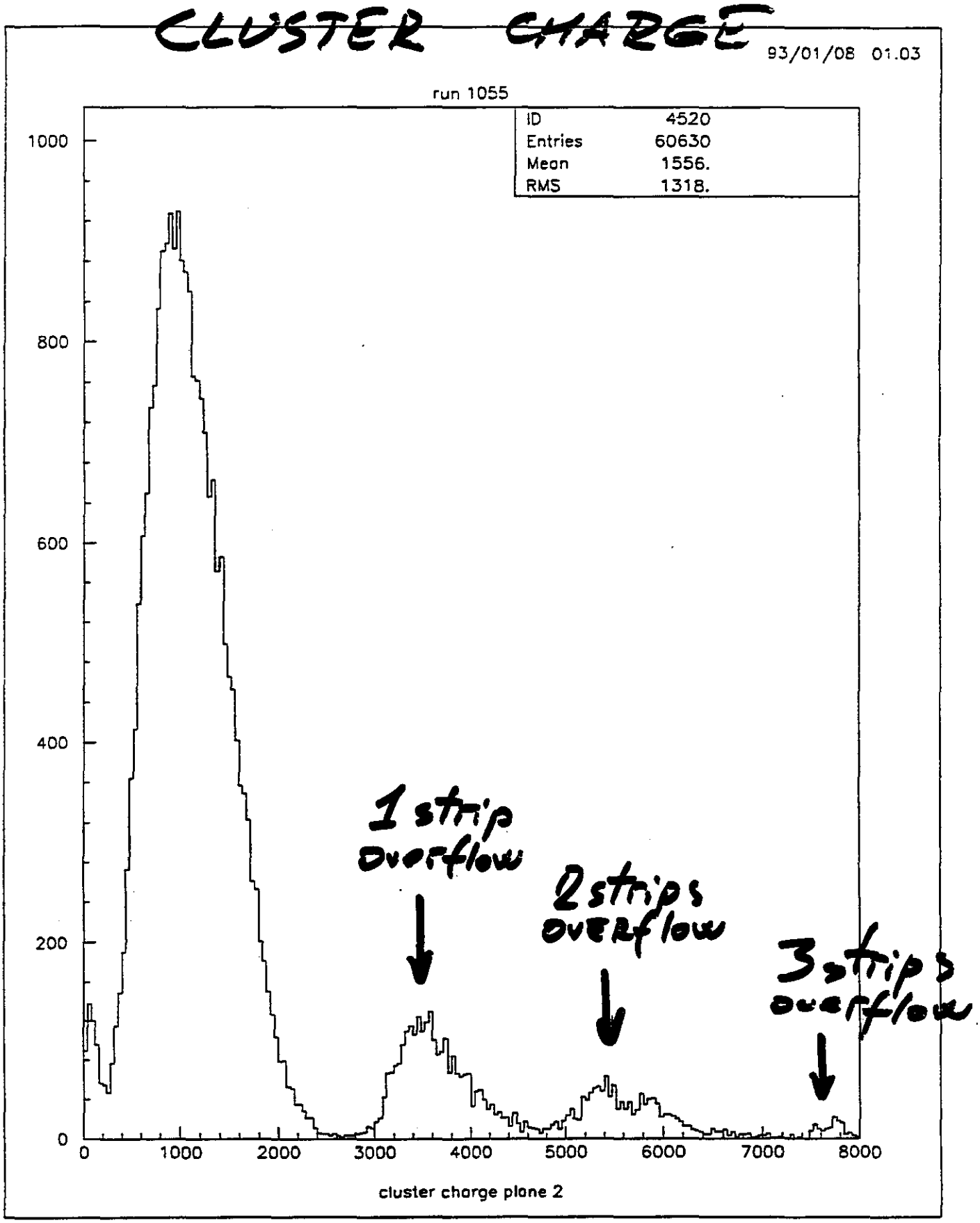
CLUSTER CHARGE
93/01/08 01.03
run 1055
ID 4520
Entries 60630
Mean 1556.
RMS 1318.
1000
800
600
400
200
0
0
1000
2000
3000
4000
5000
6000
7000
8000
cluster charge plane 2
1 strip overflow
2 strips overflow
3 strips overflow

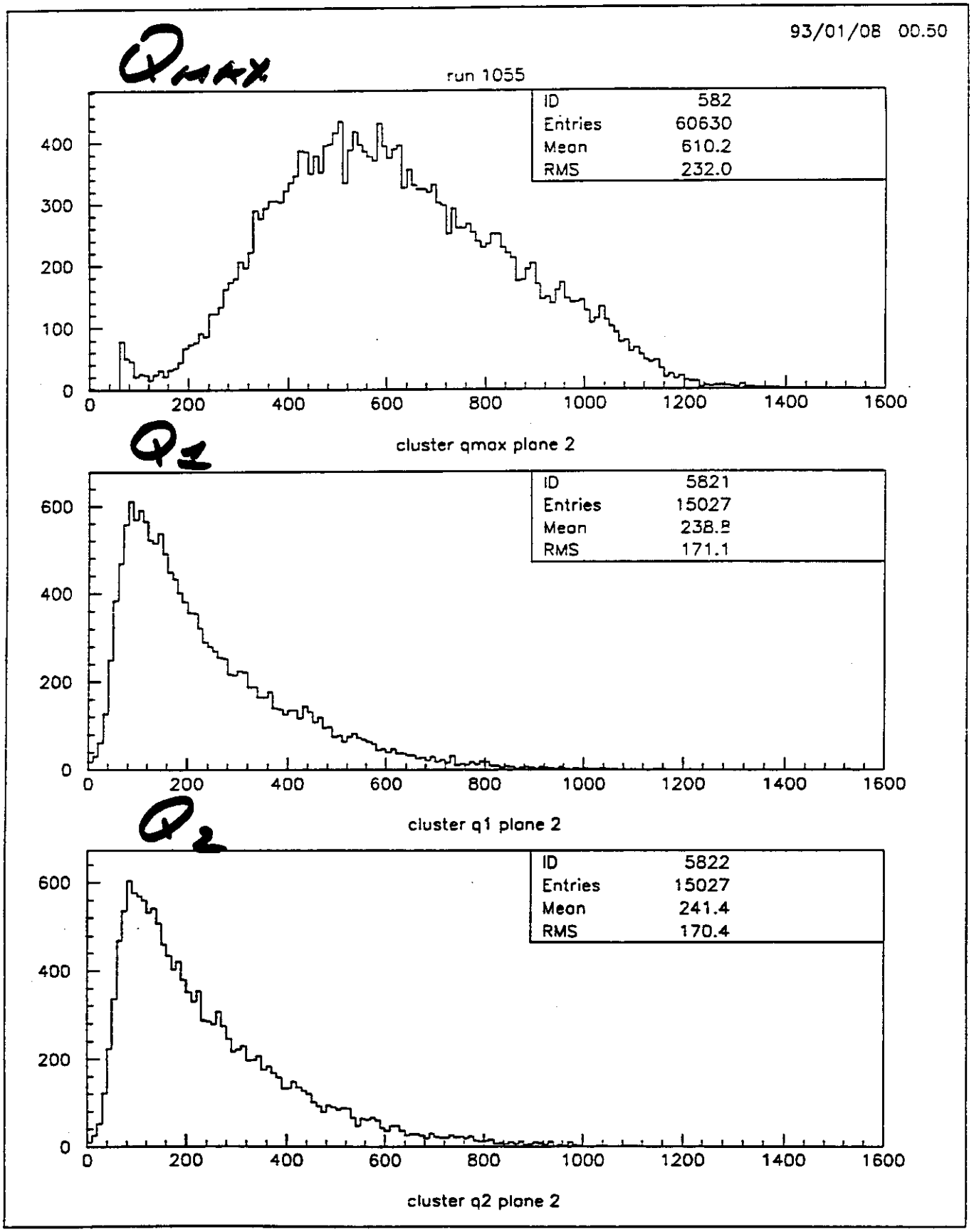
93/01/08 00.50
Qmax
run 1055
ID 582
Entries 60630
Mean 610.2
RMS 232.0
cluster qmax plane 2
Q1
ID 5821
Entries 15027
Mean 238.8
RMS 171.1
cluster q1 plane 2
Q2
ID 5822
Entries 15027
Mean 241.4
RMS 170.4
cluster q2 plane 2

93/01/04 16.03

run1055

Q_{LEFT} : Q_{RIGHT} CORRELATION

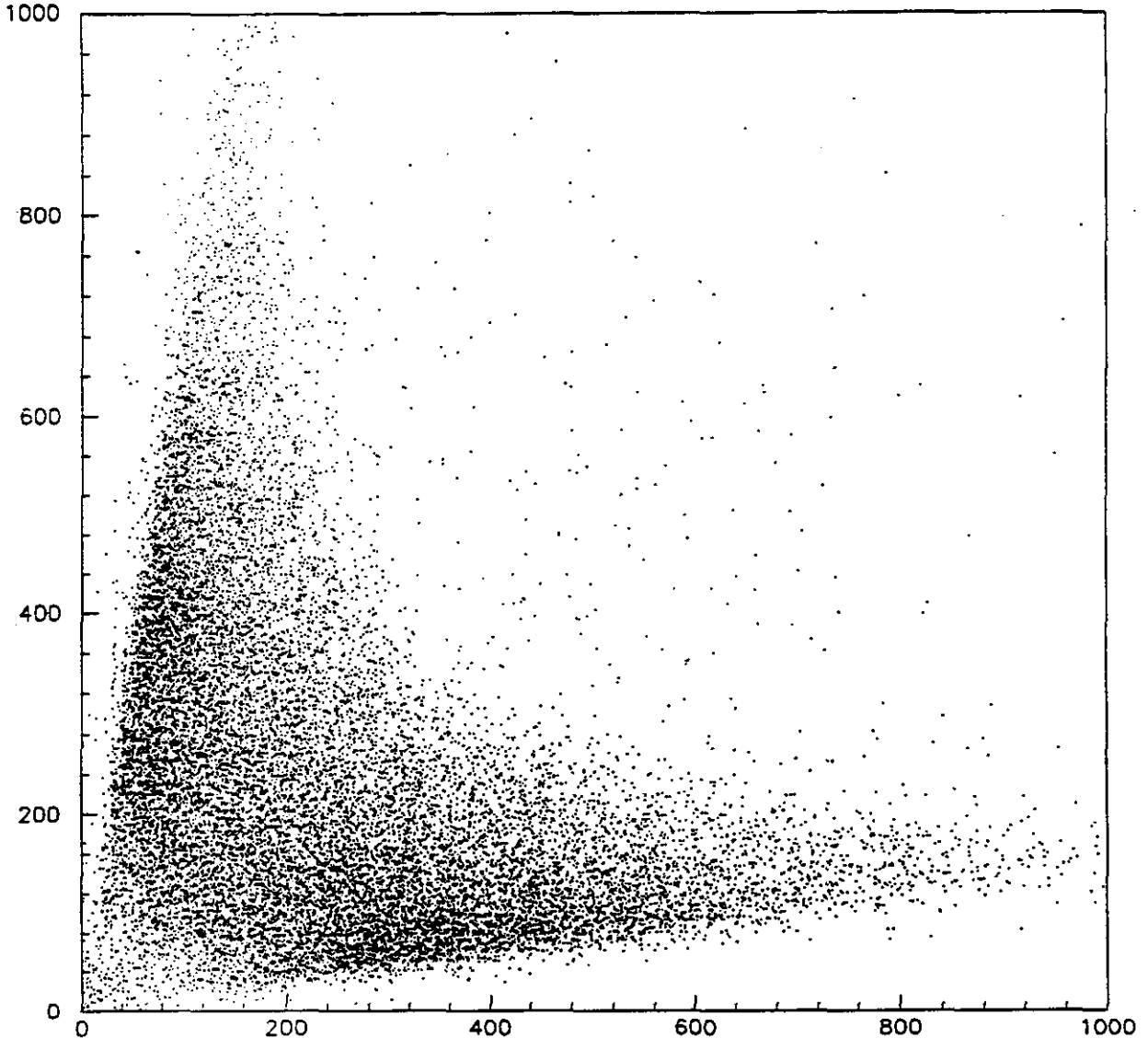

q2 vs q1 plane 2

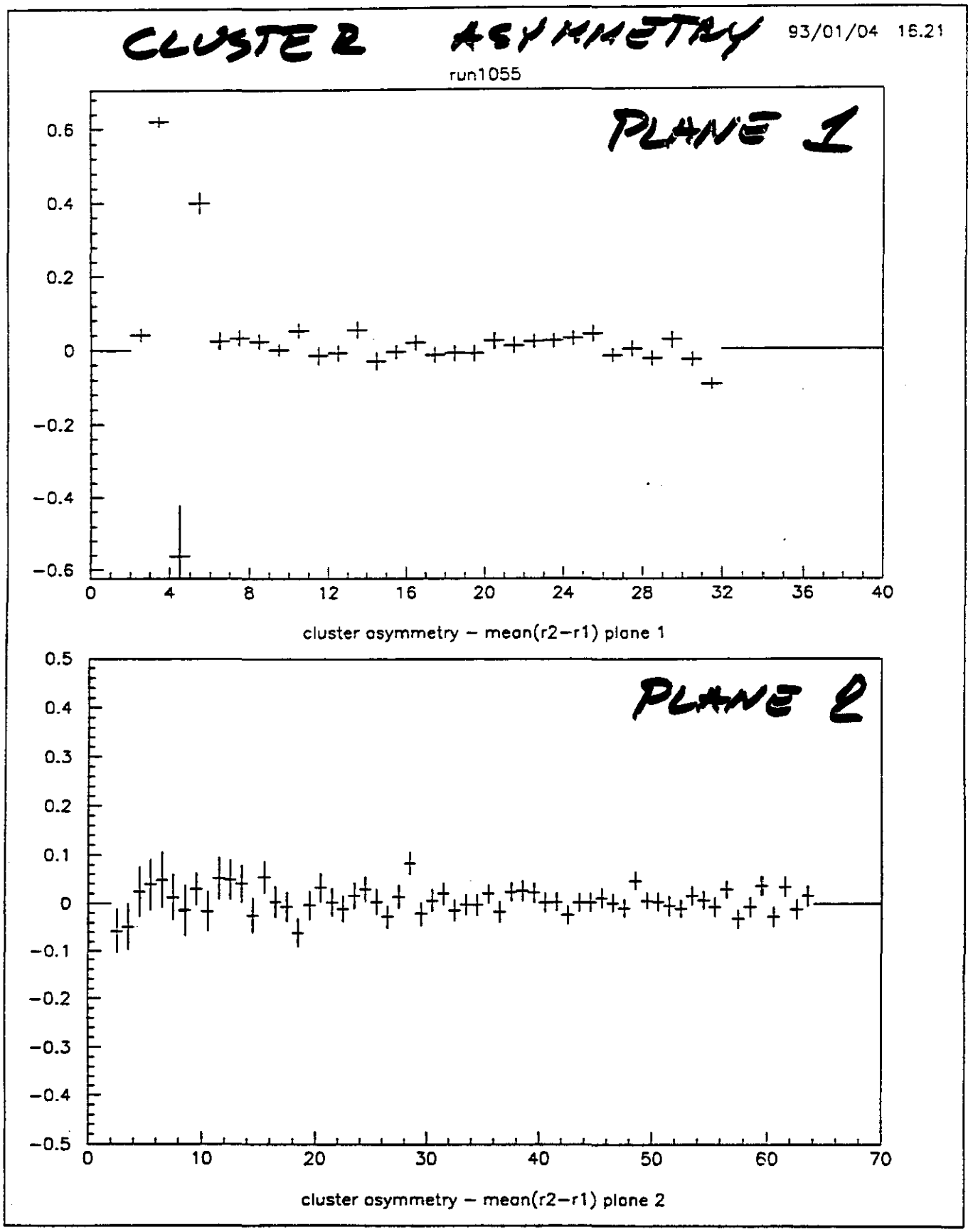
CLUSTER ASYMMETRY
93/01/04 16.21
run1055
PLANE 1
0.6
0.4
0.2
0
−0.2
−0.4
−0.6
0
4
8
12
16
20
24
28
32
36
40
cluster asymmetry − mean(r2−r1) plane 1
PLANE 2
0.5
0.4
0.3
0.2
0.1
0
−0.1
−0.2
−0.3
−0.4
−0.5
0
10
20
30
40
50
60
70
cluster asymmetry − mean(r2−r1) plane 2

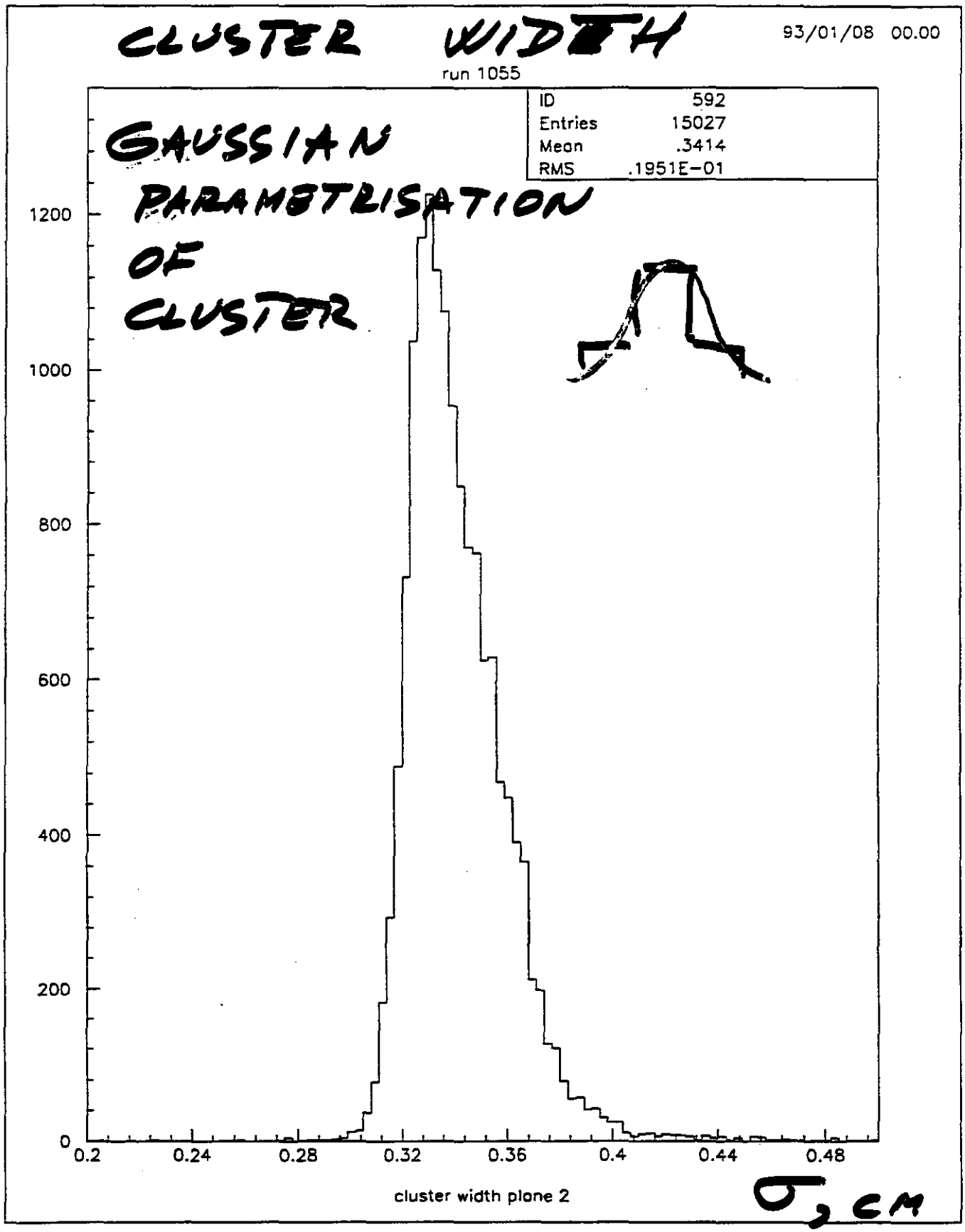
CLUSTER WIDTH
93/01/08 00.00
run 1055
ID 592
Entries 15027
Mean .3414
RMS .1951E-01
GAUSSIAN PARAMETRISATION OF CLUSTER
1200
1000
800
600
400
200
0
0.2
0.24
0.28
0.32
0.36
0.4
0.44
0.48
cluster width plane 2
σ, cm

CLUSTER WIDTH VS q_{max}

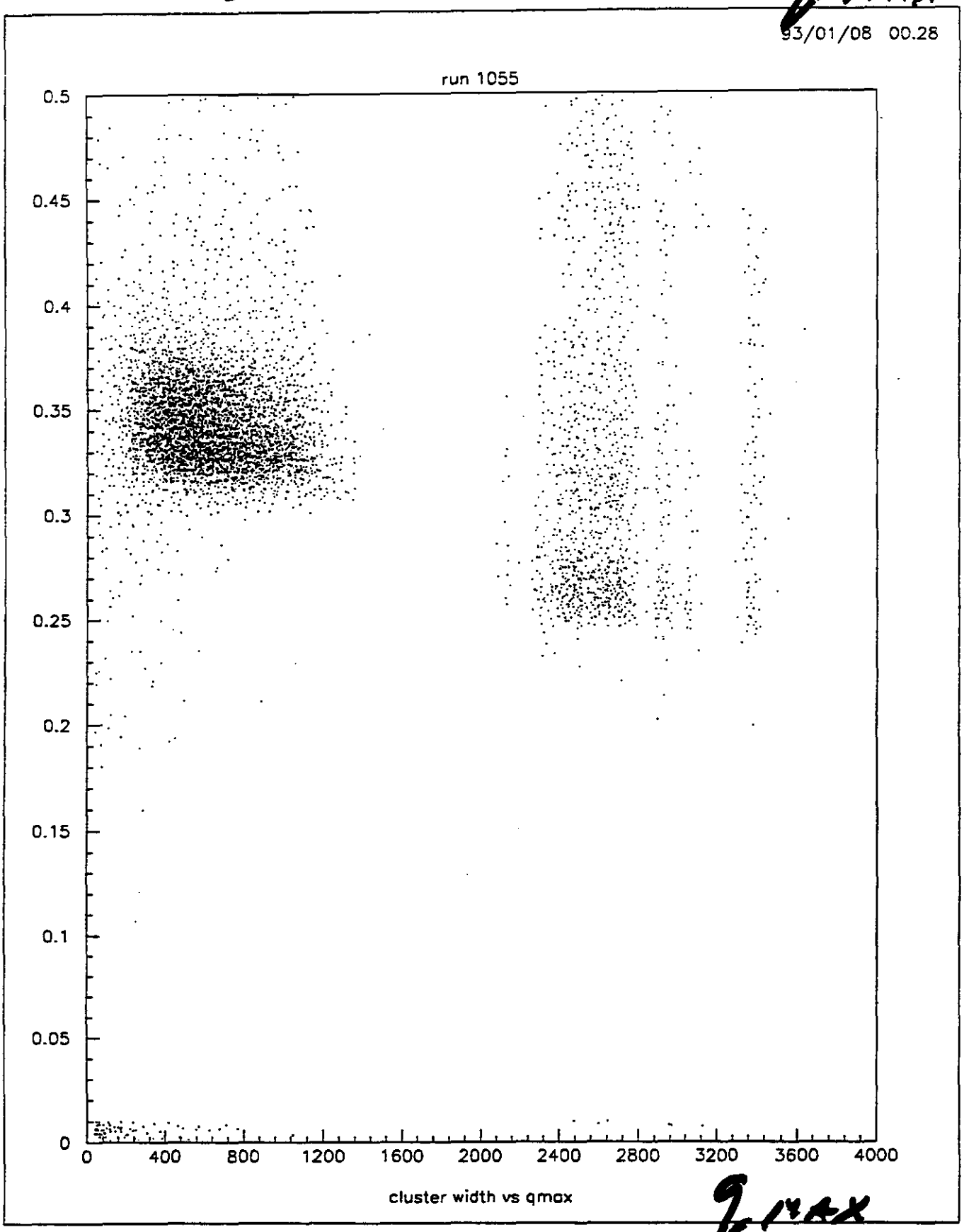

CLUSTER WIDTH VS DELTA

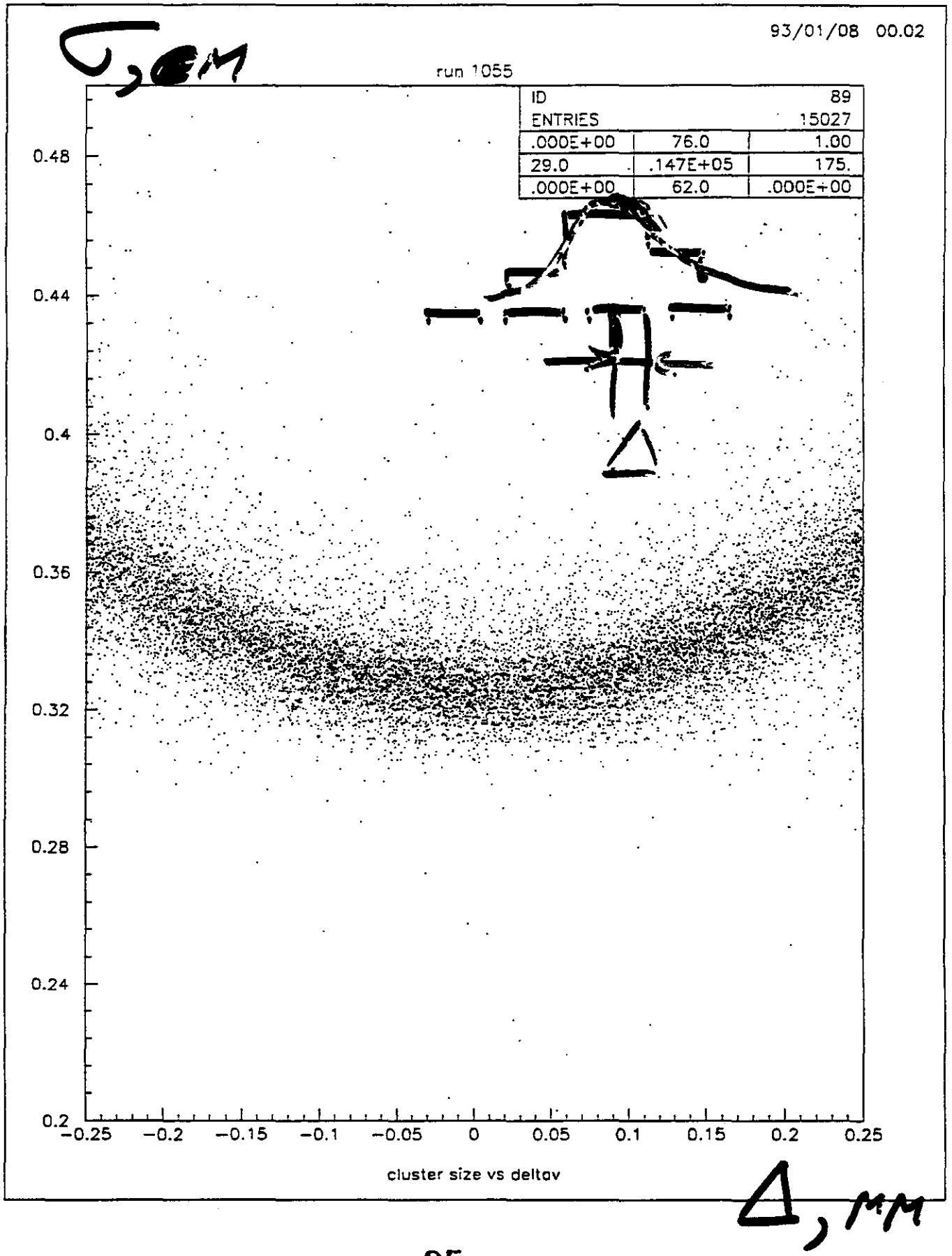

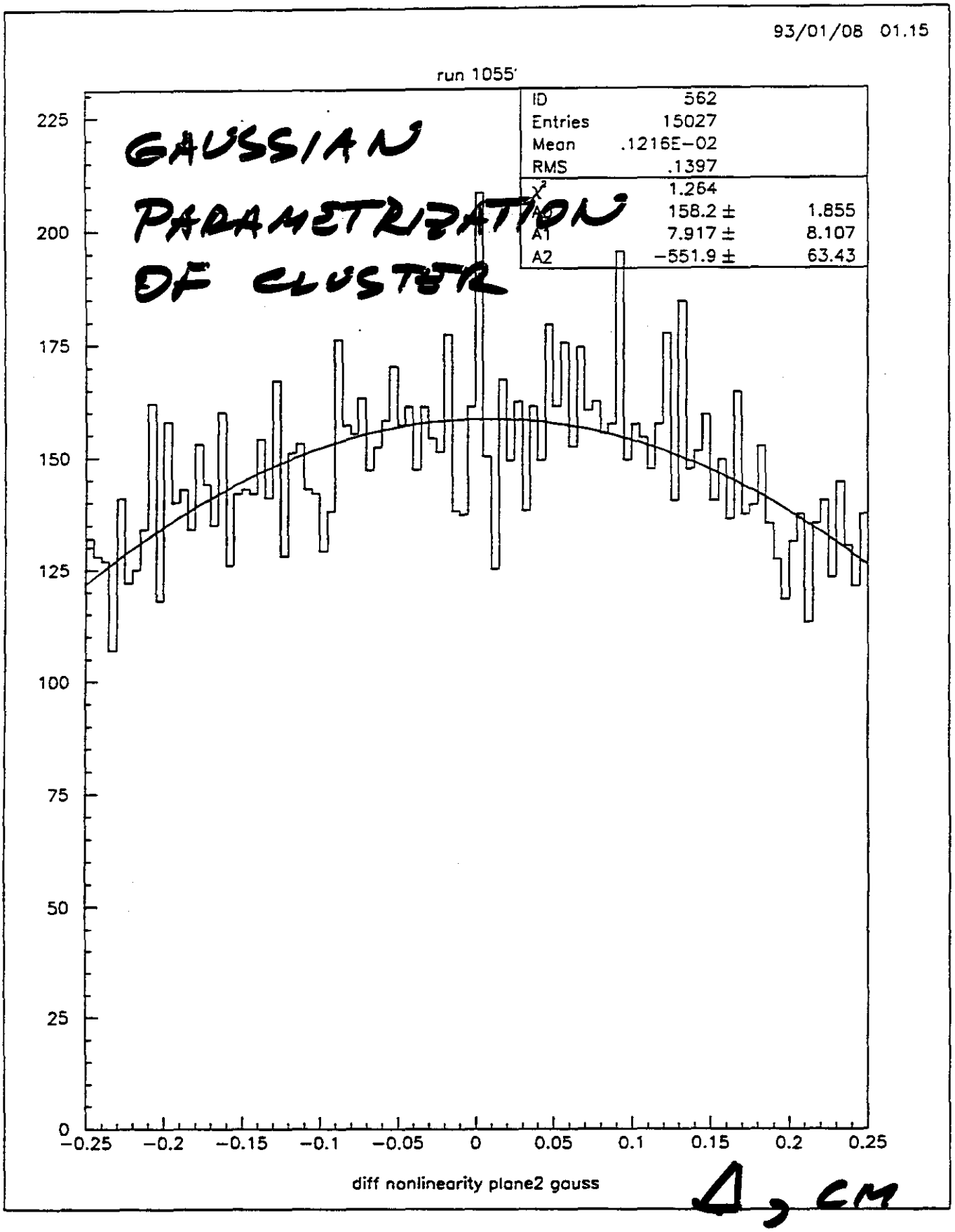
93/01/08 01.15
run 1055
ID 562
Entries 15027
Mean .1216E-02
RMS .1397
χ² 1.264
A0 158.2 ± 1.855
A1 7.917 ± 8.107
A2 −551.9 ± 63.43
GAUSSIAN PARAMETRIZATION OF CLUSTER
225
200
175
150
125
100
75
50
25
0
−0.25 −0.2 −0.15 −0.1 −0.05 0 0.05 0.1 0.15 0.2 0.25
diff nonlinearity plane2 gauss
Δ, cm

93/01/08 00.37

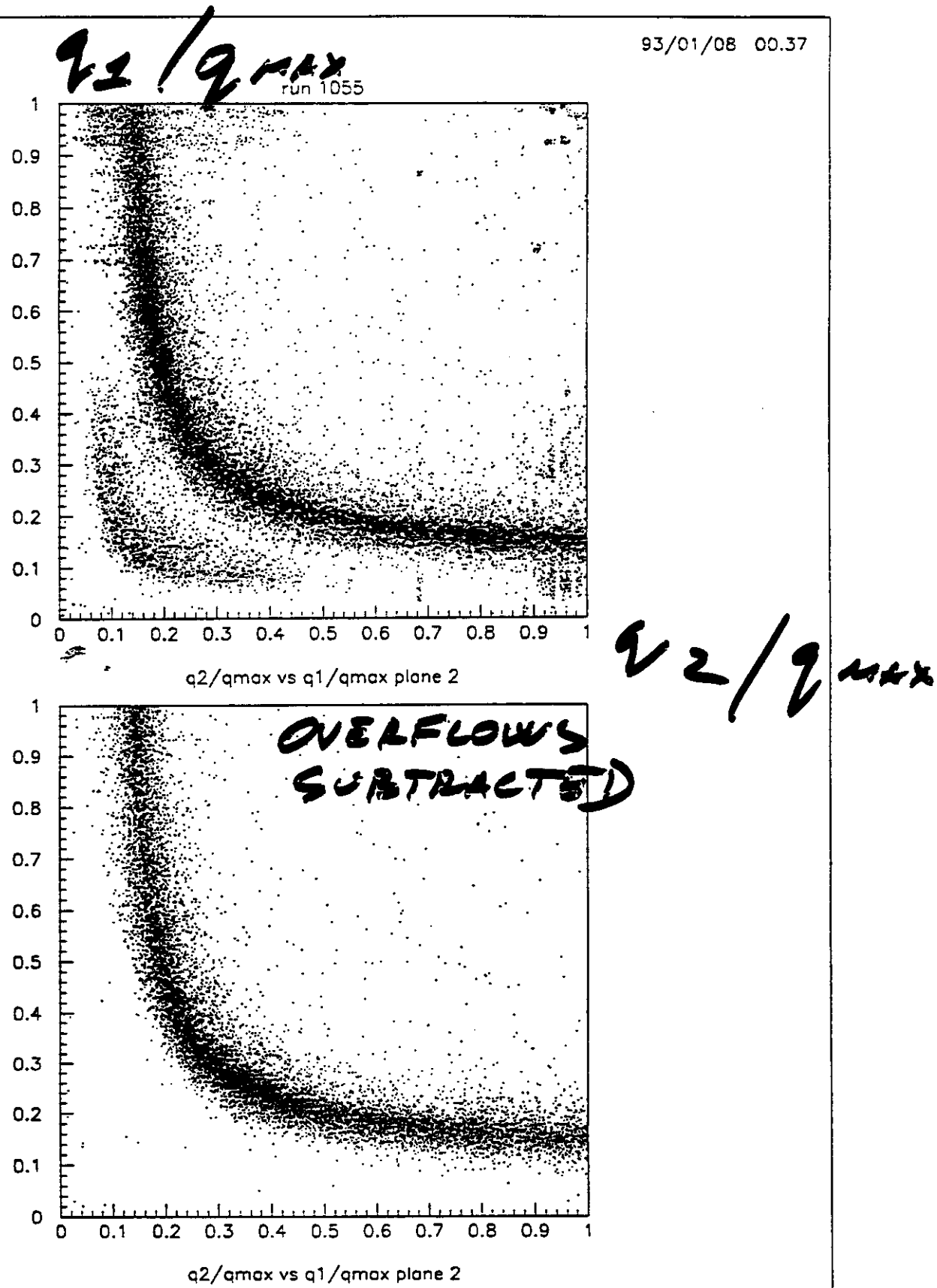
q1/qmax
run 1055
q2/qmax
q2/qmax vs q1/qmax plane 2
OVERFLOWS SUBTRACTED
q2/qmax vs q1/qmax plane 2

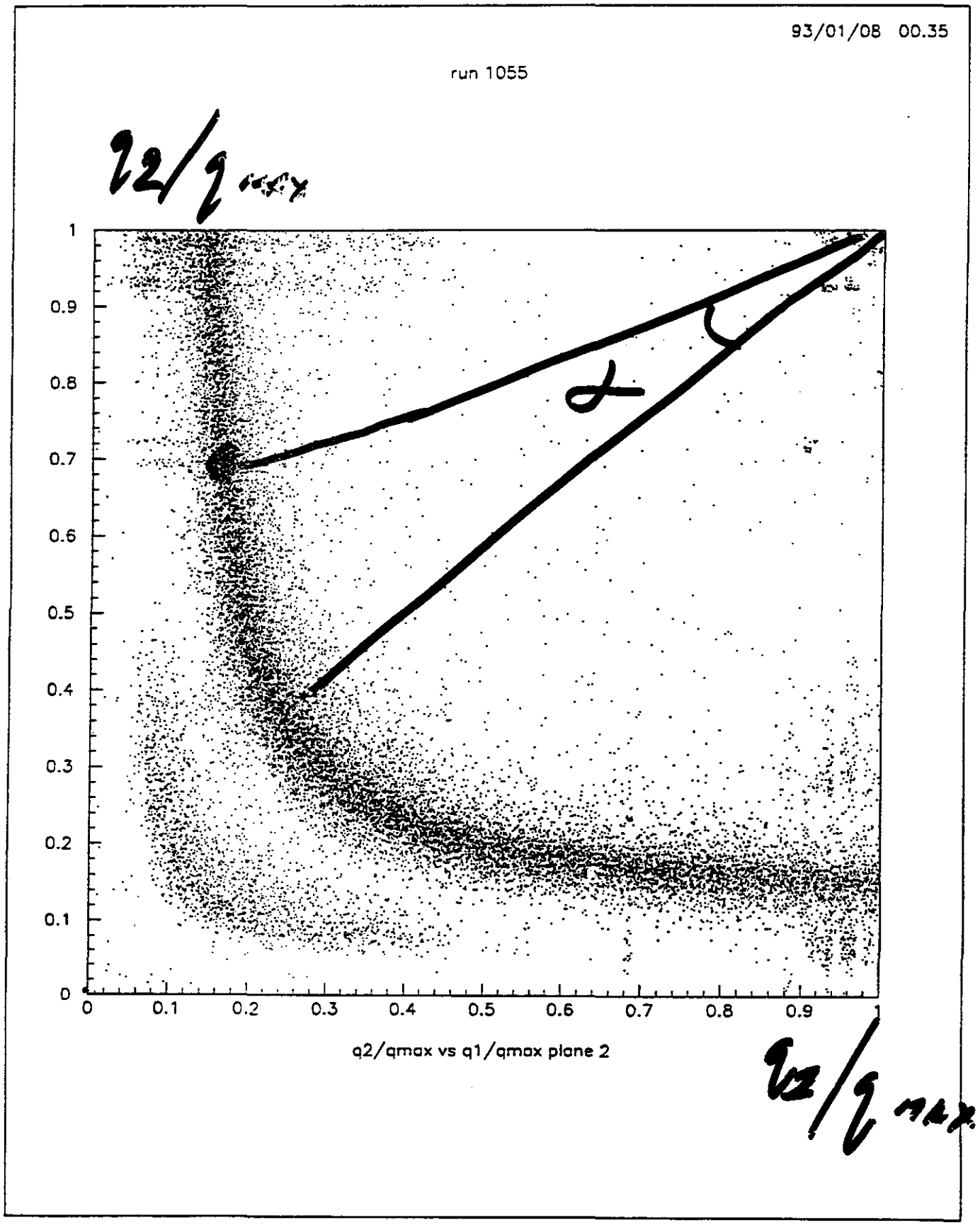
93/01/08 00.35
run 1055
q2/q max
1
0.9
0.8
0.7
0.6
0.5
0.4
0.3
0.2
0.1
0
0
0.1
0.2
0.3
0.4
0.5
0.6
0.7
0.8
0.9
1
α
q2/qmax vs q1/qmax plane 2
q2/q max

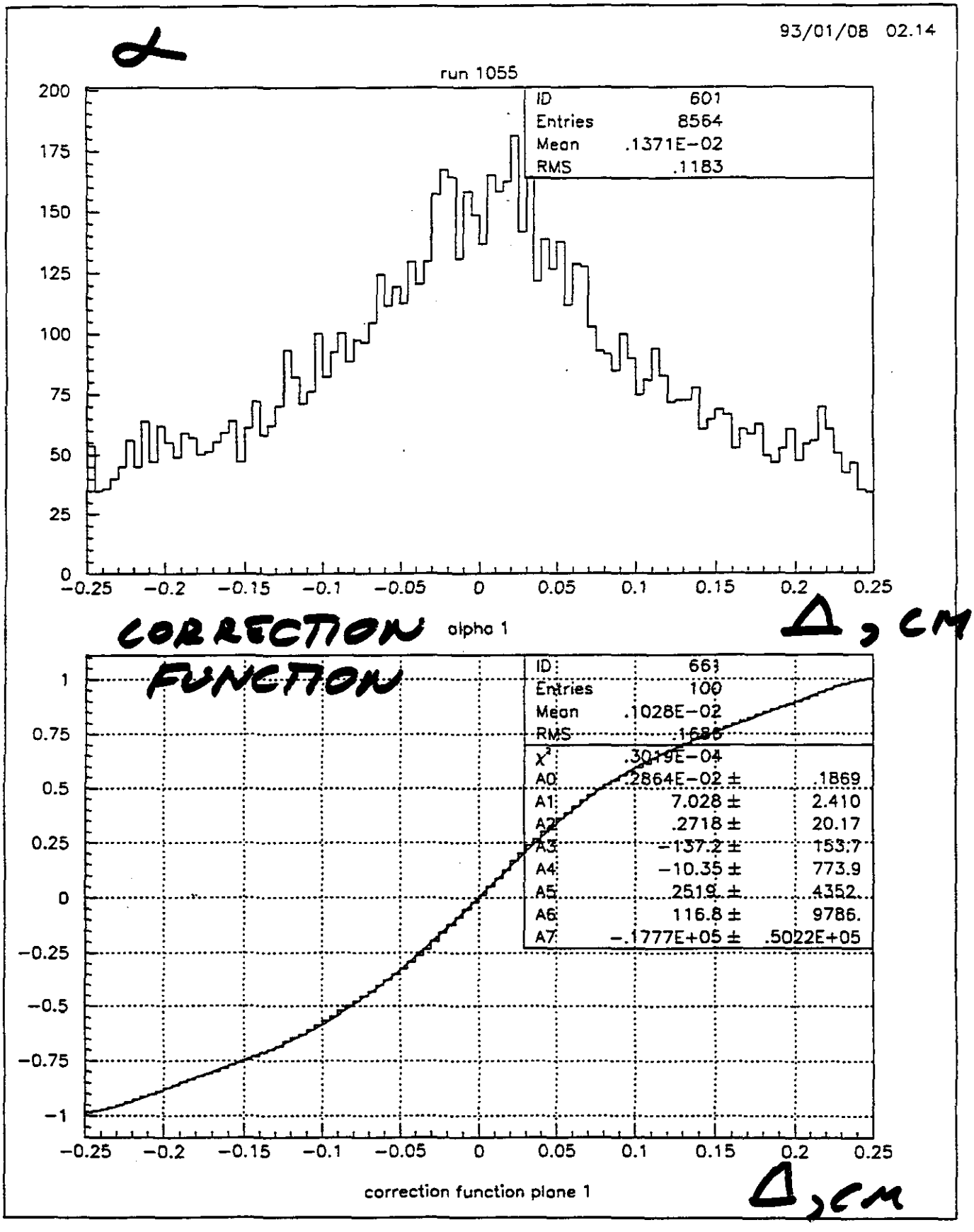
93/01/08 02.14
α
run 1055
ID 601
Entries 8564
Mean .1371E−02
RMS .1183
Δ, CM
CORRECTION FUNCTION
alpha 1
ID 661
Entries 100
Mean .1028E−02
RMS .1686
χ² .3019E−04
A0 .2864E−02 ± .1869
A1 7.028 ± 2.410
A2 .2718 ± 20.17
A3 −137.2 ± 153.7
A4 −10.35 ± 773.9
A5 .2519 ± .4352
A6 116.8 ± 9786.
A7 −.1777E+05 ± .5022E+05
correction function plane 1
Δ, CM

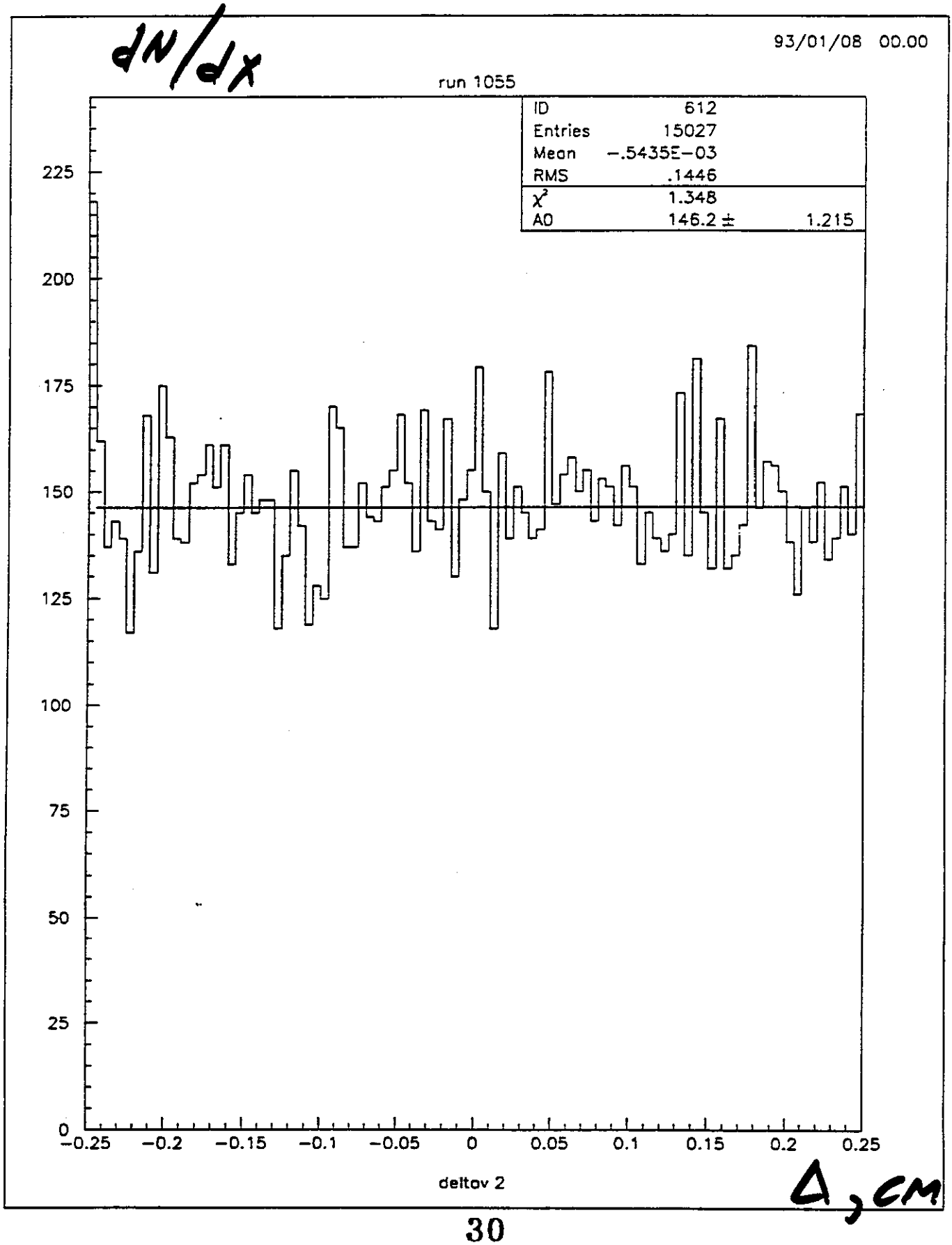

DIFFERENTIAL NONLINEARITY CORRECTED FOR

gem

γeμ

Presentation by:

B. Mayes

Spatial Resolution Measurements of UH (open profile) CSC Prototype at TTR

University of Houston

SSCL (TTR)

Dubna

Presented by Bill Mayes

GEM CSC meeting 1/8/93

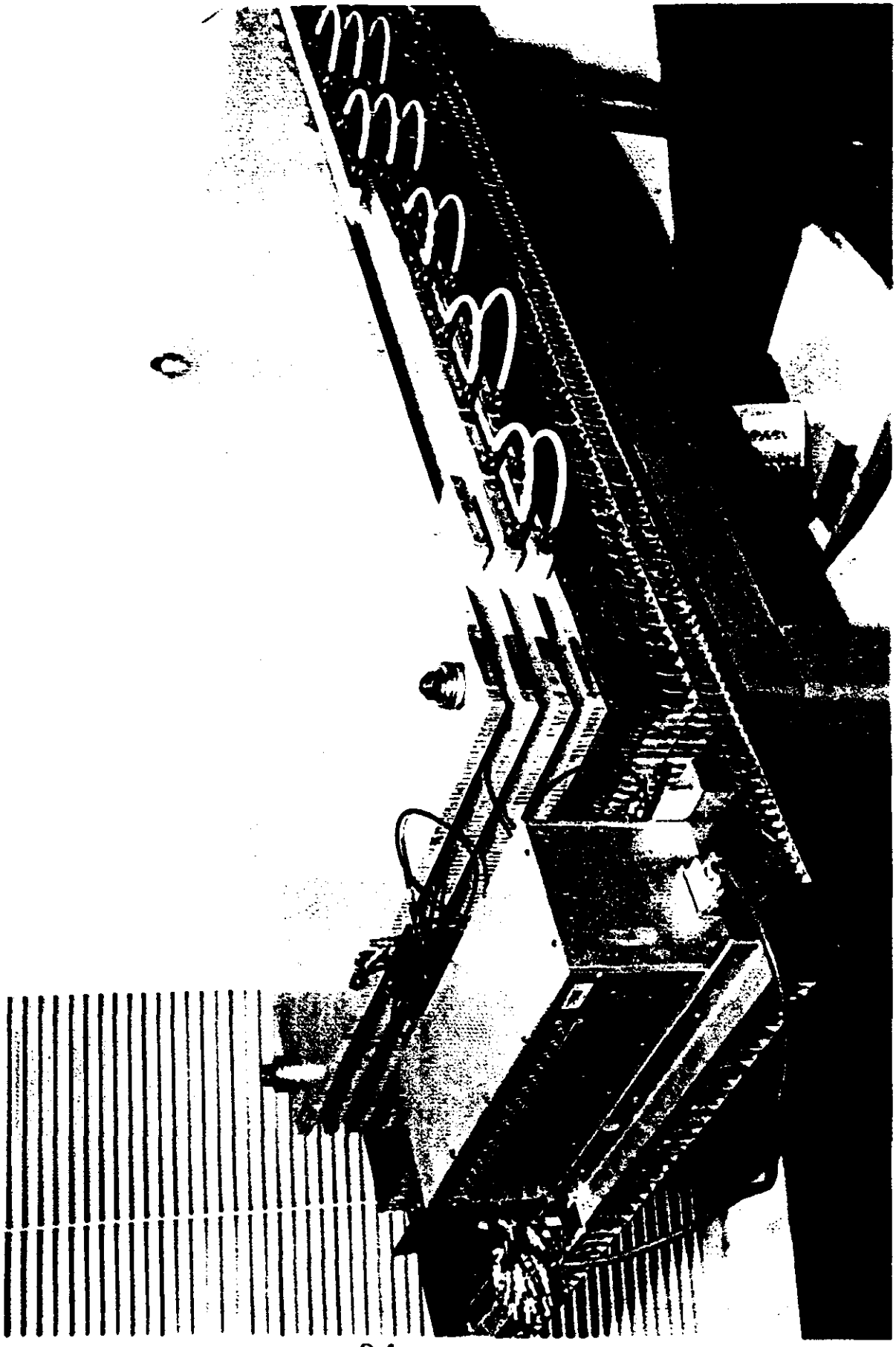

UH CSC Prototype

- 3 layers of 1.0 m (long) x 0.5 m precision strips (pitch = 5.0 mm = 4 mm Cu + 1 mm gap)
- 3 layers (12 chambers per layer) of 66-cm Iarocci-type carbon-coated (4 kΩ per square) profiles with 45 μm gold-plated tungsten wires
- standard (75/25 Isobutane-argon) gas mixture in proportional mode (3.0 - 3.3 kV)
- 10 (top), 9 (middle), and 10 (bottom) strips at center from the three layers are instrumented with preamps (gain $\simeq$ 1000) and ADCs.
- preamp outputs are routed via 53-m RG174 coaxial cables to Lecroy 2249W ADCs with an integration time of 500 ns
- trigger on 2 top scintillators and all bottom scintillators

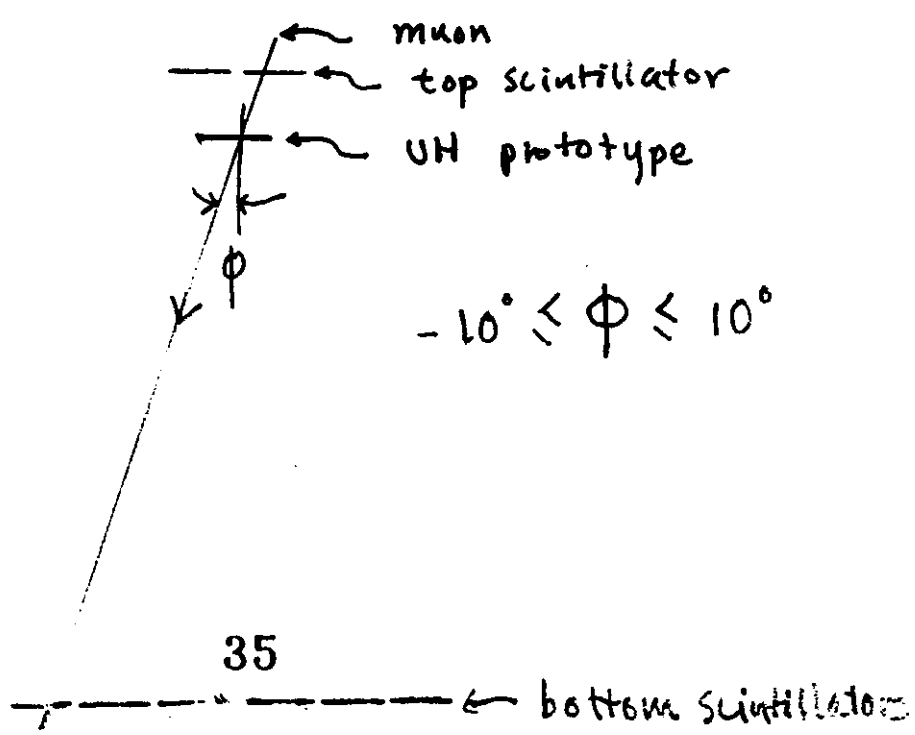

Analysis Procedure

- Fast Filter at TTR
  - select events with at least 1 strip with $\geq$ 100 ADC counts in each layer

- Pedestal and Gain Corrections
  - apply pedestal (20-40 ADC counts) subtraction and gain correction (1.00 $\pm$ 0.10) to all ADC counts.
  - ADC counts set to 0 if corrected counts are $\leq$ 0.

- Fiducial Cut
  - locate peak channel in each layer and require peak channel to be at least 1 or 2 channels from uninstrumented strips

- δ-ray Cut
  - remove any event with 1 or more ADC overflows ($\geq$ 1900 raw ADC counts)

- Locate Cluster Centroid
  - determine c.o.g. of the hits for each layer (z_{cog}) by using a weighted mean of 3-strip ($z^{(3)}$) and 4-strip ($z^{(4)}$) c.o.g.'s

$$z_{cog} = \frac{z^{(3)}}{1 + \frac{2}{w}\left(z^{(3)} - z^{(4)}\right)}$$

w = strip pitch = 5.0 mm

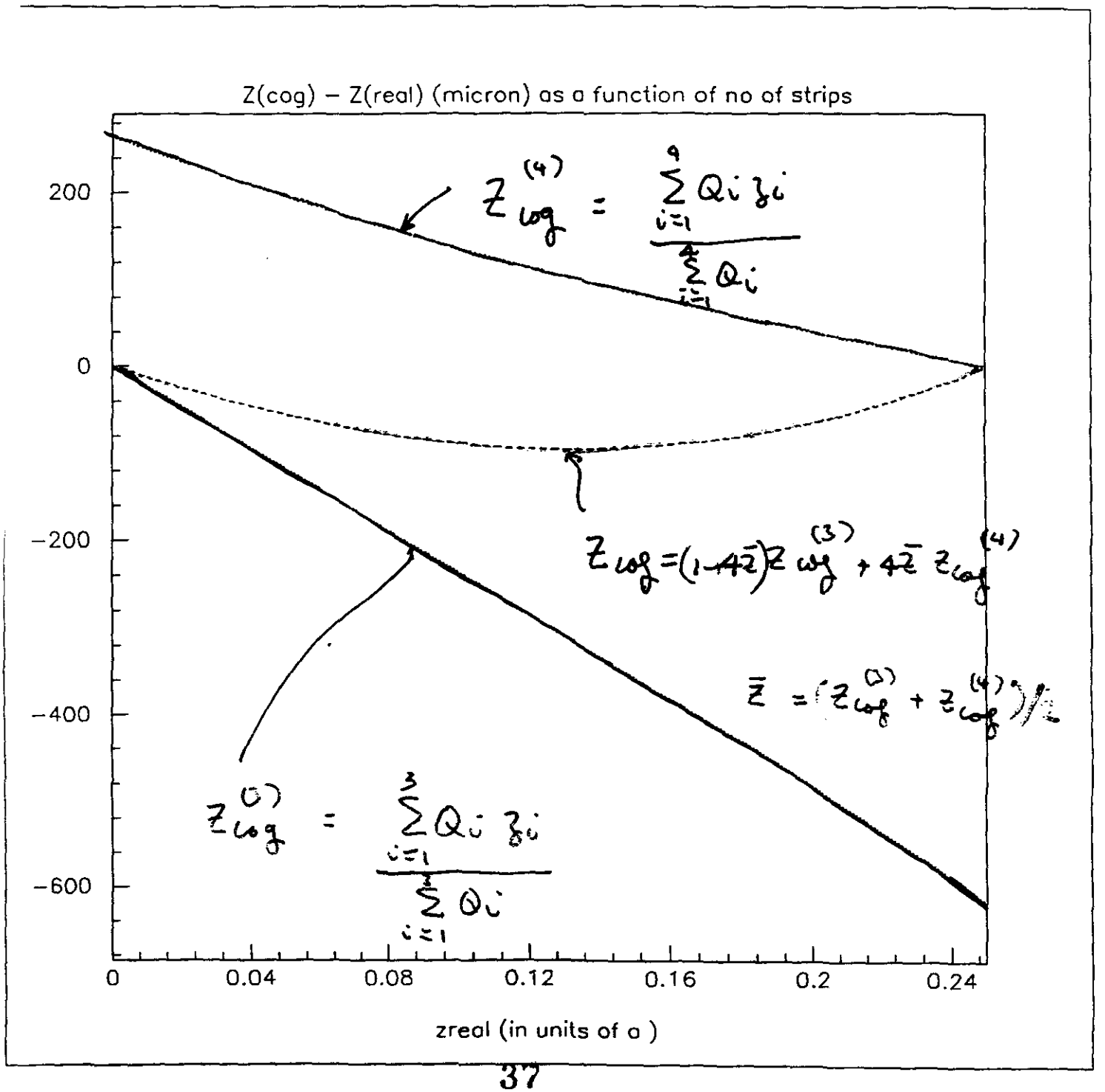
Z(cog) – Z(real) (micron) as a function of no of strips
200
0
−200
−400
−600
0
0.04
0.08
0.12
0.16
0.2
0.24
zreal (in units of a)
$Z_{cog}^{(4)} = \frac{\sum_{i=1}^{4} Q_i z_i}{\sum_{i=1}^{4} Q_i}$
$Z_{cog} = (1-4\bar{z}) Z_{cog}^{(3)} + 4\bar{z}\, Z_{cog}^{(4)}$
$\bar{z} = (Z_{cog}^{(3)} + Z_{cog}^{(4)})/2$
$Z_{cog}^{(3)} = \frac{\sum_{i=1}^{3} Q_i z_i}{\sum_{i=1}^{3} Q_i}$

- Systematic Correction
  - apply a 3-term-Fourier-series systematic correction of the following form

$$\Delta z = A \times [sin(\frac{2\pi z_{cog}}{w}) - 0.077 \times sin(\frac{4\pi z_{cog}}{w}) + 0.041 \times sin(\frac{6\pi z_{cog}}{w})]$$

A is varied in the range : $60 \leq A \leq 100$ μm

A = 117.1 μm according to monte carlo with a point inducing charge

A $\simeq$ 80-90 μm gives best results

- Systematic Alignment Correction
  - middle plane is found to be off by $\simeq 33 \pm 5$ μm relative to top and bottom layers.
  - correct z_{cog}s in the middle plane by a systematic shift of 33 μm.

- Track Fitting
  - fit the corrected points (least square) to a straight line
- Resolution per Plane
  - residuals in the top layer (R_1) within $\pm$ 150 μm are fitted to a Gaussian + a constant.
  - resolution per plane $\sigma = \sqrt{6}\ \sigma_{R_1}$

$$\Delta z = -117.07 \sin\left(\frac{2\pi z}{0.5\ \text{cm}}\right) \qquad 0 \le z \le 0.25\ \text{cm}$$

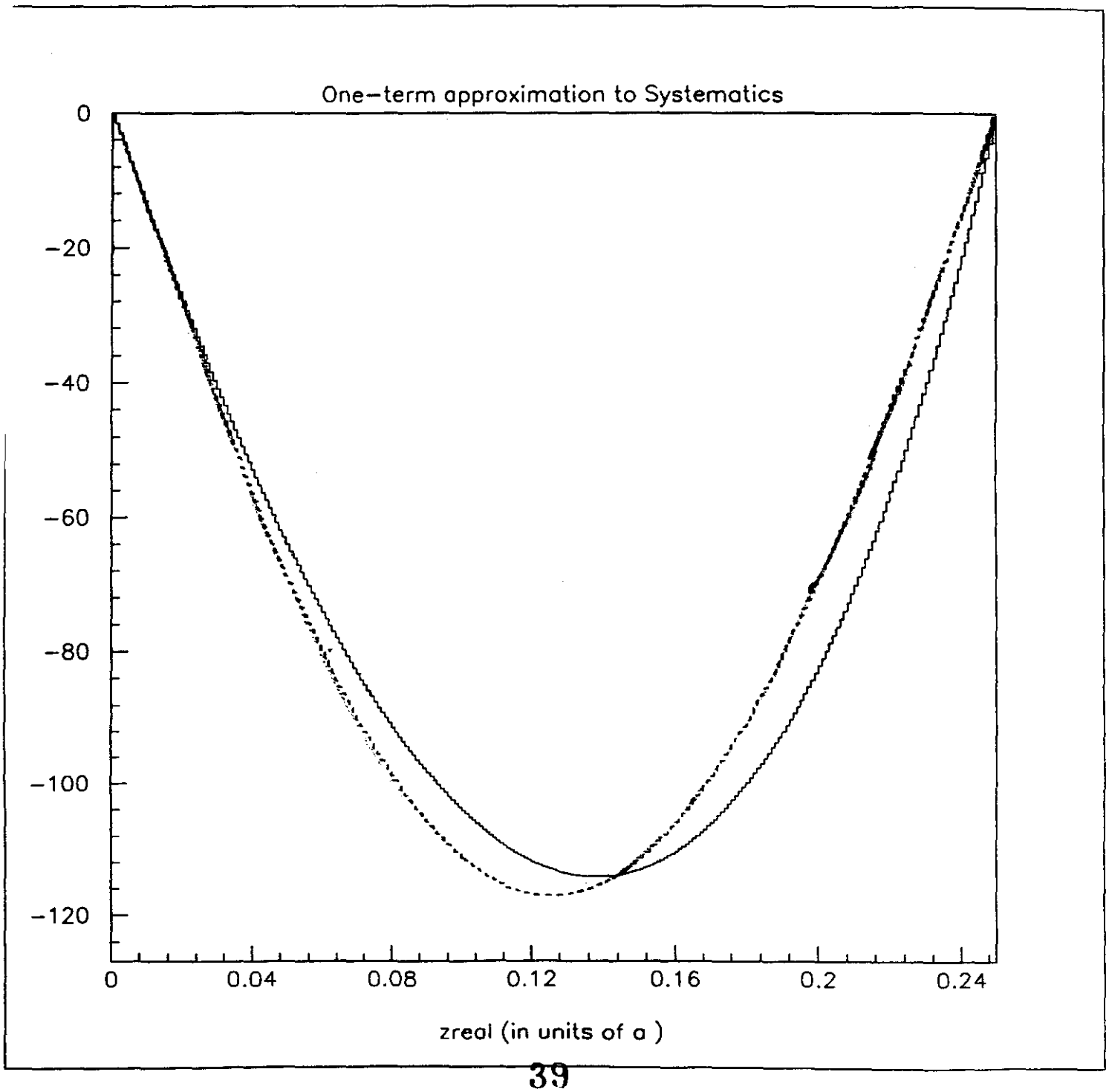

$$\Delta z = -117.07 \sin\left(\frac{2\pi z}{0.5\,cm}\right) + 9.07 \sin\left(\frac{4\pi z}{0.5\,cm}\right)$$

$$0 < z < 0.25\,cm$$

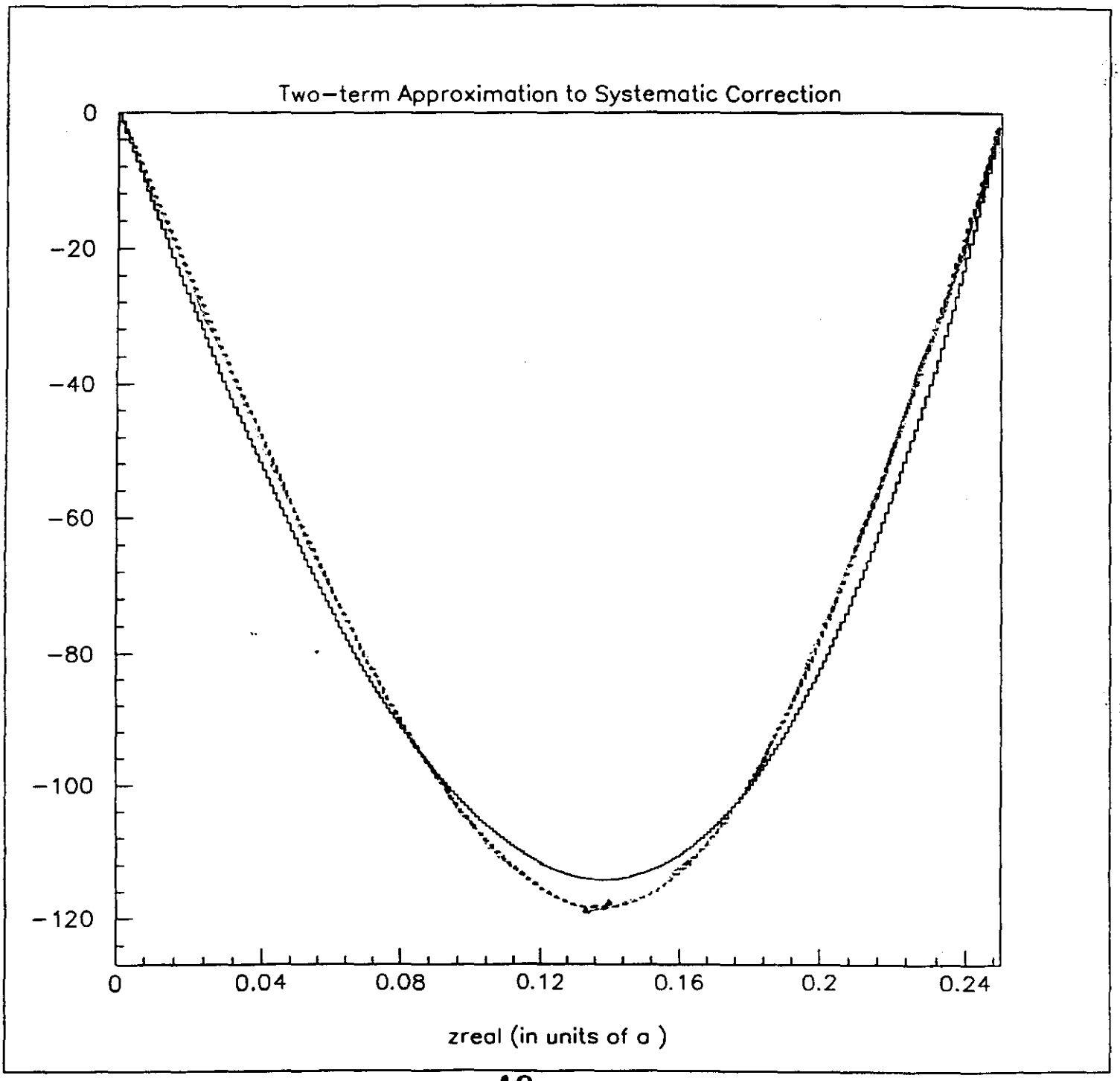

$$\Delta z = -117.07 \sin\left(\frac{2\pi z}{0.5\,km}\right) + 9.07 \sin\left(\frac{4\pi z}{0.5\,km}\right) - 4.85 \sin\left(\frac{6\pi z}{0.5\,km}\right)$$

$$0 < z < 0.25\,km$$

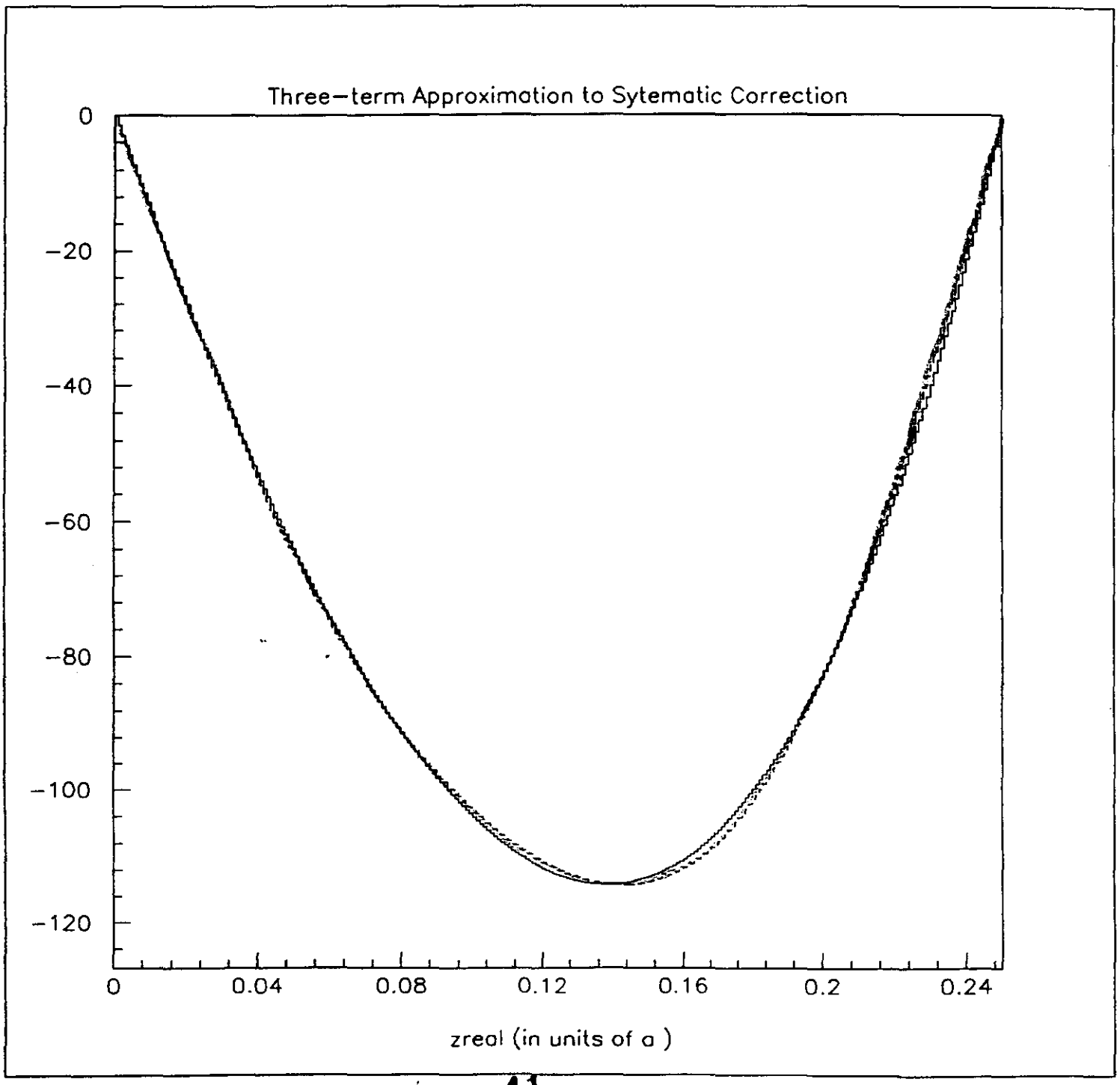

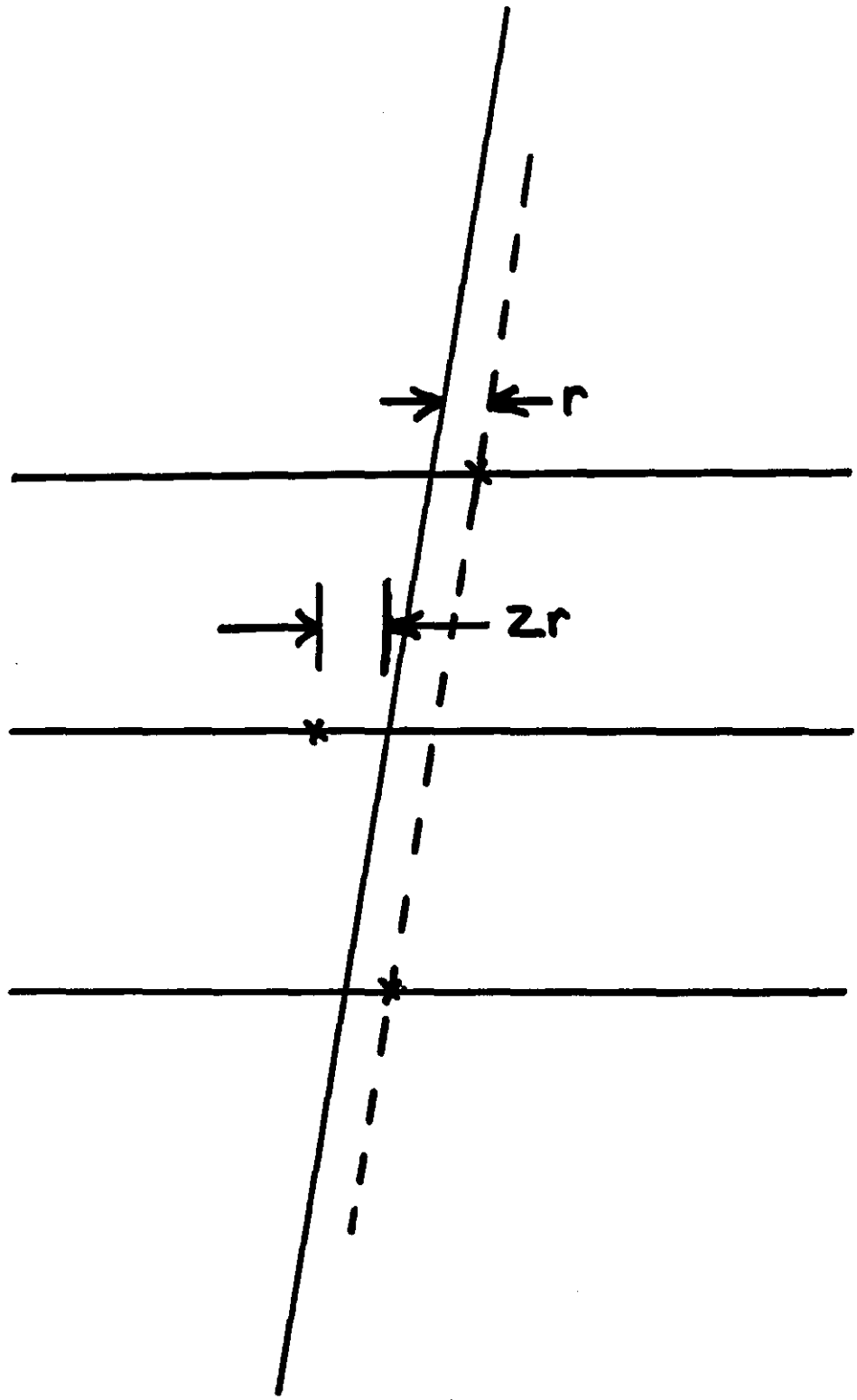

$\sigma_{plane} = \sqrt{6}\ \sigma_{residuals}$

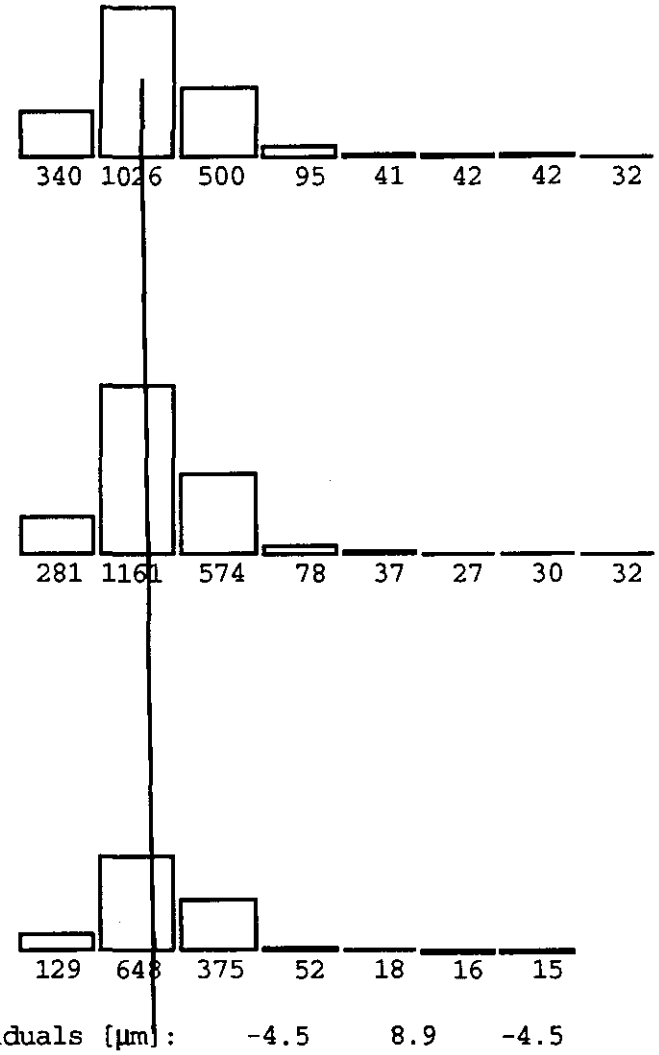

Residuals [µm]: -4.5 8.9 -4.5
Centroid [mm]: 12.576 12.945 13.340
Σ counts: 1961 2094 1204 Σ unused : 157 126 49 Angle:-0.9°

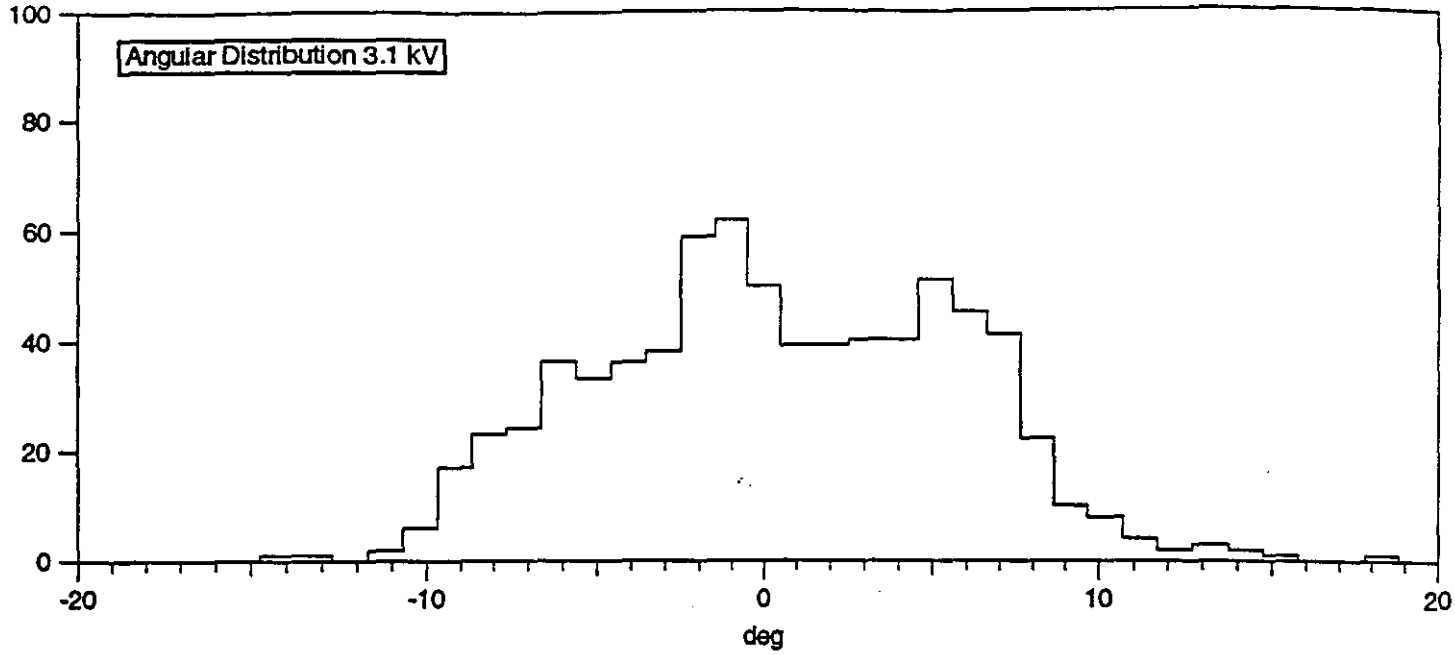
Angular Distribution 3.1 kV
100
80
60
40
20
0
-20
-10
0
10
20
deg

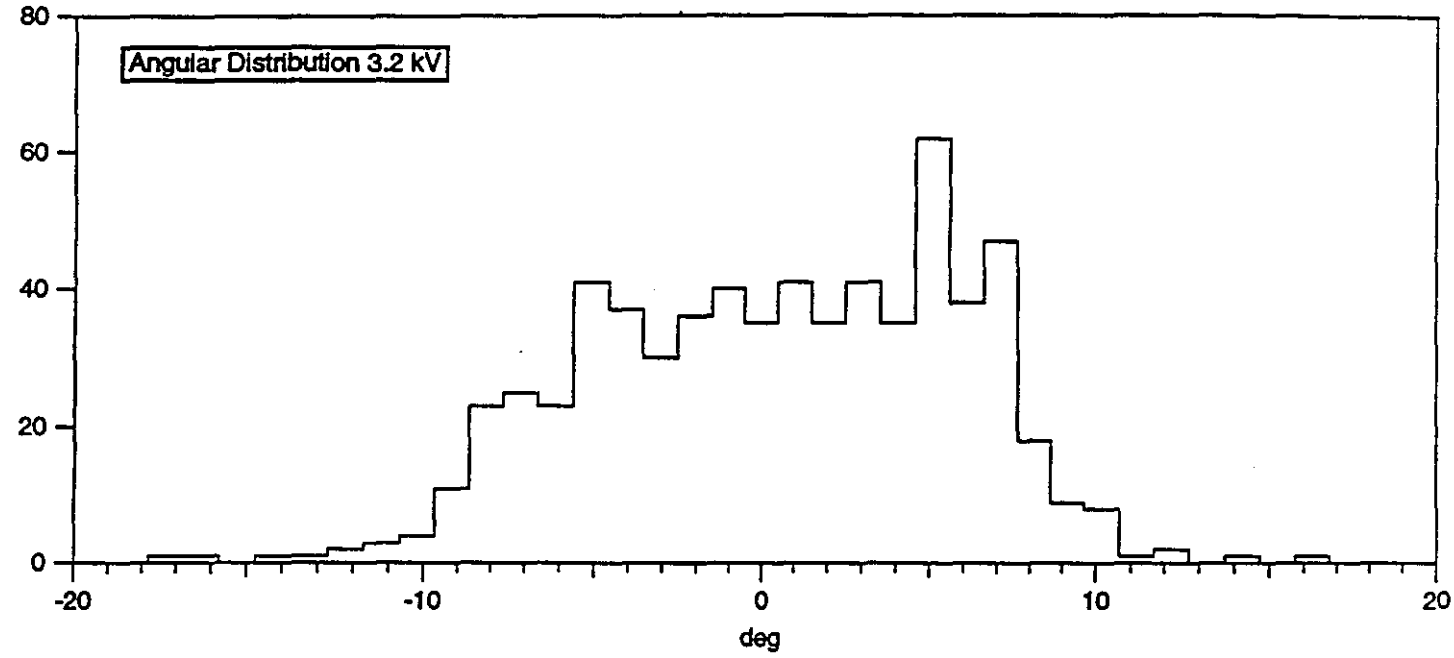
Angular Distribution 3.2 kV
80
60
40
20
0
-20
-10
0
10
20
deg

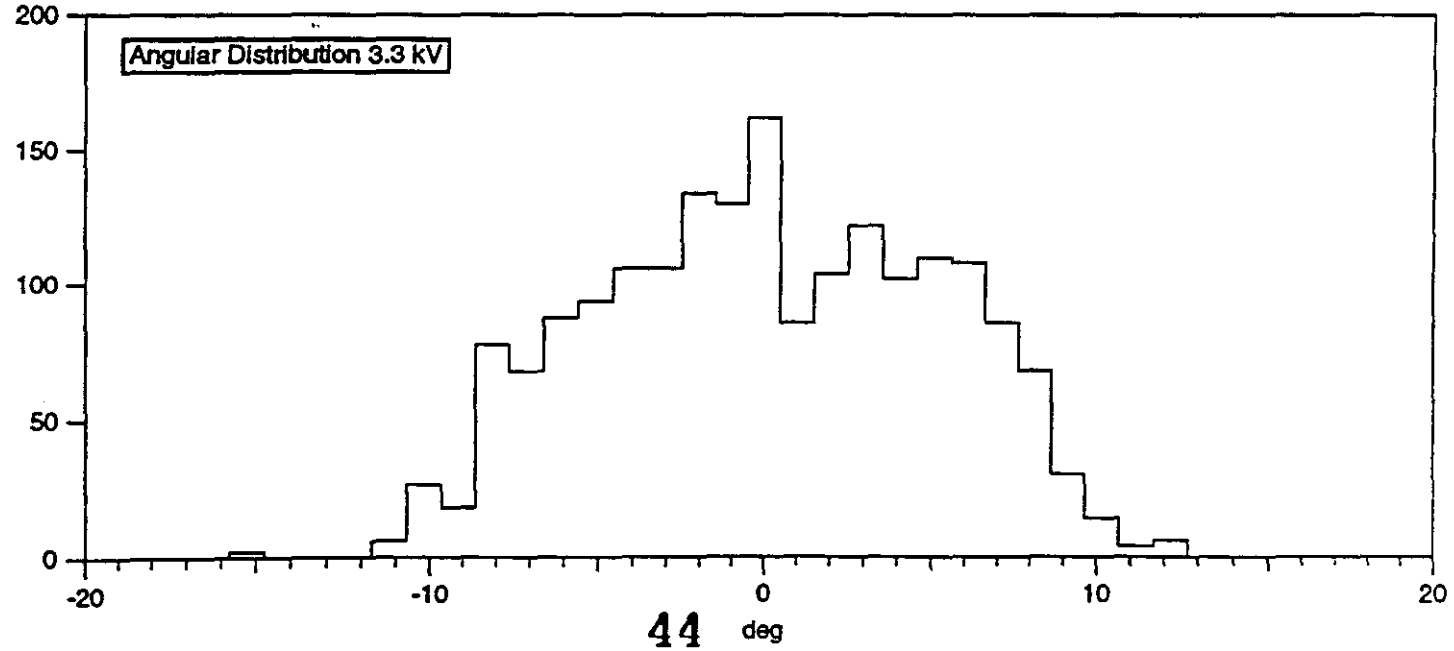
Angular Distribution 3.3 kV
200
150
100
50
0
-20
-10
0
10
20
deg

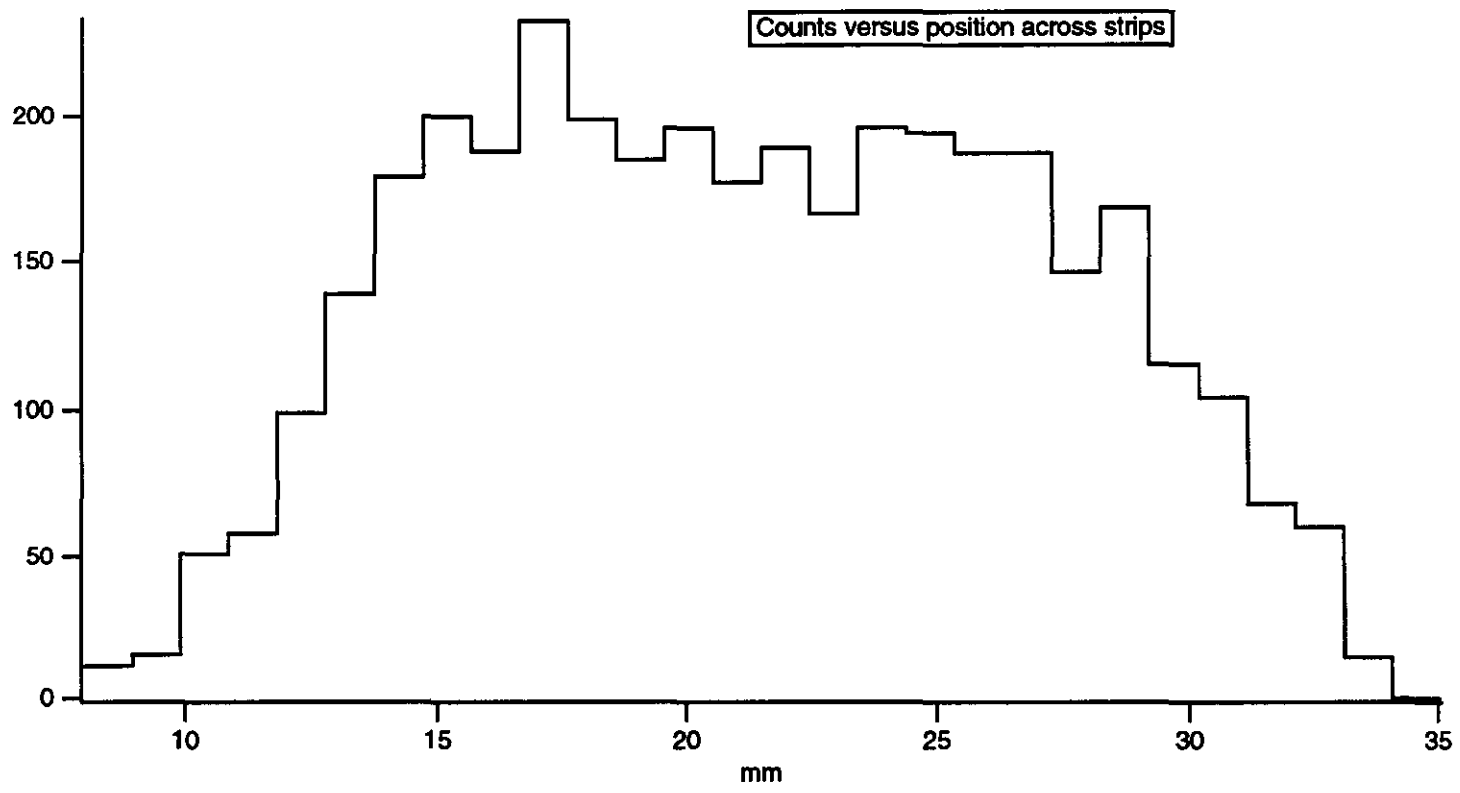
Counts versus position across strips
200
150
100
50
0
10
15
20
25
30
35
mm

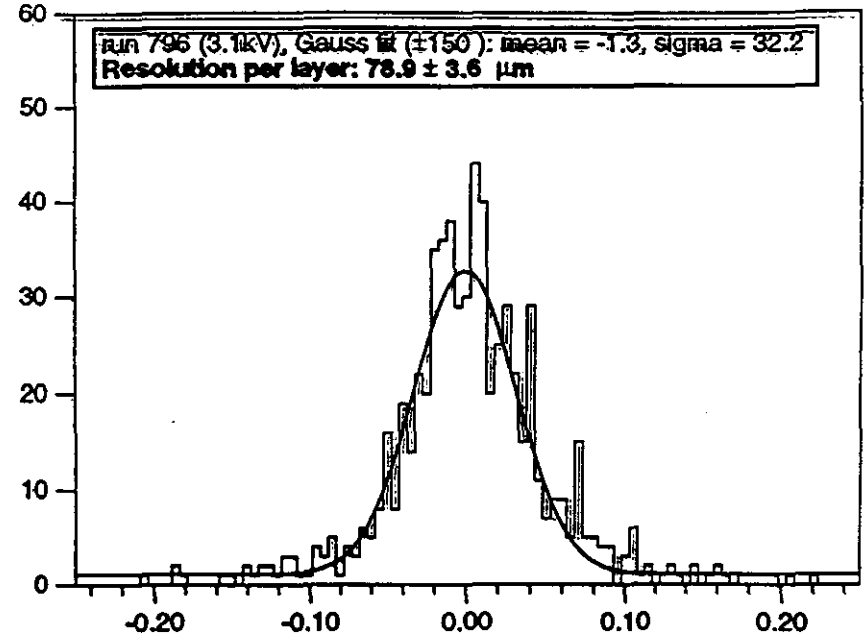
run 796 (3.1kV), Gauss fit (±150): mean = -1.3, sigma = 32.2
Resolution per layer: 78.9 ± 3.6 µm
60
50
40
30
20
10
0
-0.20
-0.10
0.00
0.10
0.20

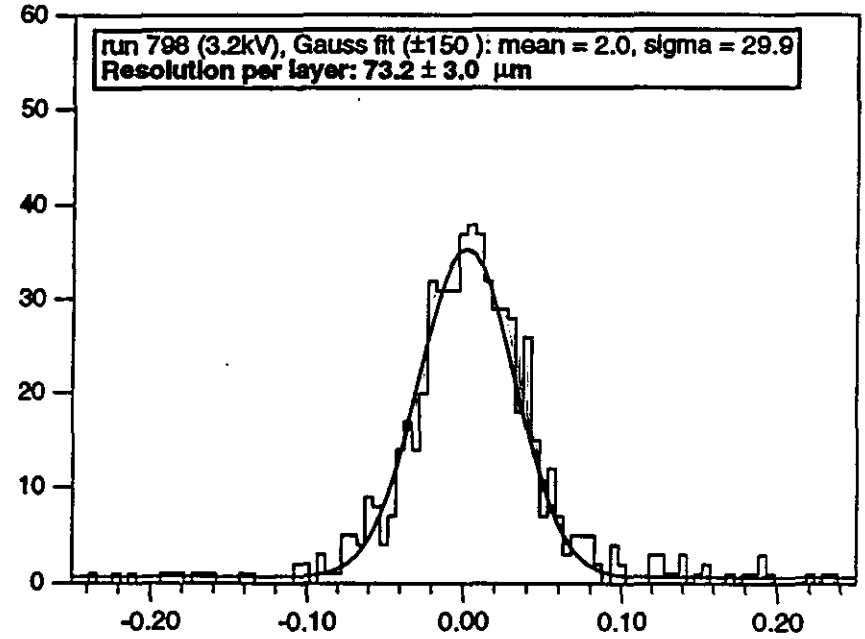
run 798 (3.2kV), Gauss fit (±150): mean = 2.0, sigma = 29.9
Resolution per layer: 73.2 ± 3.0 µm
60
50
40
30
20
10
0
-0.20
-0.10
0.00
0.10
0.20

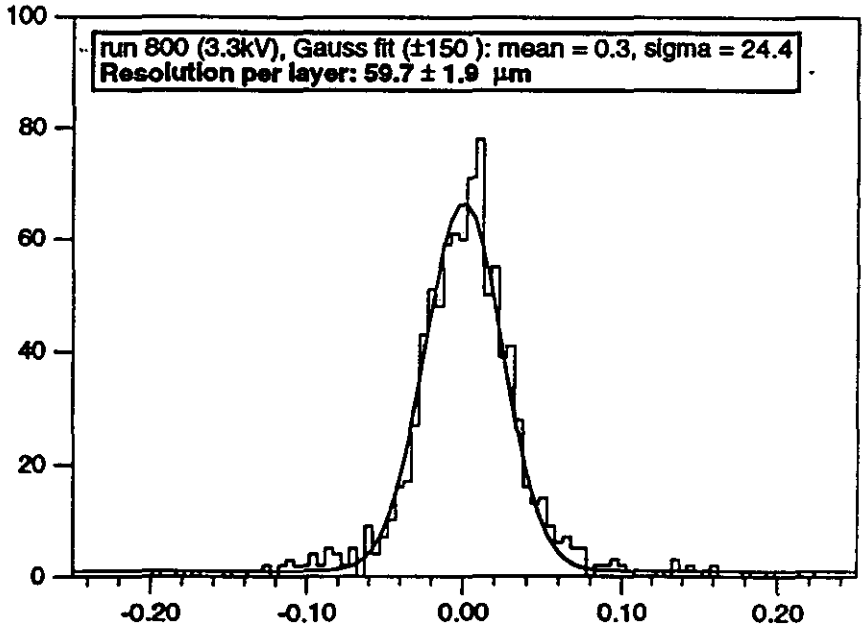
run 800 (3.3kV), Gauss fit (±150): mean = 0.3, sigma = 24.4
Resolution per layer: 59.7 ± 1.9 µm
100
80
60
40
20
0
-0.20
-0.10
0.00
0.10
0.20
mm

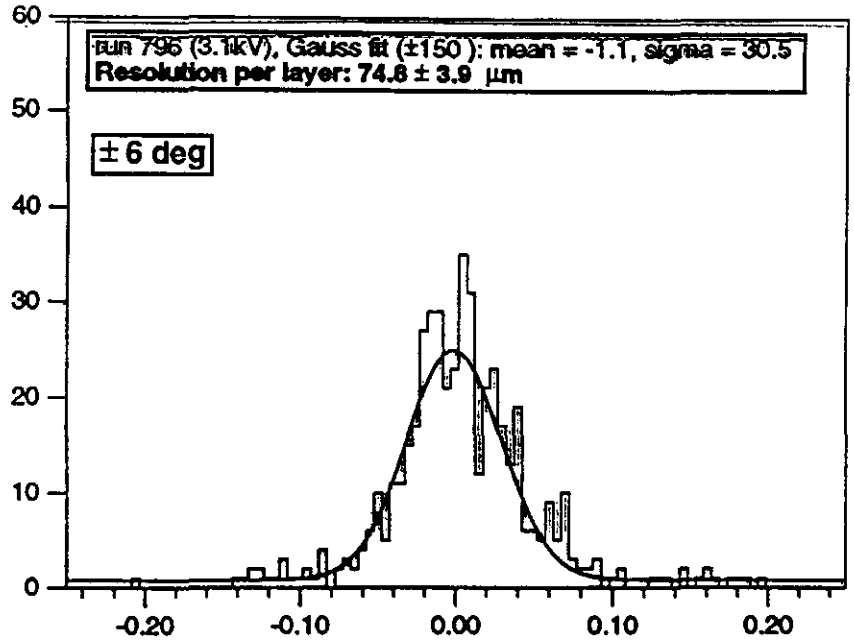
run 796 (3.1kV), Gauss fit (±150): mean = -1.1, sigma = 30.5
Resolution per layer: 74.8 ± 3.9 μm
± 6 deg
60
50
40
30
20
10
0
-0.20
-0.10
0.00
0.10
0.20

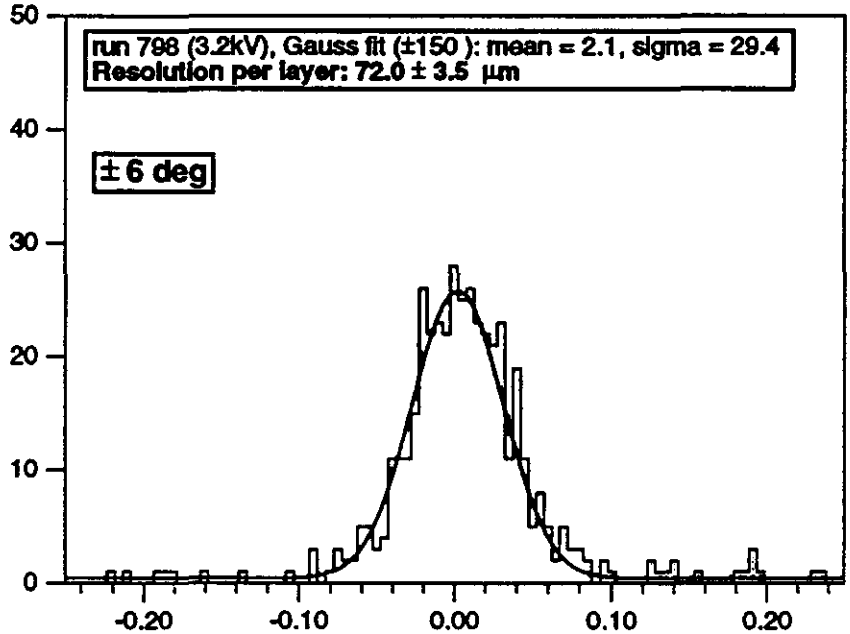
run 798 (3.2kV), Gauss fit (±150): mean = 2.1, sigma = 29.4
Resolution per layer: 72.0 ± 3.5 μm
± 6 deg
50
40
30
20
10
0
-0.20
-0.10
0.00
0.10
0.20

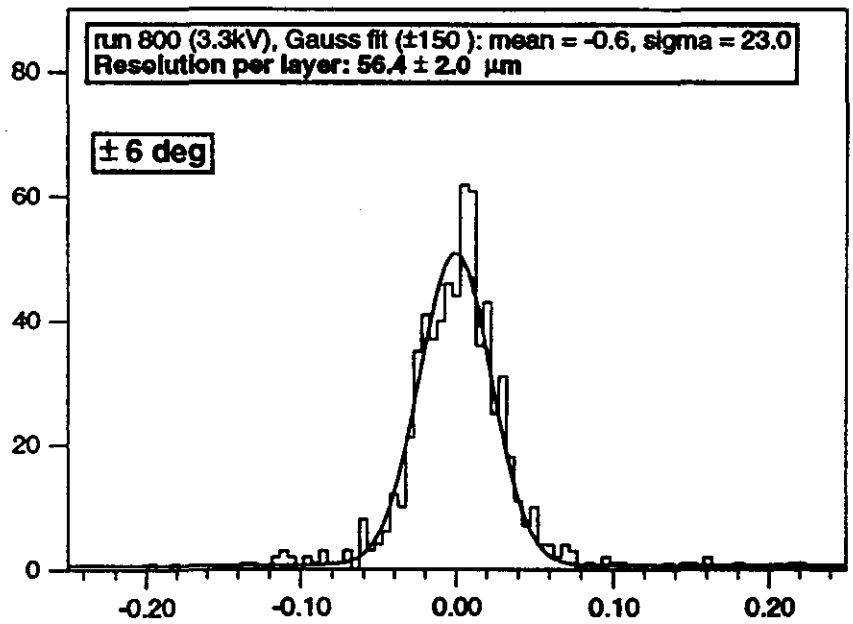
run 800 (3.3kV), Gauss fit (±150): mean = -0.6, sigma = 23.0
Resolution per layer: 56.4 ± 2.0 μm
± 6 deg
80
60
40
20
0
-0.20
-0.10
0.00
0.10
0.20
mm

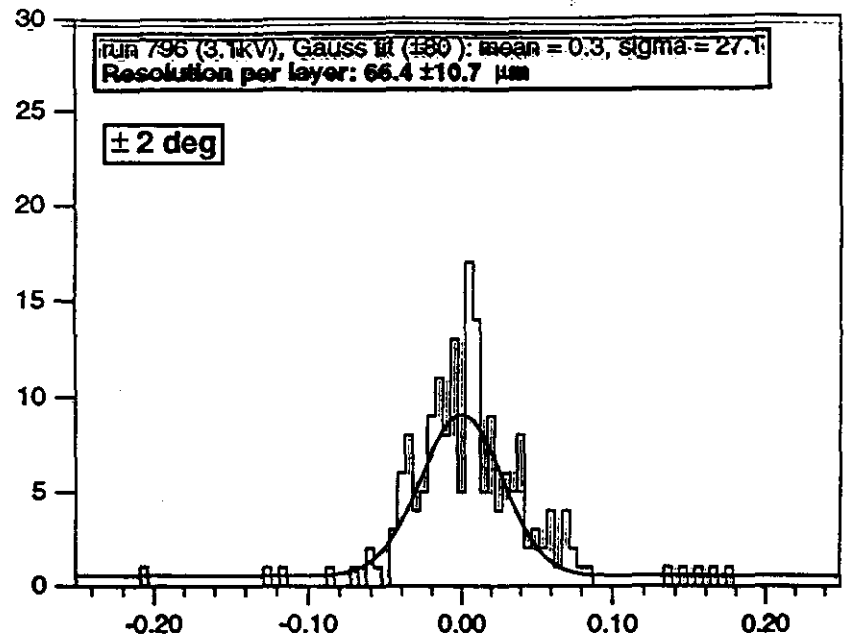
run 796 (3.1kV), Gauss fit (±80): mean = 0.3, sigma = 27.1
Resolution per layer: 66.4 ±10.7 μm
± 2 deg
30
25
20
15
10
5
0
-0.20
-0.10
0.00
0.10
0.20

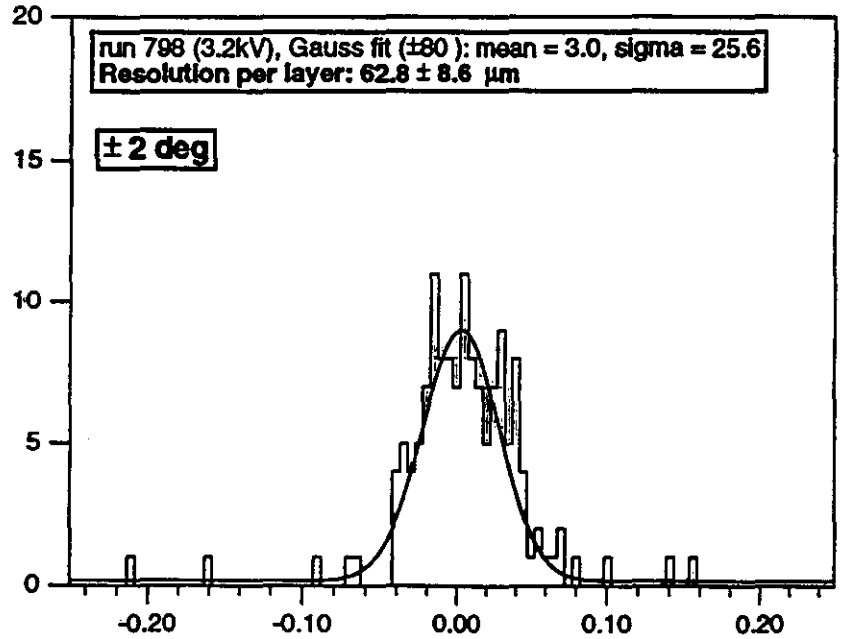
run 798 (3.2kV), Gauss fit (±80): mean = 3.0, sigma = 25.6
Resolution per layer: 62.8 ± 8.6 μm
± 2 deg
20
15
10
5
0
-0.20
-0.10
0.00
0.10
0.20

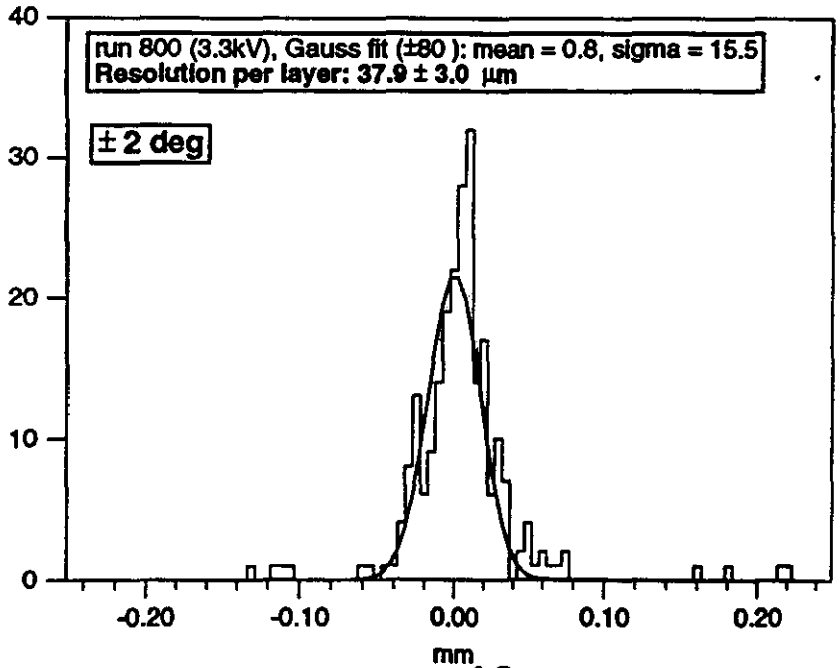
run 800 (3.3kV), Gauss fit (±80): mean = 0.8, sigma = 15.5
Resolution per layer: 37.9 ± 3.0 μm
± 2 deg
40
30
20
10
0
-0.20
-0.10
0.00
0.10
0.20
mm

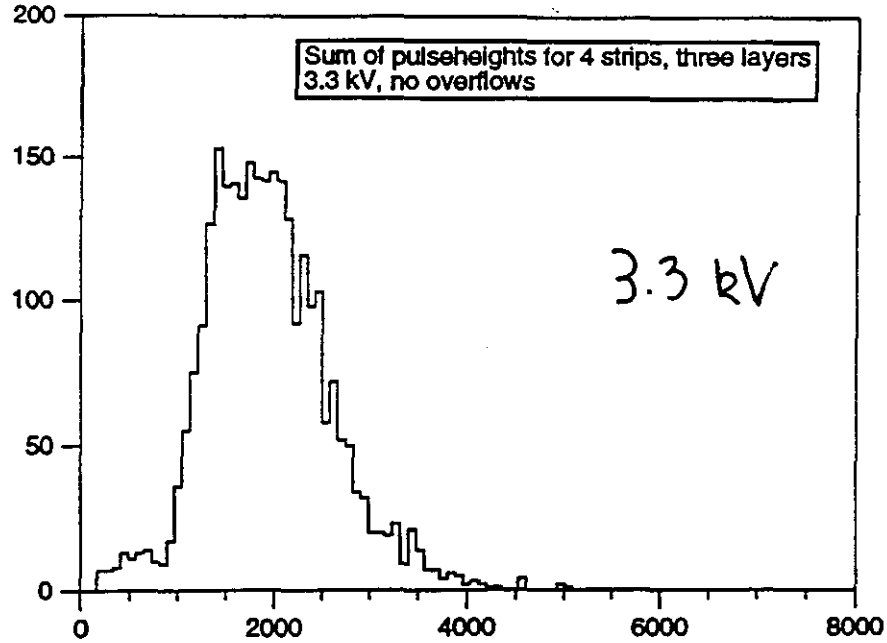
Sum of pulseheights for 4 strips, three layers
3.3 kV, no overflows
3.3 kV
200
150
100
50
0
0
2000
4000
6000
8000

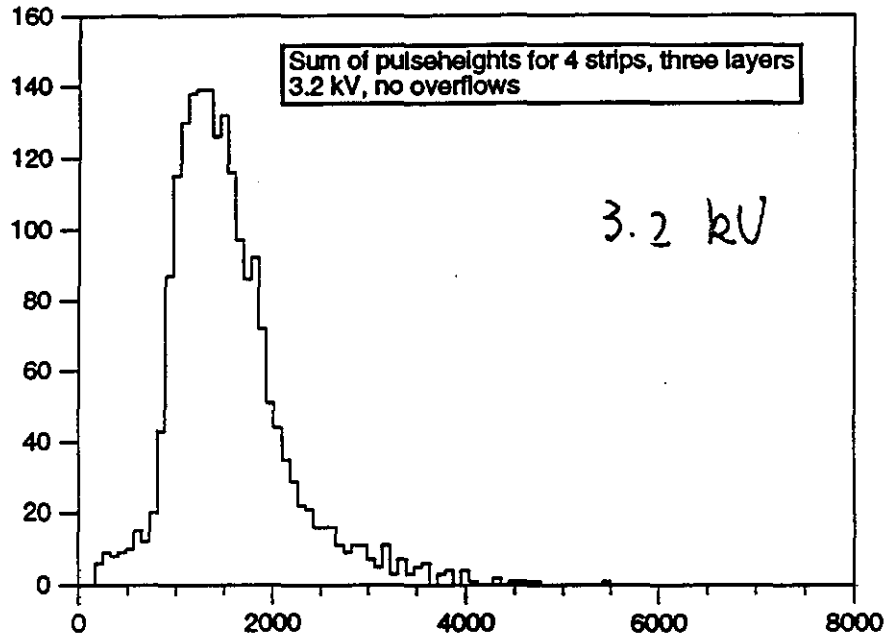
Sum of pulseheights for 4 strips, three layers
3.2 kV, no overflows
3.2 kV
160
140
120
100
80
60
40
20
0
0
2000
4000
6000
8000

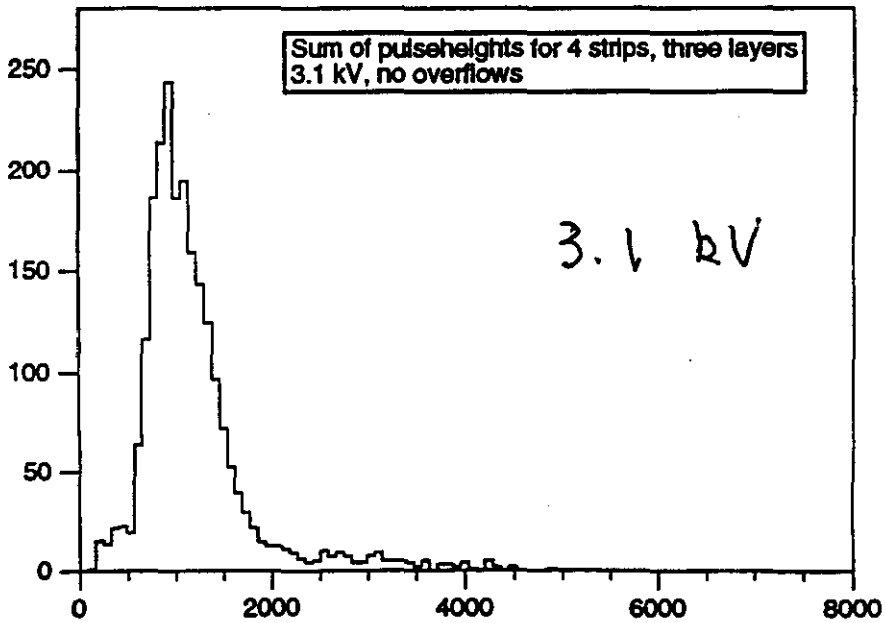
Sum of pulseheights for 4 strips, three layers
3.1 kV, no overflows
3.1 kV
250
200
150
100
50
0
0
2000
4000
6000
8000
cnt

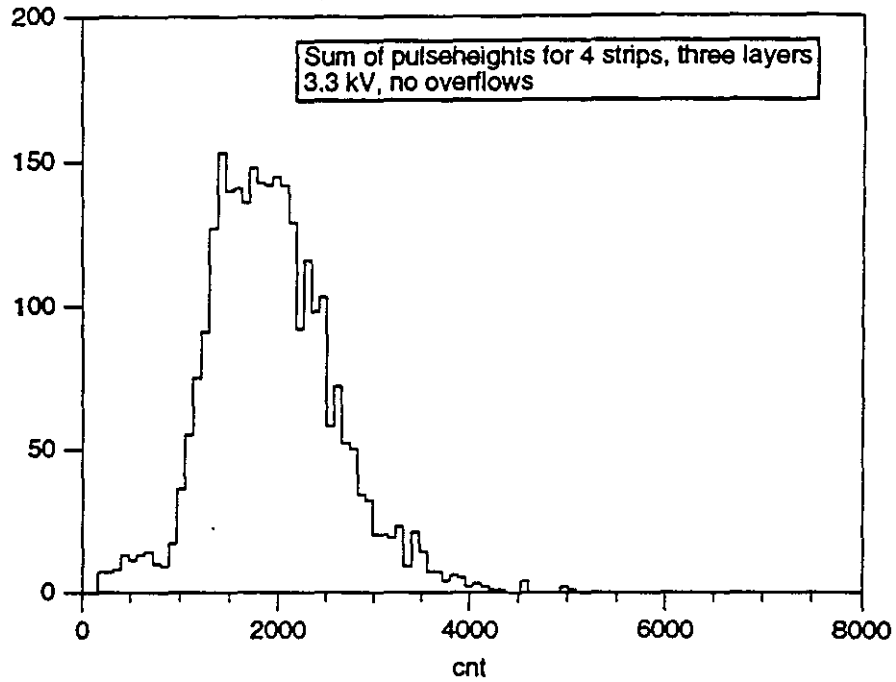
Sum of pulseheights for 4 strips, three layers
3.3 kV, no overflows
200
150
100
50
0
0
2000
4000
6000
8000
cnt

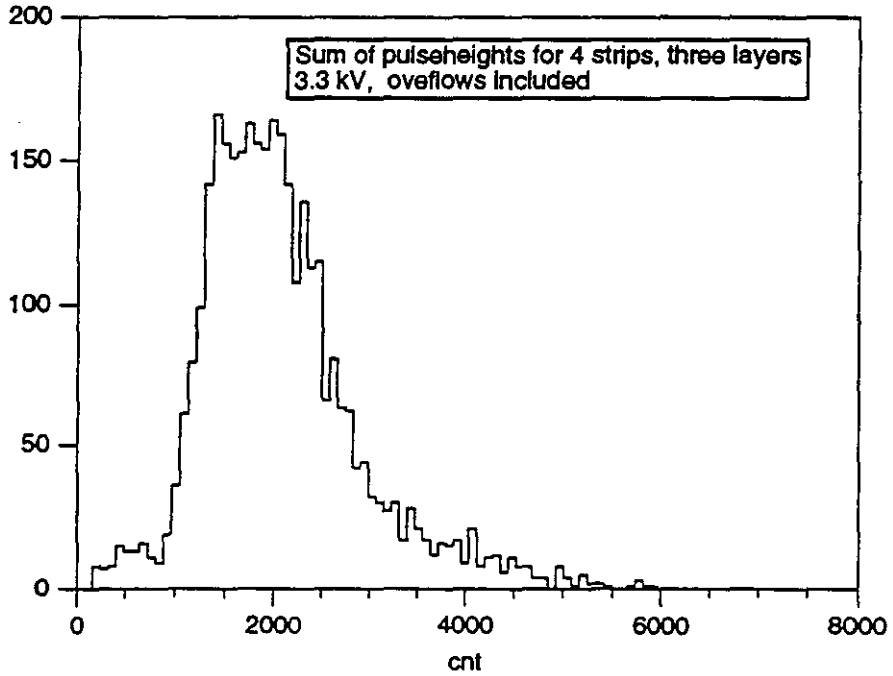
Sum of pulseheights for 4 strips, three layers
3.3 kV, oveflows included
200
150
100
50
0
0
2000
4000
6000
8000
cnt

Summary of Results (Preliminary)

- Averaged over $\pm \simeq 6°$

HV(kV)	$\sigma(\mu m)$
3.1	74.8 ± 3.9
3.2	72.0 ± 3.5
3.3	56.4 ± 2.0

- Averaged over all angles $\pm \simeq 8°$

HV(kV)	$\sigma(\mu m)$
3.1	78.9 ± 3.6 (96.3)
3.2	73.2 ± 3.0
3.3	59.7 ± 1.9

- Normal incidence $\pm$ 2.0°

HV(kV)	$\sigma(\mu m)$
3.1	66.4 ± 10.7
3.2	62.8 ± 8.6
3.3	37.9 ± 3.0

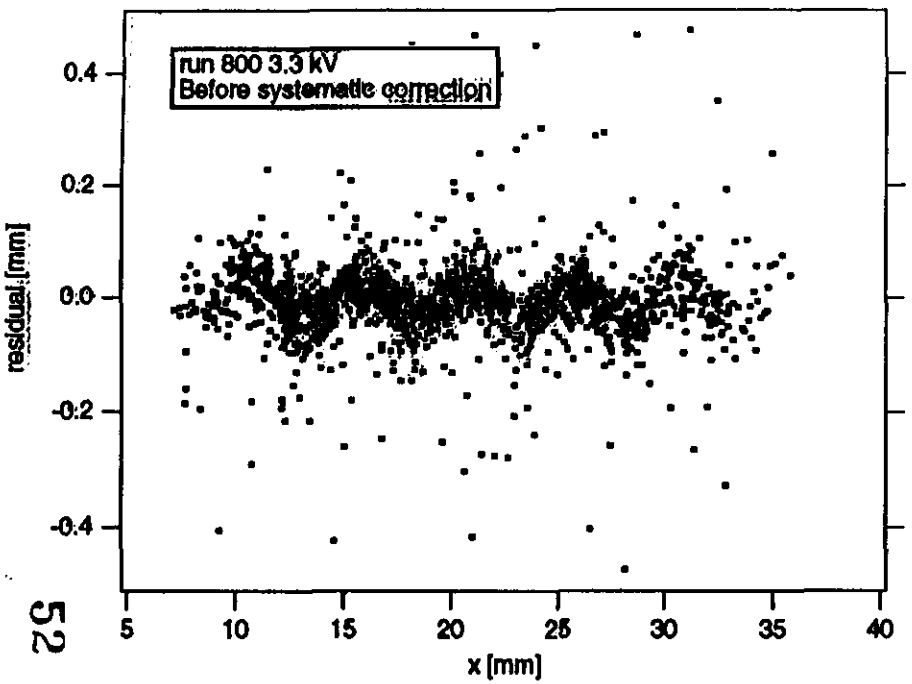
run 800 3.3 kV
Before systematic correction
residual [mm]
x [mm]

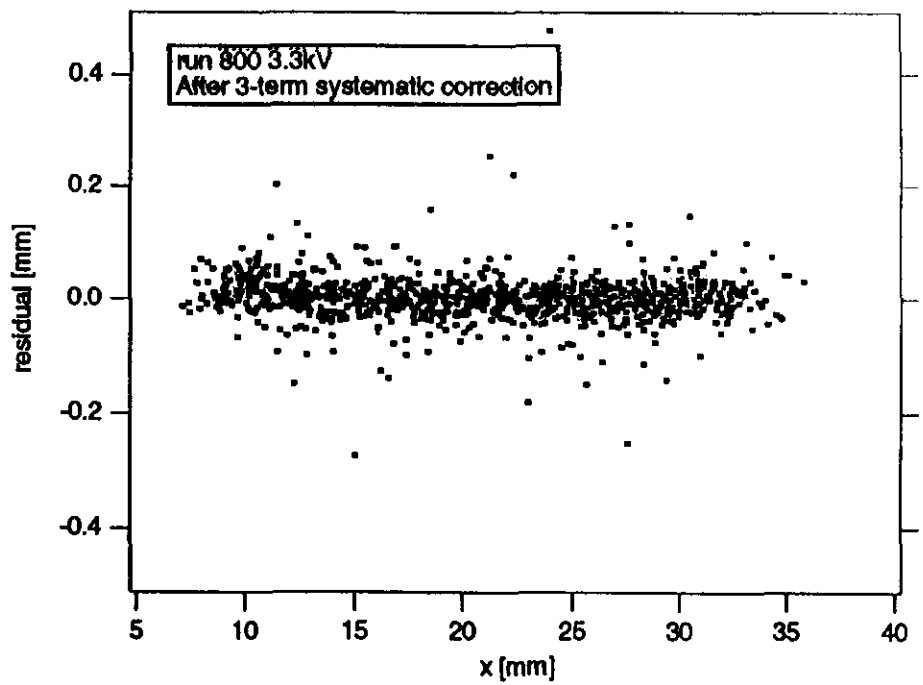
run 800 3.3kV
After 3-term systematic correction
residual [mm]
x [mm]

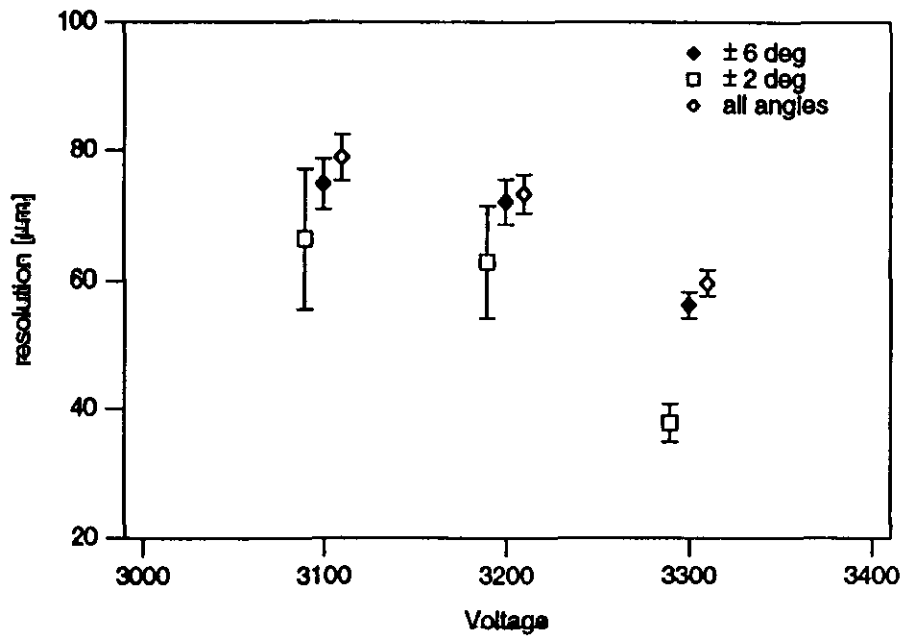
± 6 deg
± 2 deg
all angles
resolution [μm]
Voltage

Presentation by:

Yu. Kiryushin

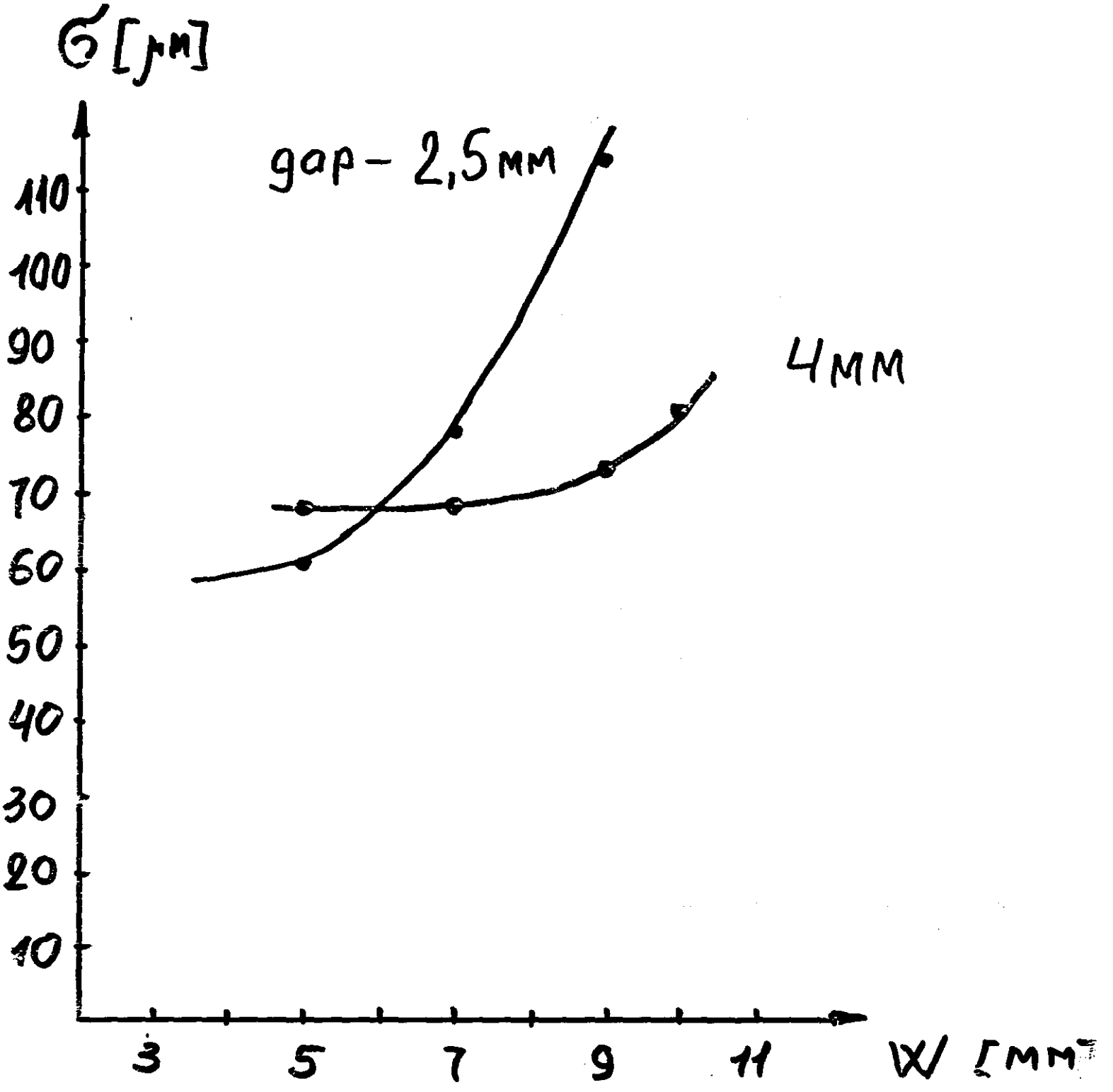
σ [μm]
gap – 2,5 мм
4 мм
110
100
90
80
70
60
50
40
30
20
10
3
5
7
9
11
W [мм]

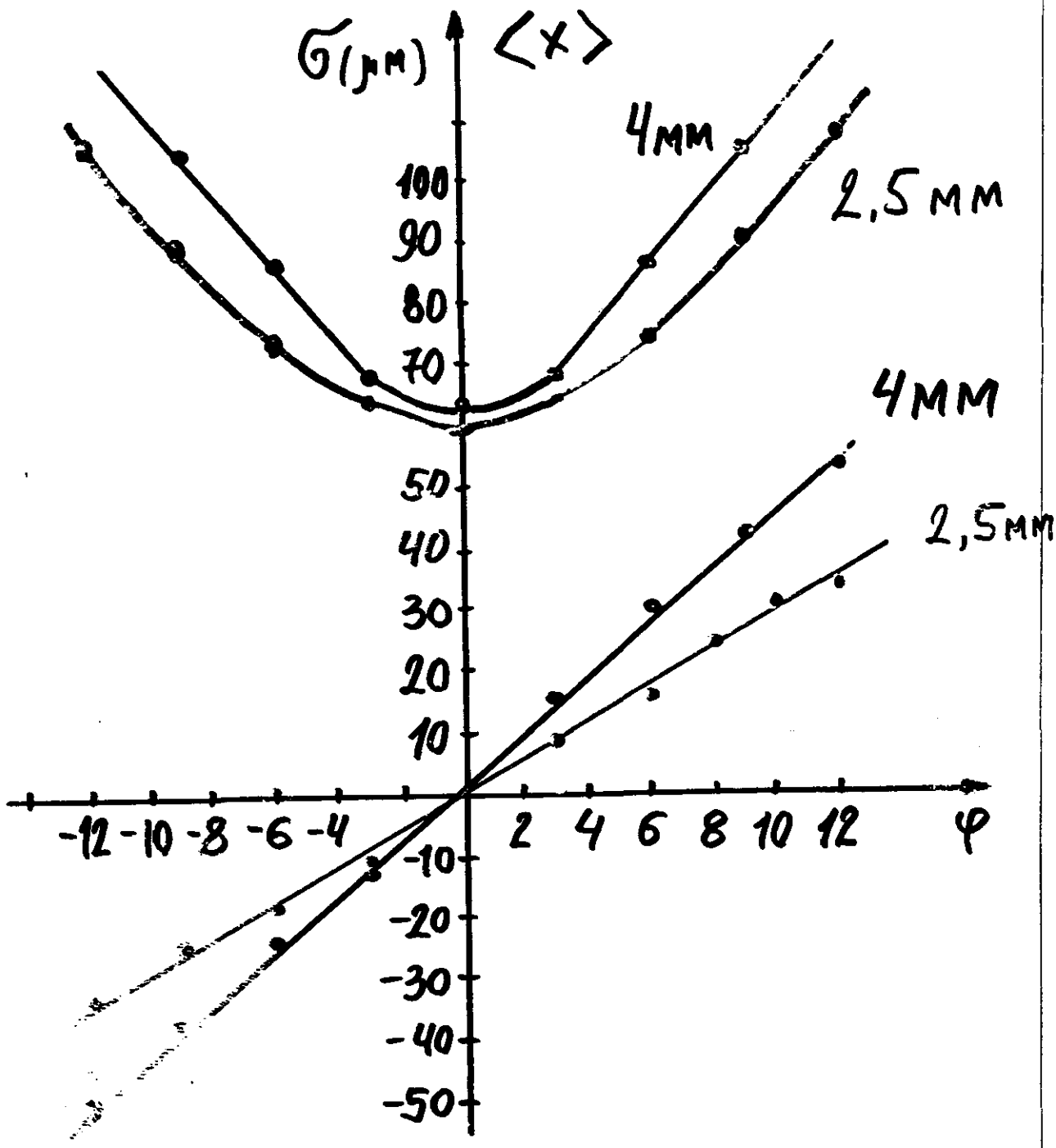
σ(μm)
⟨x⟩
4мм
2,5мм
4мм
2,5мм
100
90
80
70
50
40
30
20
10
-10
-20
-30
-40
-50
-12 -10 -8 -6 -4
2 4 6 8 10 12
φ

Inner layer

	8 gaps	6 gaps
Gap	3 mm	3 mm
Fine strip pitch	200 mils	216 mils
N chann. plane	128	112
chamber	1024	672
sup. layer	131 072	86016
Corse strip pitch	4000 mils	2519 mils
N chan. plane	30	48
chamber	236	384
sup. layer	30208	49152

MIDDLE LAYER

	4 gaps	6 gaps
Gap	3 MM	4 MM
Fine strip pitch	200 miles	327 miles
N chann. plane	256	144
chamber	1024	864
sup. layer	262144	221184
Corse strip pitch	4000 miles	2994 miles
N chann. plane	24	32
chamber	96	192
sup. layer	24576	49152

OUTER LAYER

	4 gaps CHAMBER	6-gaps chamber
Gap of the chamb.	3 mm	5 mm
Fine strip pitch	200 mils	410 mils
N channels plane	176	80
per cham.	704	480
superlayer	360448	245760
Corse strip pitch	4000 mils	2809 mils
N chann. plane	34	48
chamber	136	192
Sup. layer	69632	98304

What in total?

For 8 + 4 + 4

N precise = 753664

N corse = 124416

For 6 + 6 + 6

N precise = 552960

N corse = 196608

N chambers

For 8 + 4 + 4

1024 4 gap- chambers

For 6 + 6 + 6

1792 3 gap-chambers

gem

γeμ

Presentation by:

V. Polychronakos

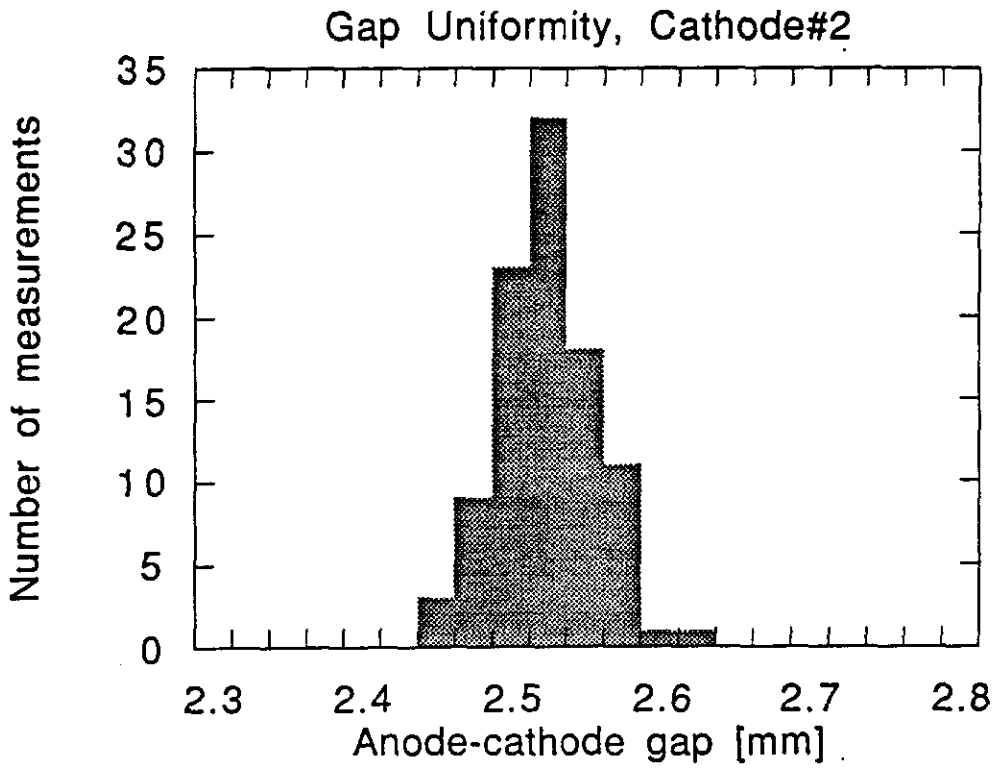
Gap Uniformity, Cathode#2
Number of measurements
35
30
25
20
15
10
5
0
2.3
2.4
2.5
2.6
2.7
2.8
Anode-cathode gap [mm]

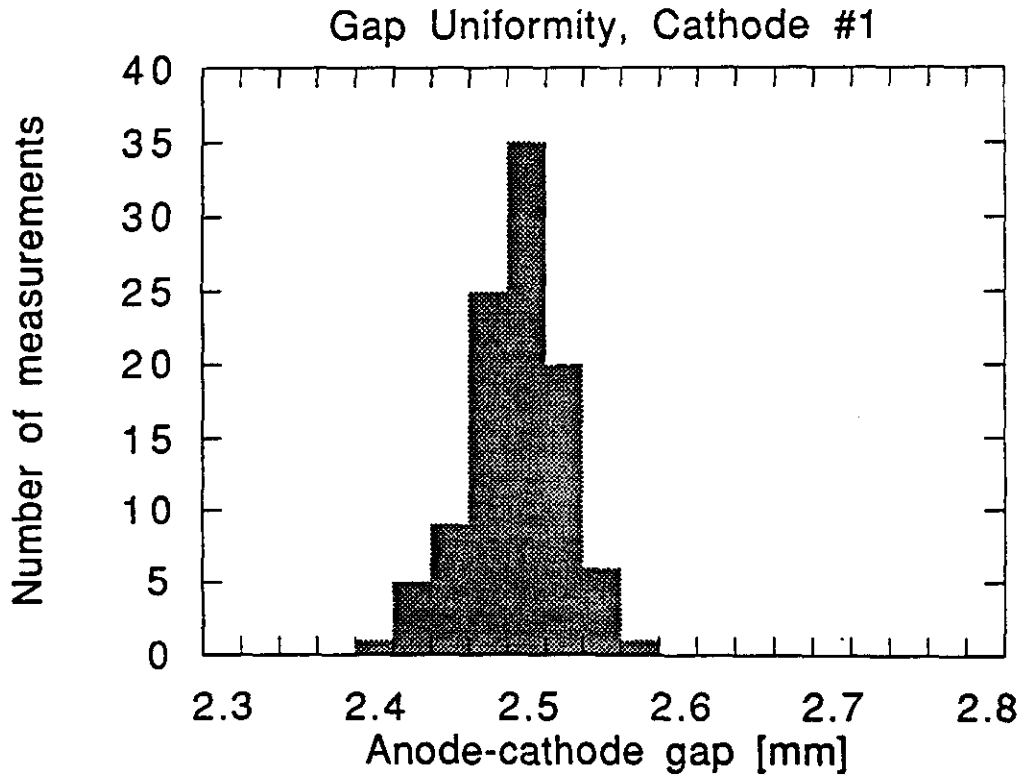
Gap Uniformity, Cathode #1
Number of measurements
40
35
30
25
20
15
10
5
0
2.3
2.4
2.5
2.6
2.7
2.8
Anode-cathode gap [mm]

Bo Yu
Graham Smith
ENL. Instr. Div.

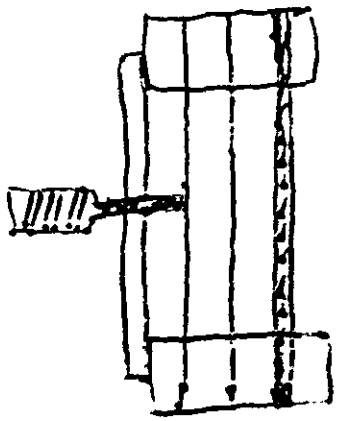

10 x 10 cm^2 test chamber
Same electrode geometry as
our current design.

Bo's small GEM detector

5.4keV X-rays, 50%CO_2/30%Ar/20%CF_4

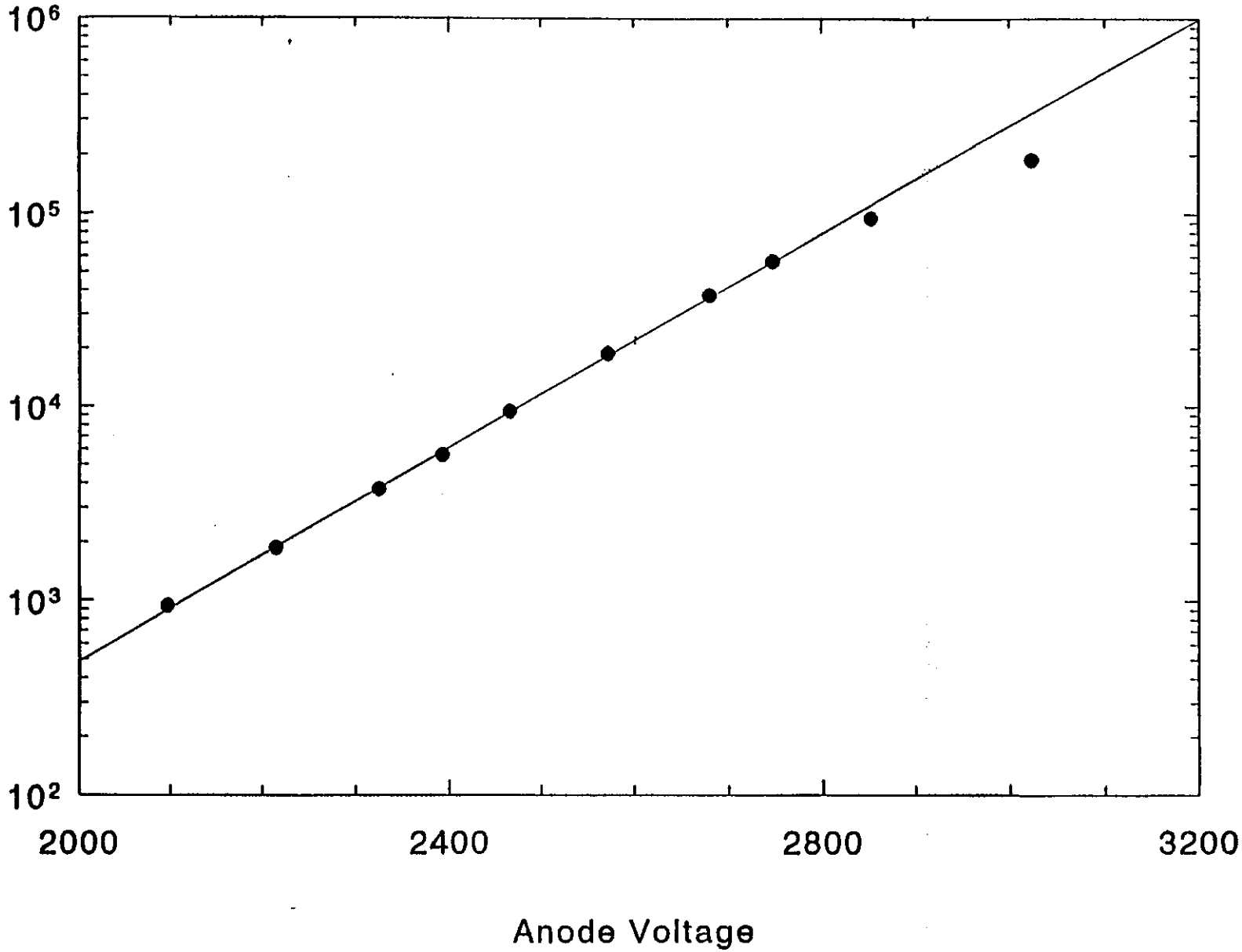

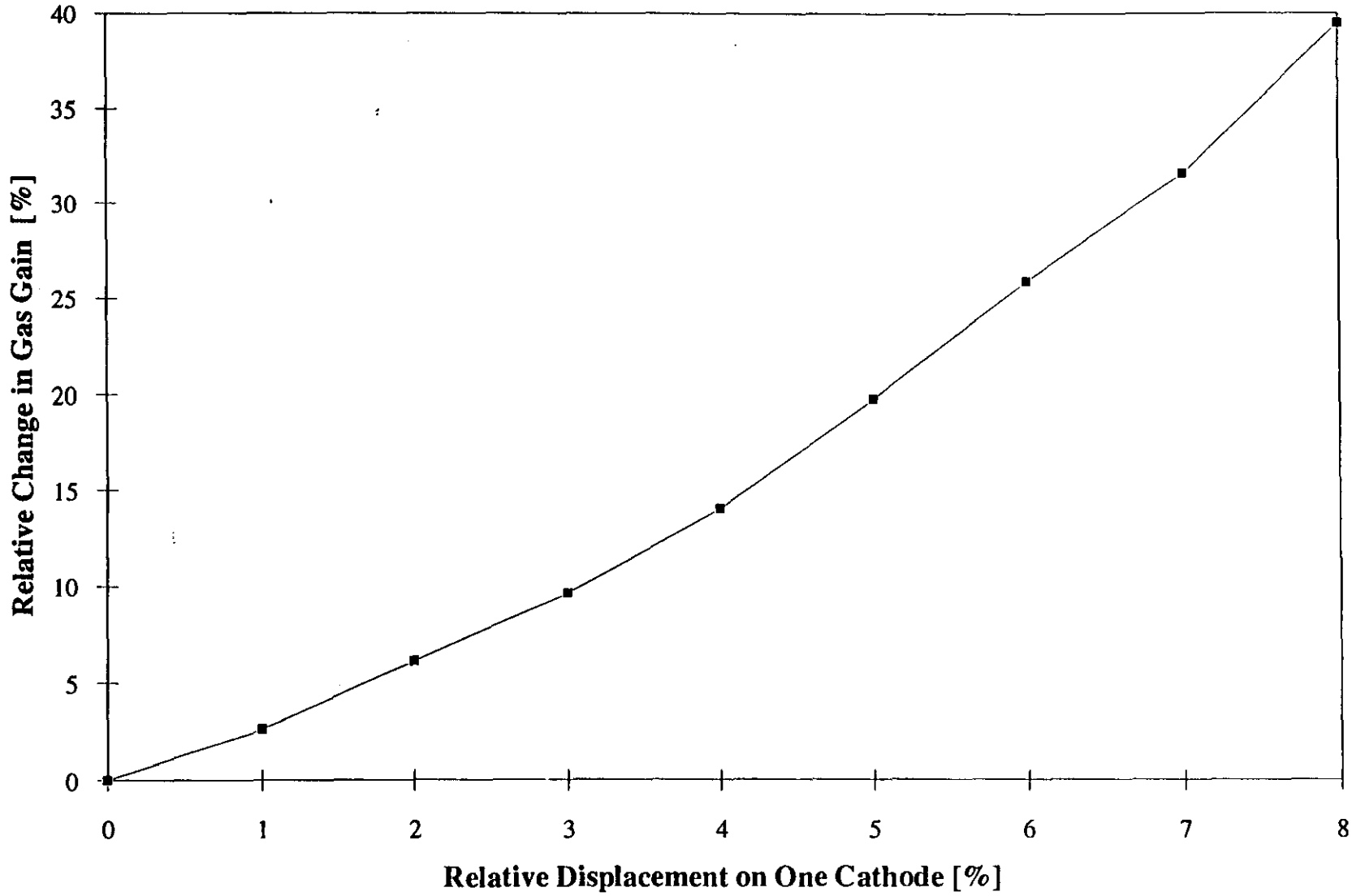
Relative Change in Gas Gain [%]
40
35
30
25
20
15
10
5
0
0
1
2
3
4
5
6
7
8
Relative Displacement on One Cathode [%]

Paul O'Connor, BNL

ICGA

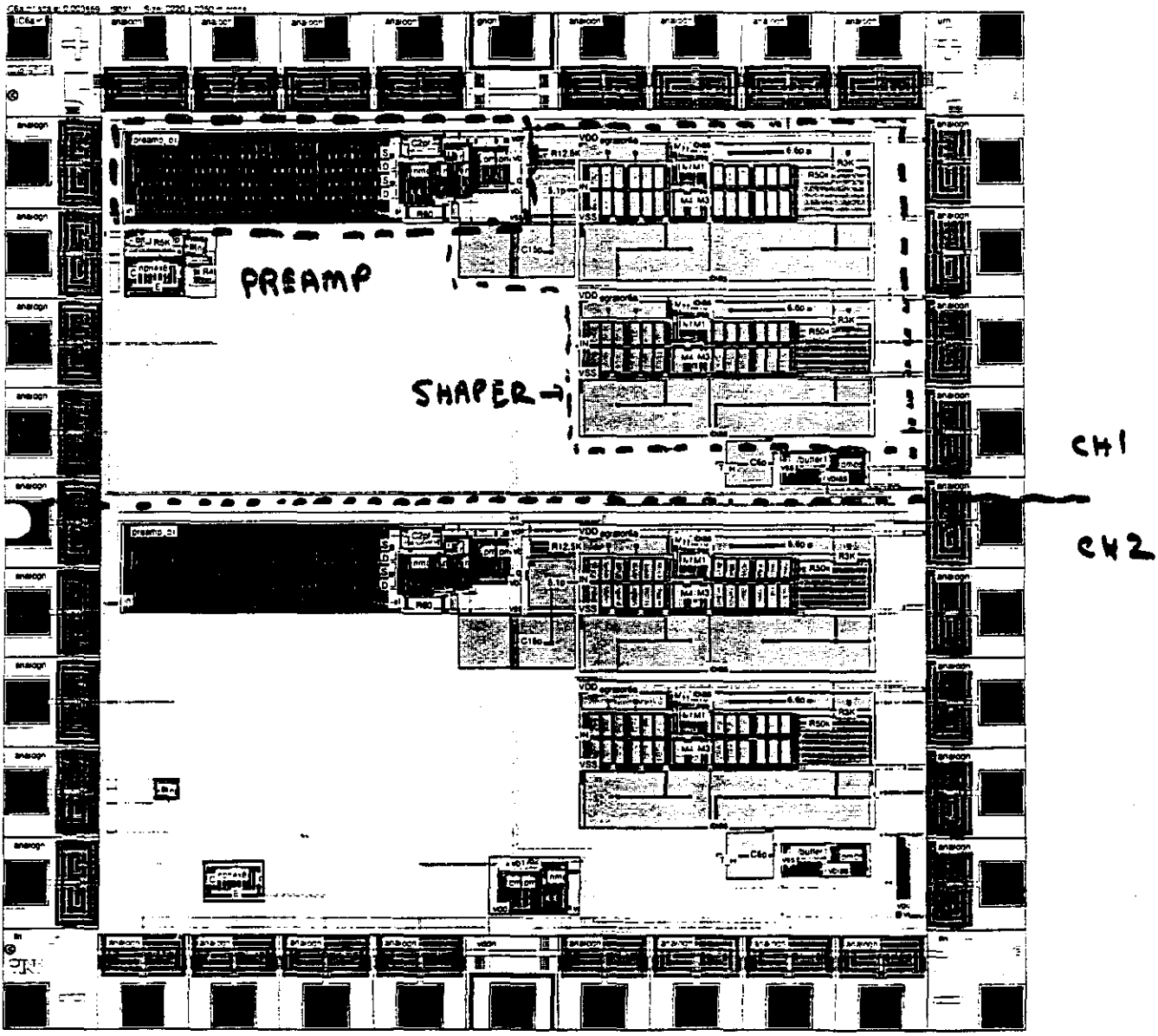

IC6A	Device #7		Qin:	5.00E-14					1/7/93
Cd	Vout	Vnoise	System	SNR	Gain	ENC	ENC	Slope	Intercept
0	1.839	6.18	0.65	299	36.78	1.67E-16	1043	6.85	1018.85
22	1.771	6.7	0.96	267	35.42	1.87E-16	1168		
47	1.697	7.13	0.64	239	33.94	2.09E-16	1306		
68	1.613	7.75	0.94	210	32.26	2.38E-16	1488		
100	1.485	8.13	0.74	183	29.70	2.73E-16	1701		
150	1.377	9.13	0.94	152	27.54	3.30E-16	2058		
pF	V p-p	mV rms	mV rms	-	mV/fC	C	e-	e-/pF	e-

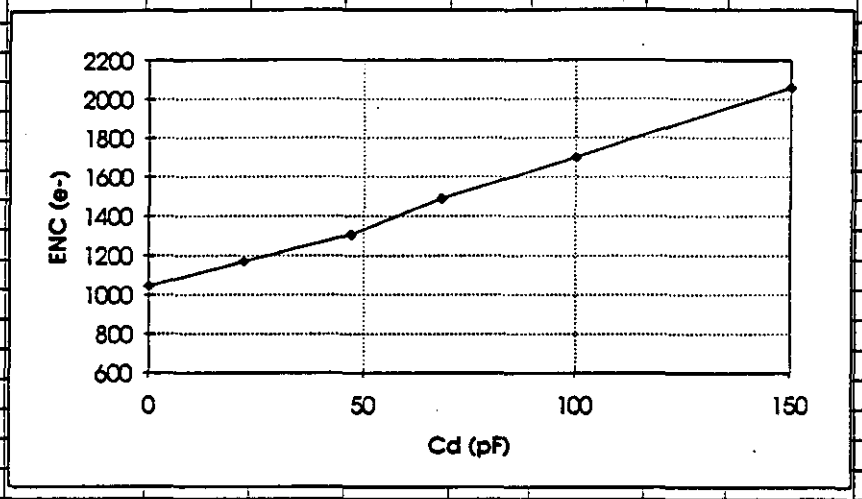

Linearity

Cd=100 pF Tp=750 nsec 1/7/93

Vin	Vout
0	0
25	734
50	1506
100	2946
140	3806
150	4020
160	4201
170	4351
180	4481
200	4700

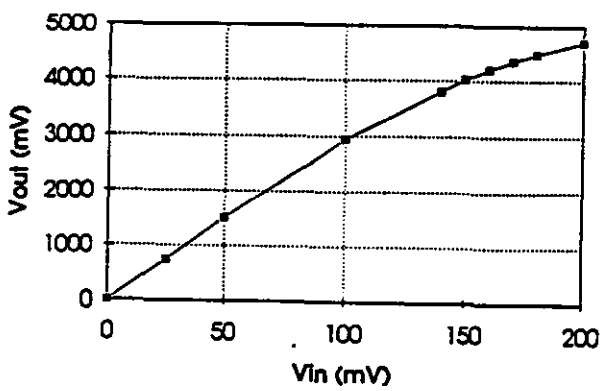

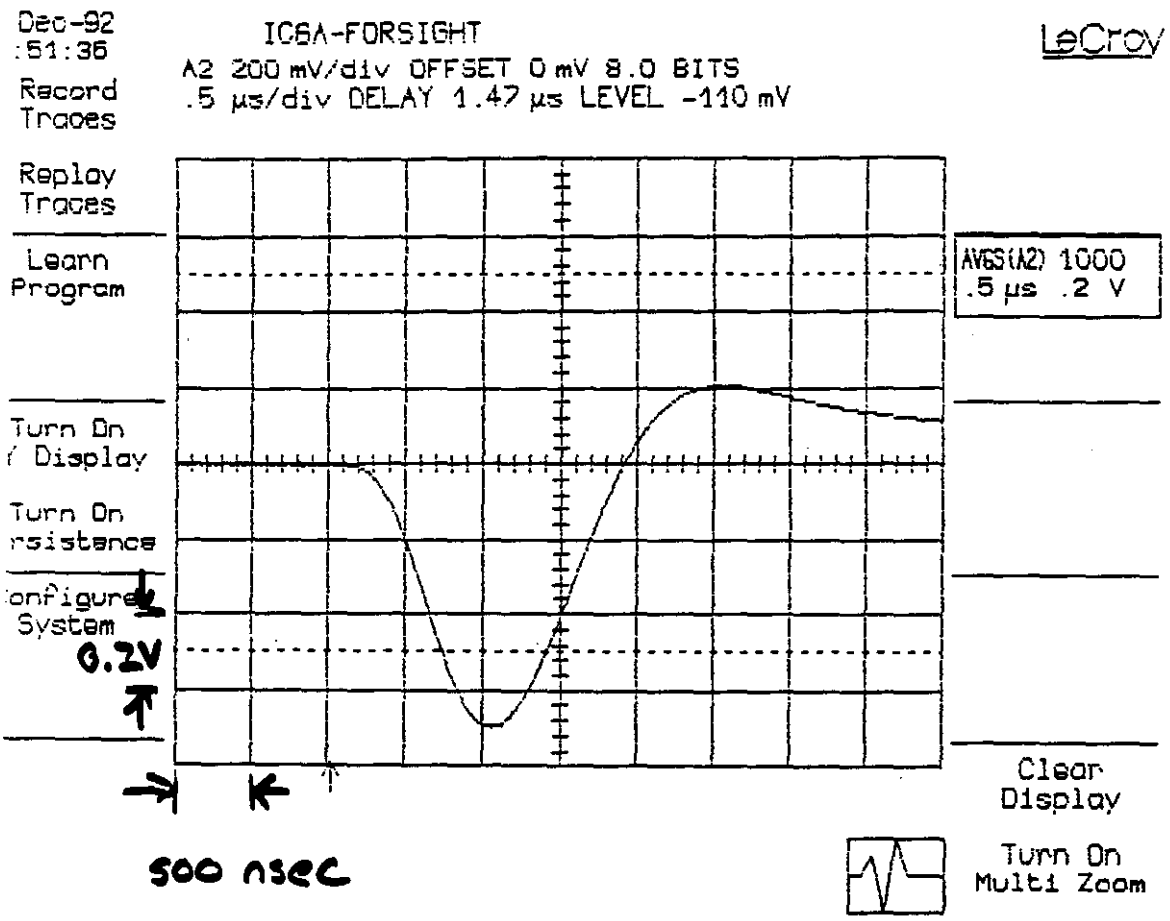
Dec-92
:51:36
ICSA-FORSIGHT
A2 200 mV/div OFFSET 0 mV 8.0 BITS
.5 µs/div DELAY 1.47 µs LEVEL -110 mV
LeCroy
Record Traces
Replay Traces
Learn Program
AVGS(A2) 1000
.5 µs .2 V
Turn On / Display
Turn On rsistance
onfigure System
0.2V
Clear Display
500 nsec
Turn On Multi Zoom

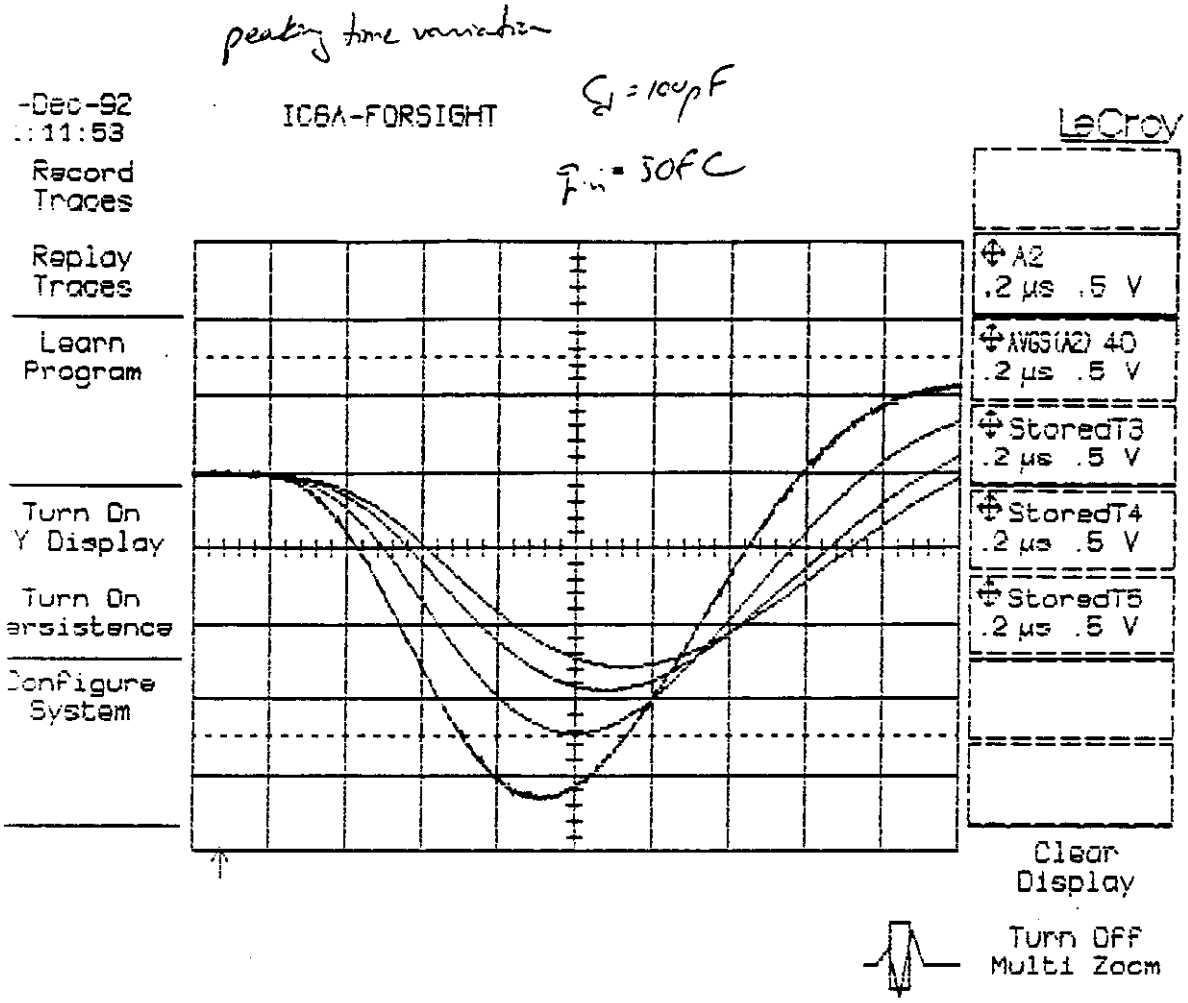
peaking time variation
-Dec-92
:11:53
ICGA-FORSIGHT
C_d = 100pF
q_{in} = 50fC
LeCroy
Record Traces
Replay Traces
Learn Program
Turn On Y Display
Turn On ersistence
Configure System
A2
.2 µs .5 V
AVGS(A2) 40
.2 µs .5 V
StoredT3
.2 µs .5 V
StoredT4
.2 µs .5 V
StoredT5
.2 µs .5 V
Clear Display
Turn Off Multi Zoom

gem

γeμ

Contributions by:

S. Boyarinov
V. Gavrilov

Presentation by:

P. Murat

PATTERN RECOGNITION IN GEM CSC BARREL VS NEUTRONS AND DEBRIS

S. BOYARINOV,
V. GAVRILOV

ITEP,
MOSCOW

01/08/93, SSCL

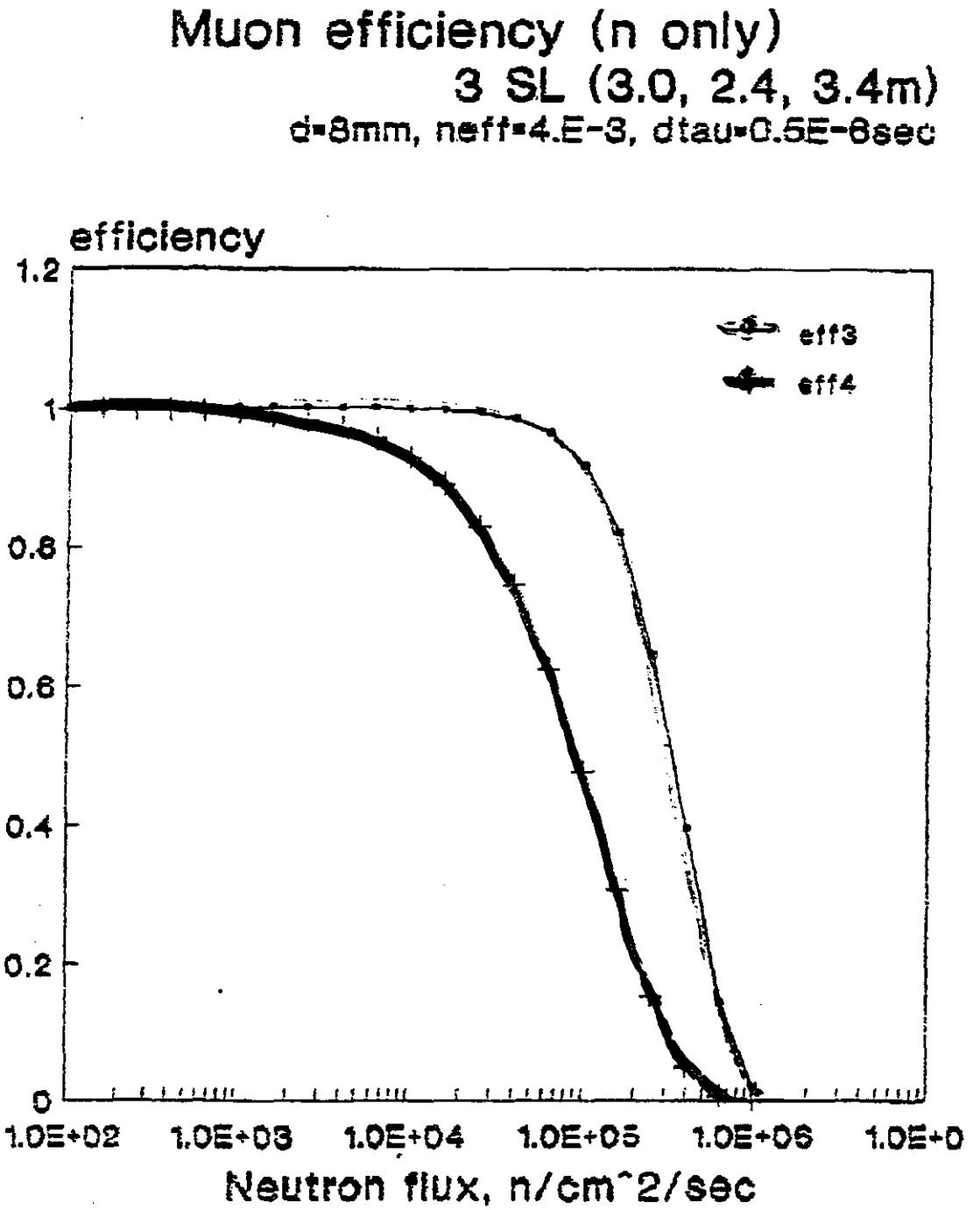
Muon efficiency (n only)
3 SL (3.0, 2.4, 3.4m)
d=8mm, neff=4.E-3, dtau=0.5E-8sec
efficiency
1.2
1
0.8
0.6
0.4
0.2
0
eff3
eff4
1.0E+02
1.0E+03
1.0E+04
1.0E+05
1.0E+06
1.0E+0
Neutron flux, n/cm^2/sec

Muon efficiency (n & electr)

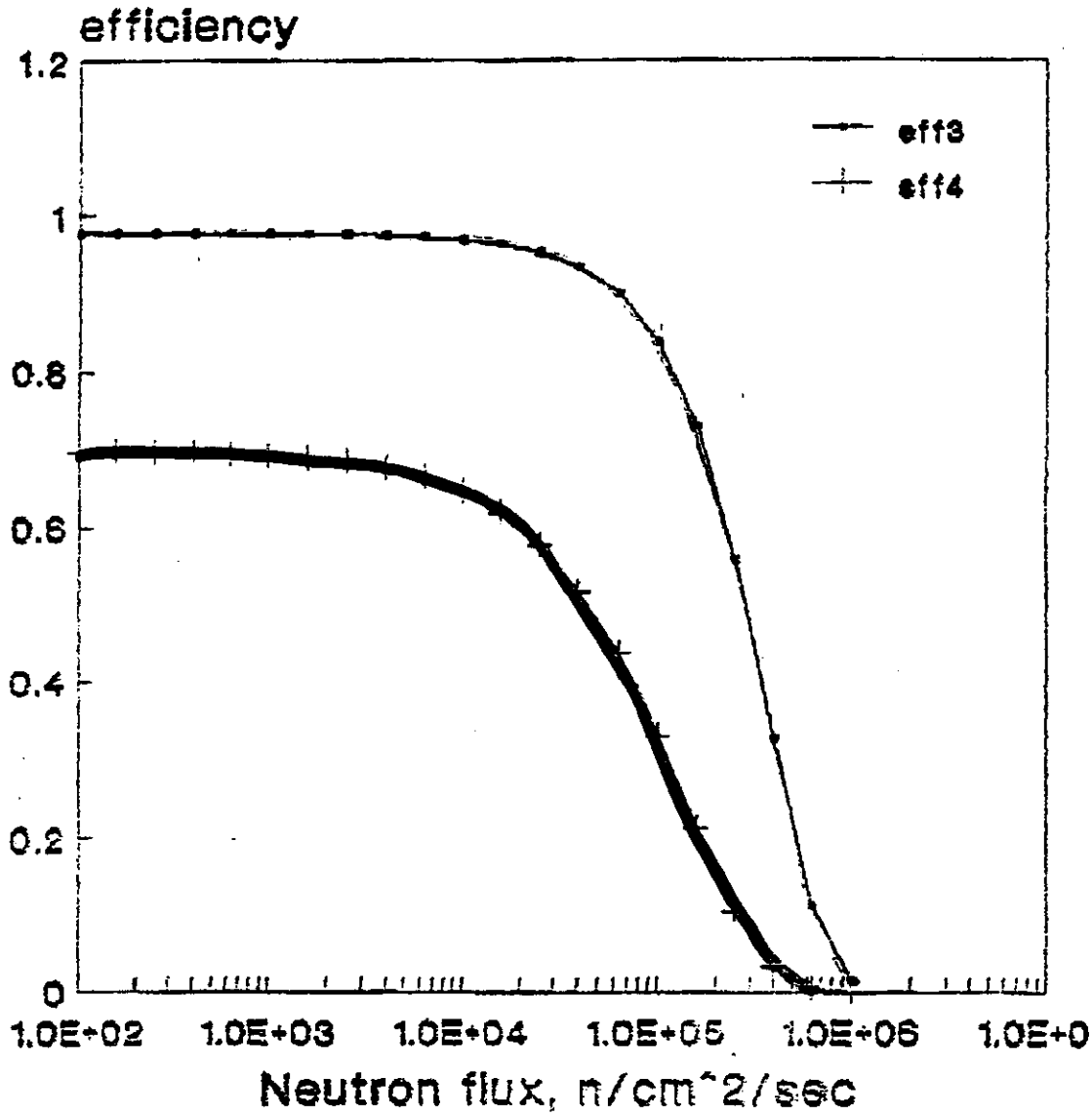

$d_{1,2} = 8$ мм
$d_3 = 10$ мм

Muon efficiency (n only)
3 SL (8/3.0, 4/2.4, 4/3.4m)
neff=4.E-3, dtau=0.5E-6sec

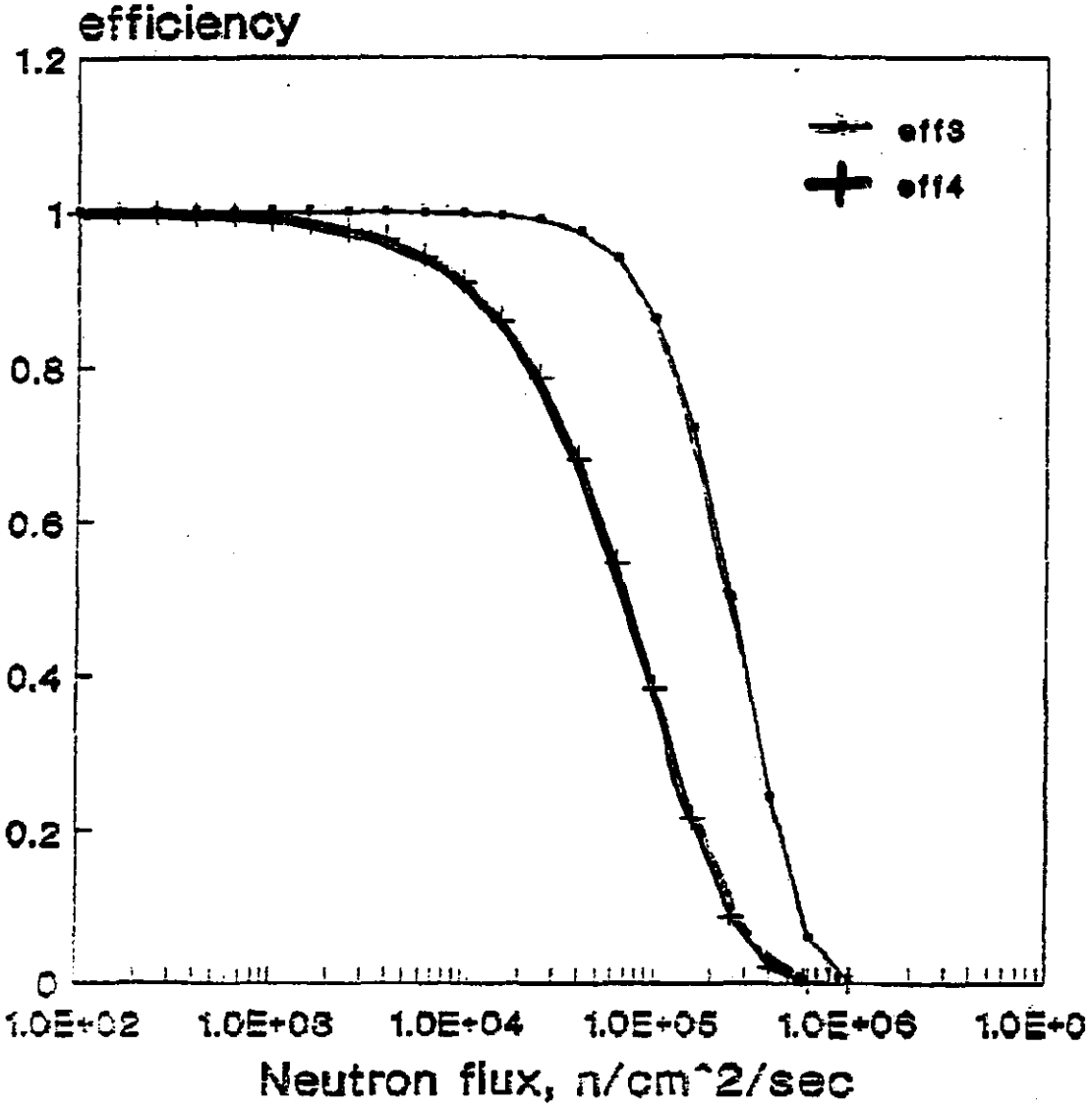

d1=d2=8mm, d3=12mm

$d_{1,2} = 8$ мм
$d_3 = 10$ мм

Muon efficiency (n & electr)
3 SL (8/3.0, 4/2.4, 4/3.4m)
neff=4.E-3, dtau=0.5E-6sec

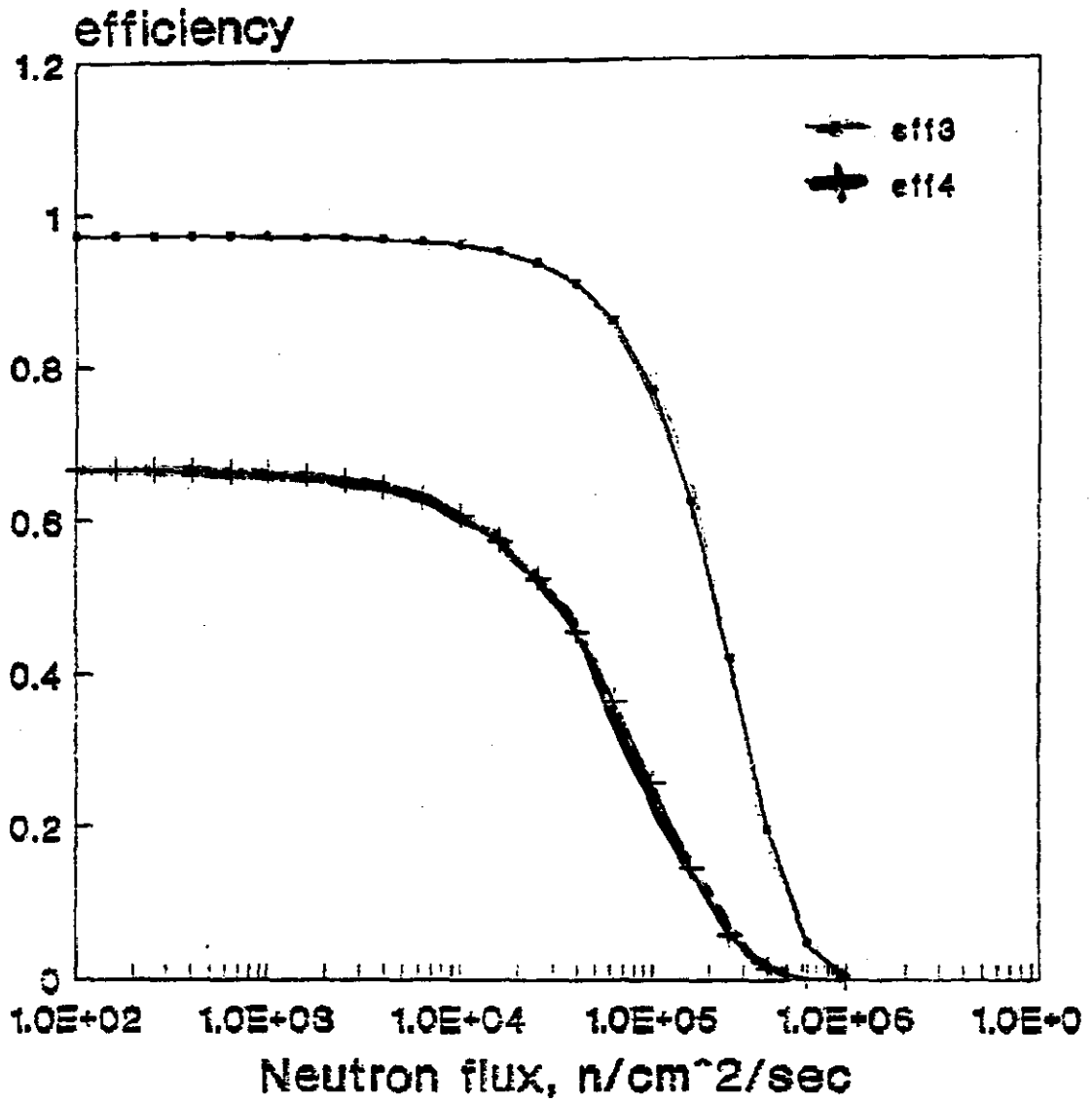

d1=d2=8mm, d3=12mm

SL_2 : 5 layers

$d_{1,2} = 8$ m
$d_3 = 12$ m

Muon efficiency (n & electr)
3 SL (8/3.0, 5/2.4, 4/3.4m)
neff=4.E-3, dtau=0.5E-6sec

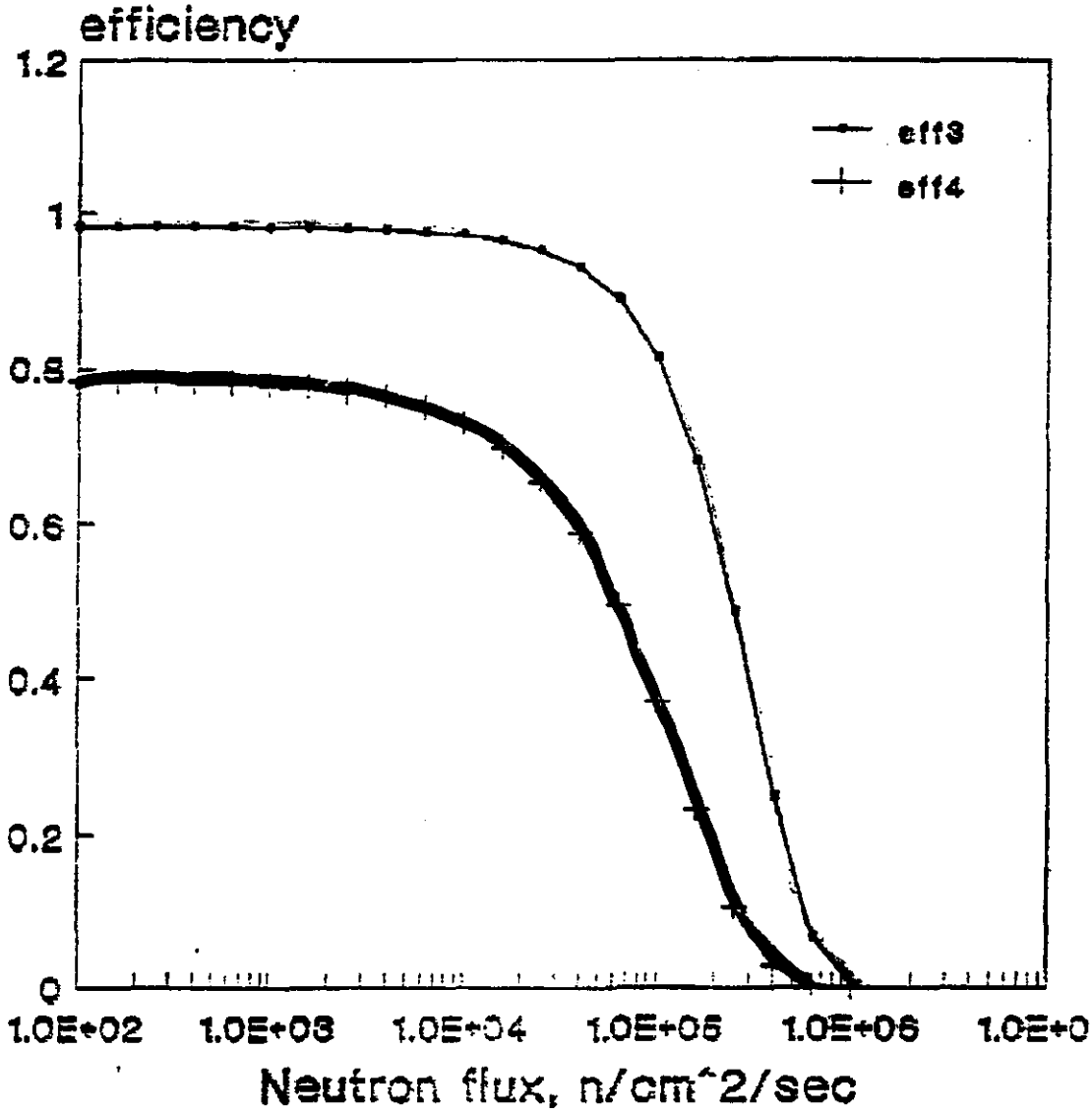

d1=d2=8mm, d3=12mm

Conclusions

* NEUTRON BACKGROUND IS NOT DANGEROUS up to $\sim 10^5 \frac{1}{cm^2 sec}$

* According to these calculations there is no significant difference between $\frac{8}{5} \oplus \frac{4}{5} \oplus \frac{4}{5}$ and $\frac{8}{5} \oplus \frac{4}{5} \oplus \frac{4}{10}$ configurations

* $\frac{8}{5} \oplus \frac{5}{5} \oplus \frac{4}{10}$ configuration is better than $\frac{8}{5} \oplus \frac{4}{5} \oplus \frac{4}{5}$ AND THE TOTAL NUMBER OF CHANNELS IS SMALLER

gem

γeμ

Presentation by:

C. Yanagisawa

1/8/93
Chiaki Yanagisawa
Stony Brook.
at SSCL.

Momentum reconstruction and Effect of double-hit.

- 1 TeV/c μ in Barrel.
- Uniform field 0.8 T
- 8-4-4

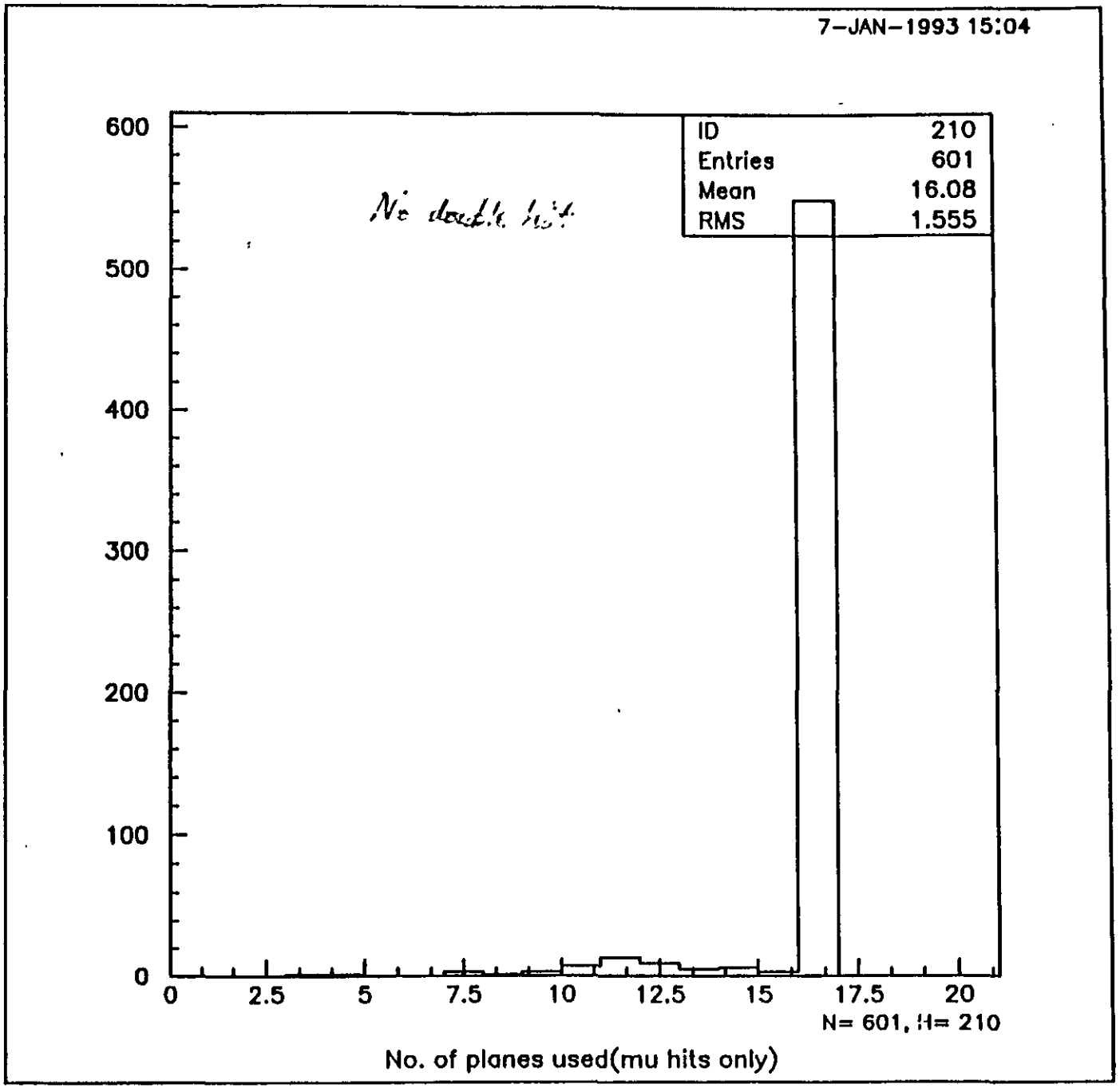
7-JAN-1993 15:04
ID 210
Entries 601
Mean 16.08
RMS 1.555
No double hit
600
500
400
300
200
100
0
0
2.5
5
7.5
10
12.5
15
17.5
20
N= 601, H= 210
No. of planes used(mu hits only)

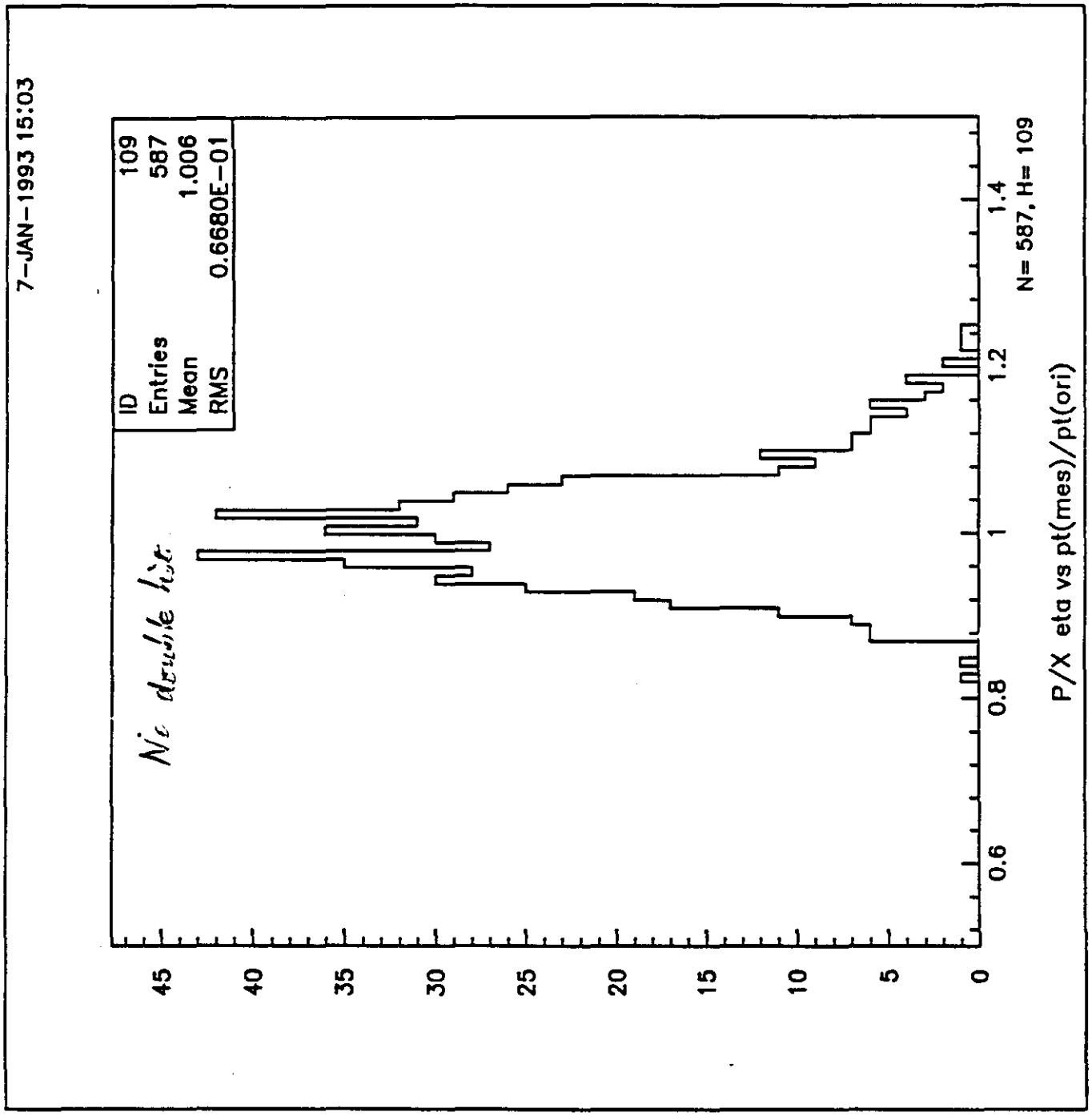
7-JAN-1993 15:03
ID 109
Entries 587
Mean 1.006
RMS 0.6680E-01
N= 587, H= 109
P/X eta vs pt(mes)/pt(ori)
0.6
0.8
1
1.2
1.4
0
5
10
15
20
25
30
35
40
45

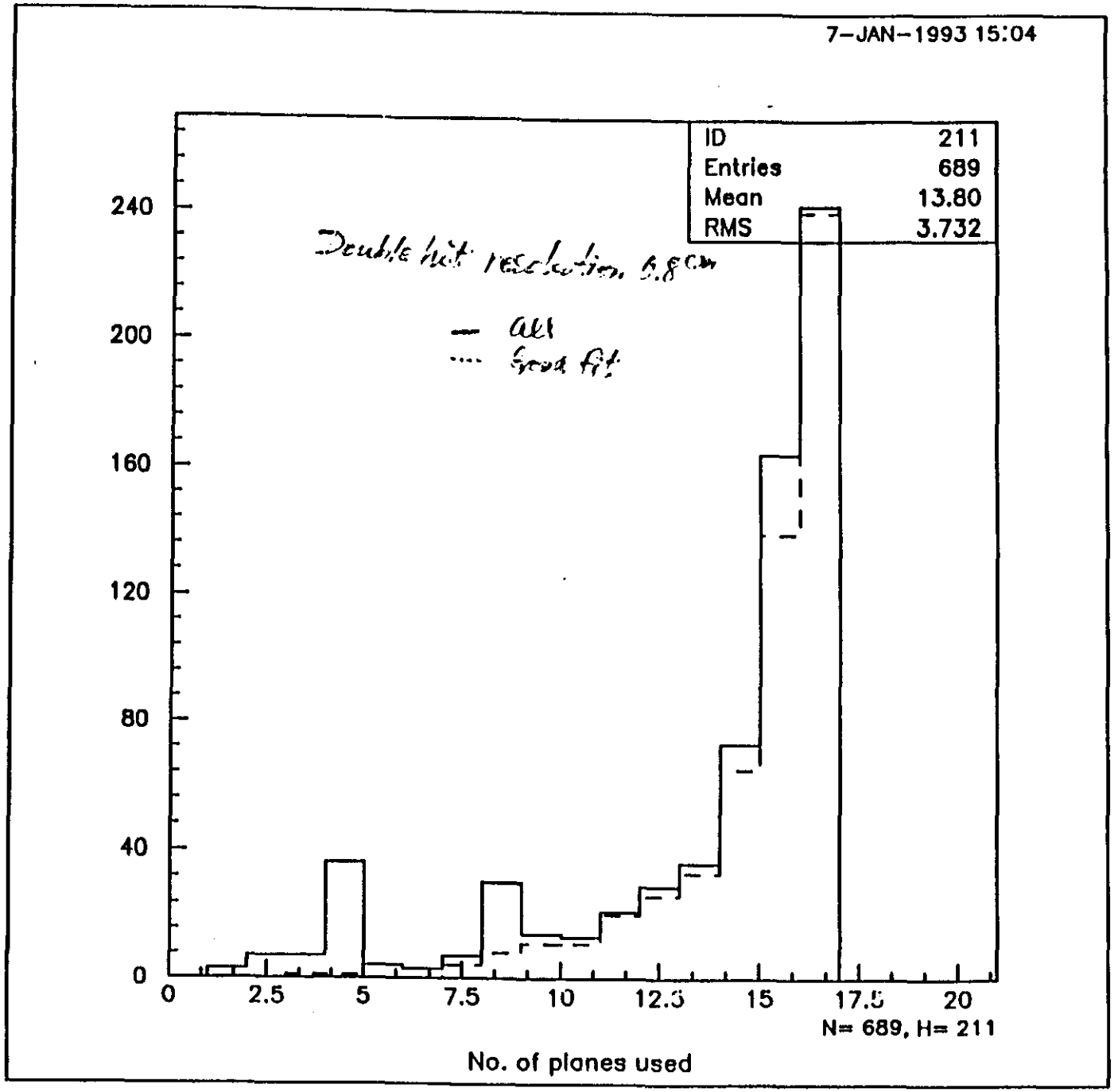
7-JAN-1993 15:04
ID 211
Entries 689
Mean 13.80
RMS 3.732
Double hit resolution 6.8 cm
all
Good fit
240
200
160
120
80
40
0
0
2.5
5
7.5
10
12.5
15
17.5
20
N= 689, H= 211
No. of planes used

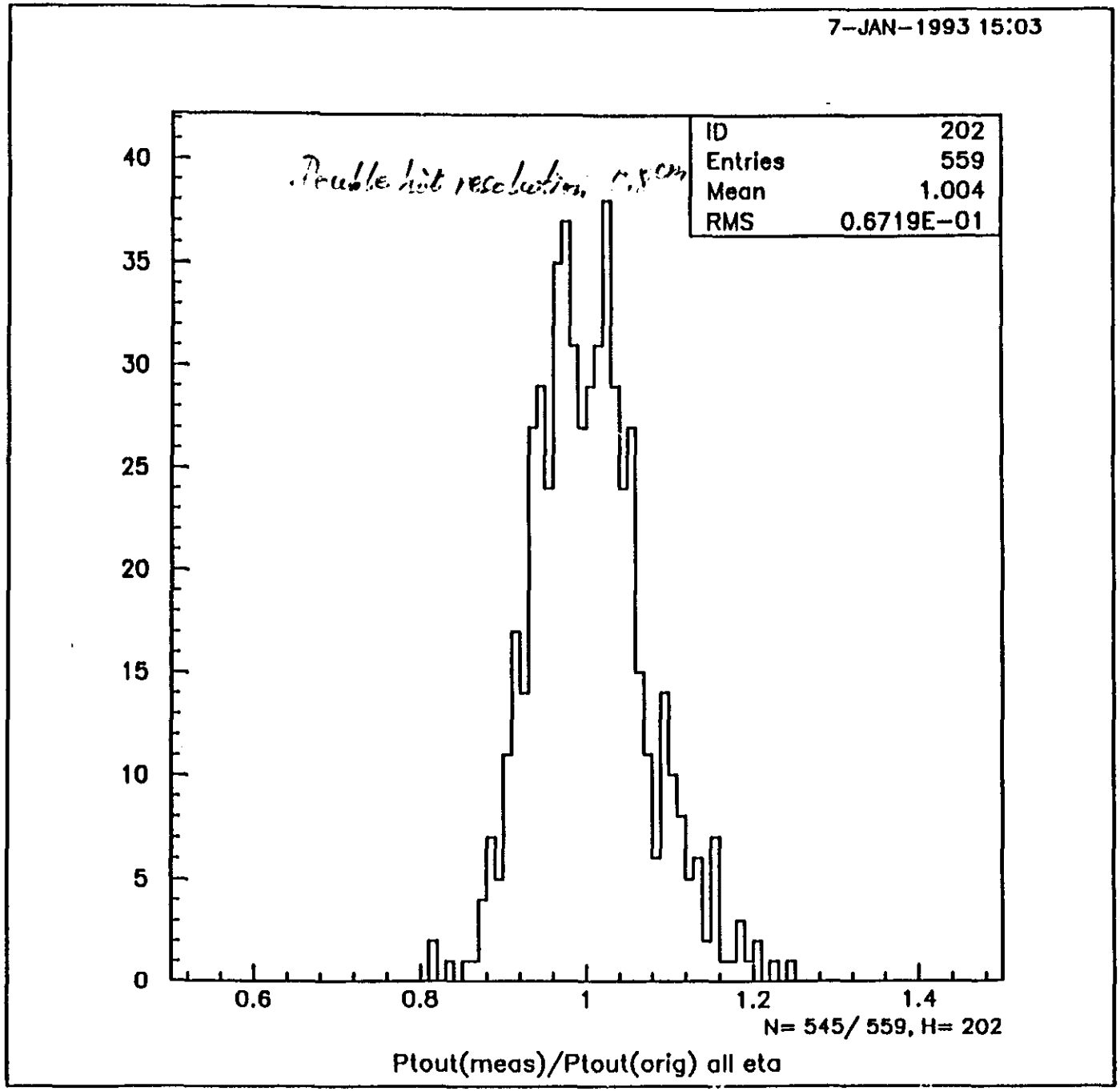
7-JAN-1993 15:03
Double hit resolution 0.8cm
ID 202
Entries 559
Mean 1.004
RMS 0.6719E-01
40
35
30
25
20
15
10
5
0
0.6
0.8
1
1.2
1.4
N= 545/ 559, H= 202
Ptout(meas)/Ptout(orig) all eta

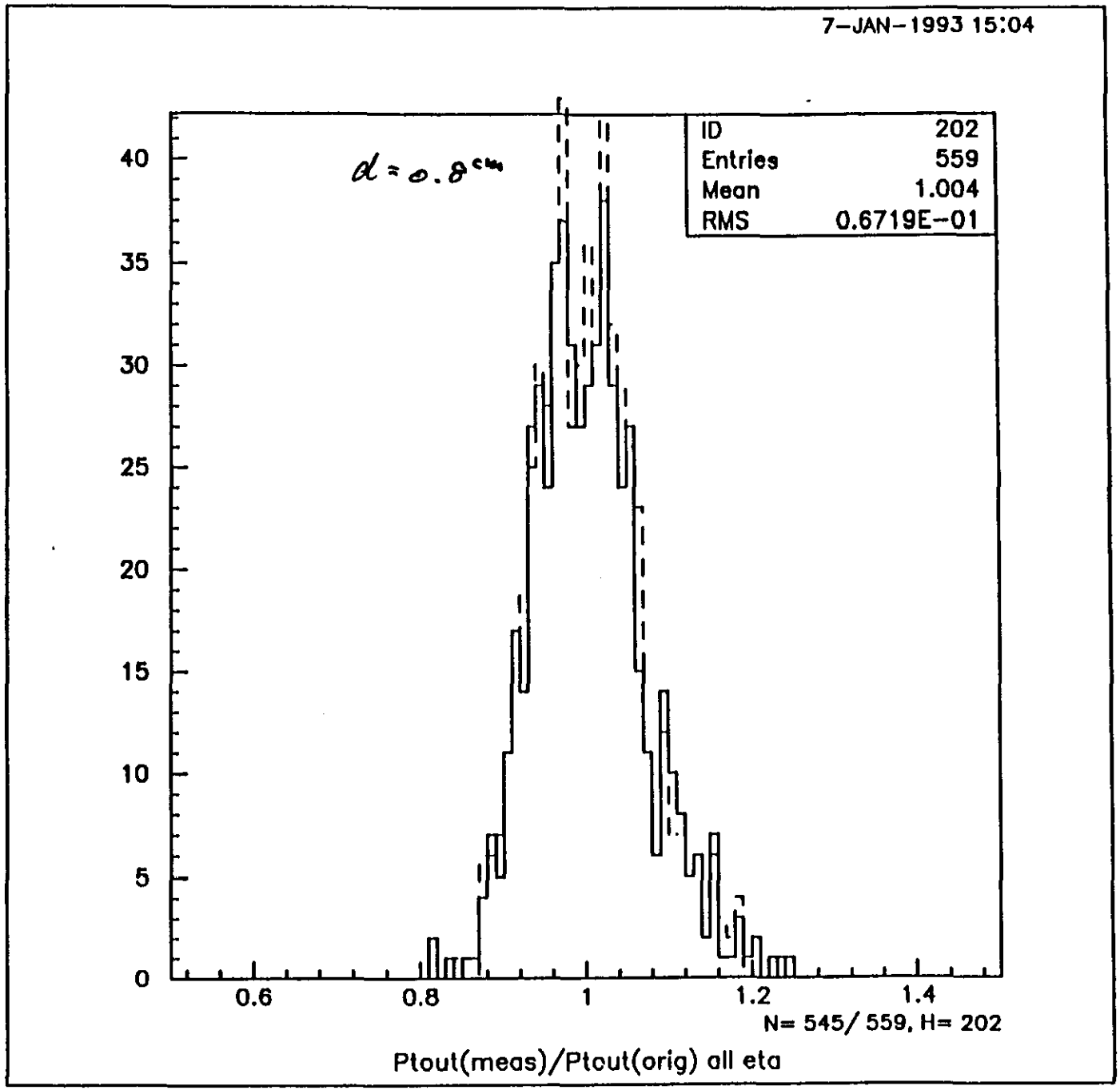
7-JAN-1993 15:04
ID 202
Entries 559
Mean 1.004
RMS 0.6719E-01
d = 0.8 cm
0
5
10
15
20
25
30
35
40
0.6
0.8
1
1.2
1.4
N= 545/ 559, H= 202
Ptout(meas)/Ptout(orig) all eta

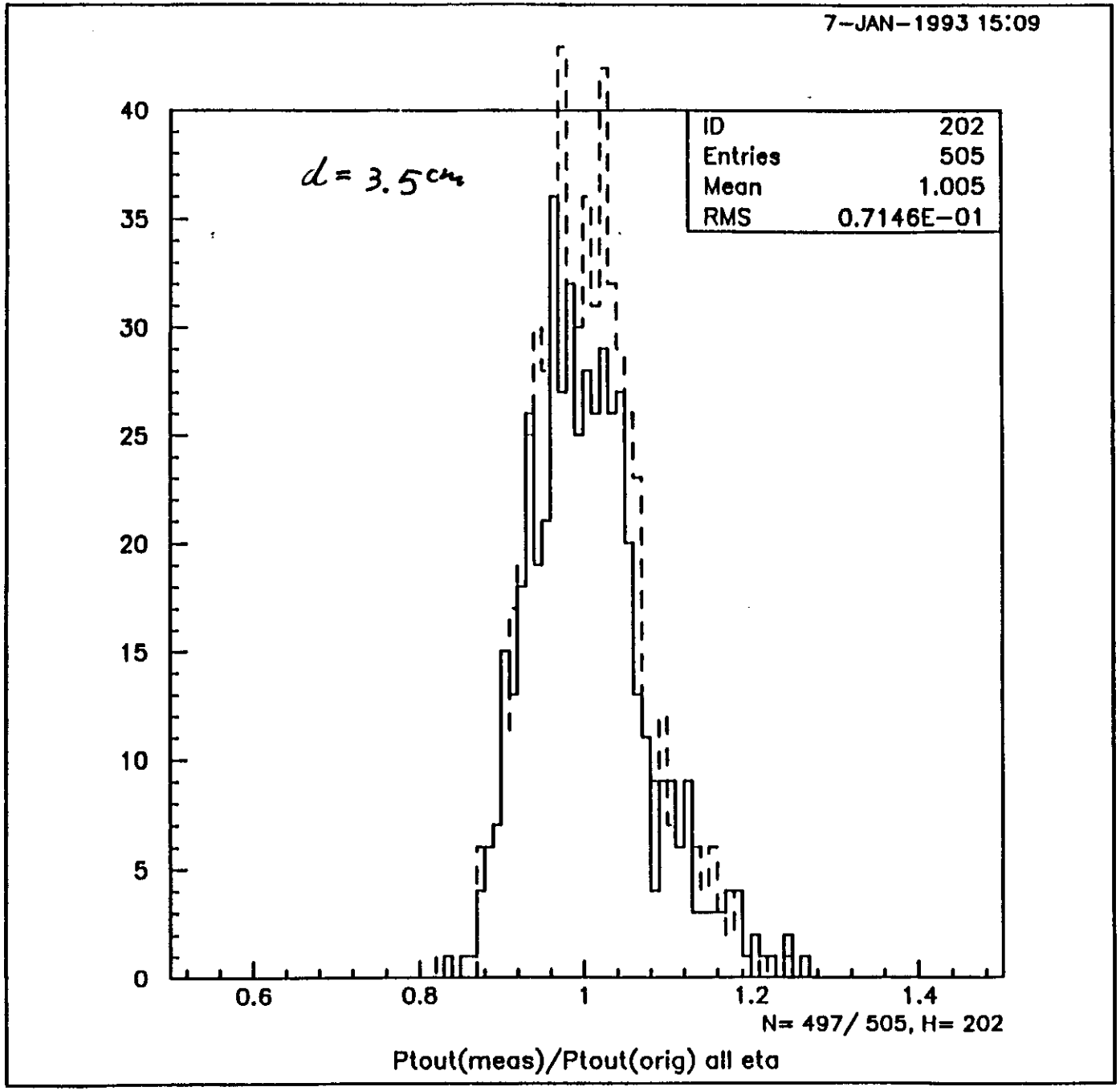
7-JAN-1993 15:09
d = 3.5 cm
ID 202
Entries 505
Mean 1.005
RMS 0.7146E-01
40
35
30
25
20
15
10
5
0
0.6
0.8
1
1.2
1.4
N= 497/ 505, H= 202
Ptout(meas)/Ptout(orig) all eta

gem

γeμ

Presentation by:

D. Marlow

CSC Electronics

D. Marlow

1/8/93

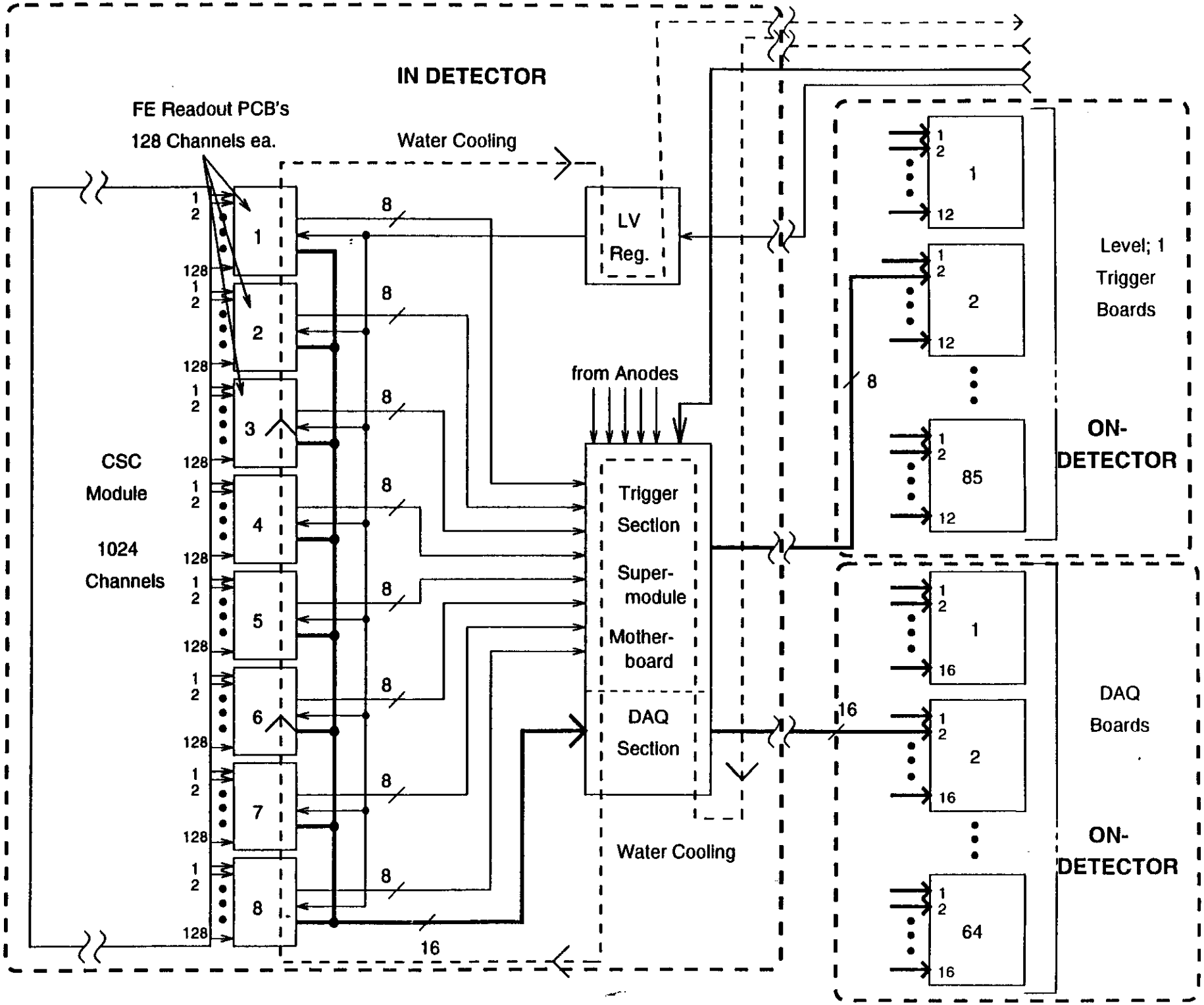
IN DETECTOR
FE Readout PCB's
128 Channels ea.
Water Cooling
CSC
Module
1024
Channels
LV
Reg.
from Anodes
Trigger
Section
Super-
module
Mother-
board
DAQ
Section
Water Cooling
Level; 1
Trigger
Boards
ON-
DETECTOR
DAQ
Boards
ON-
DETECTOR
8
16
128
12
85
64

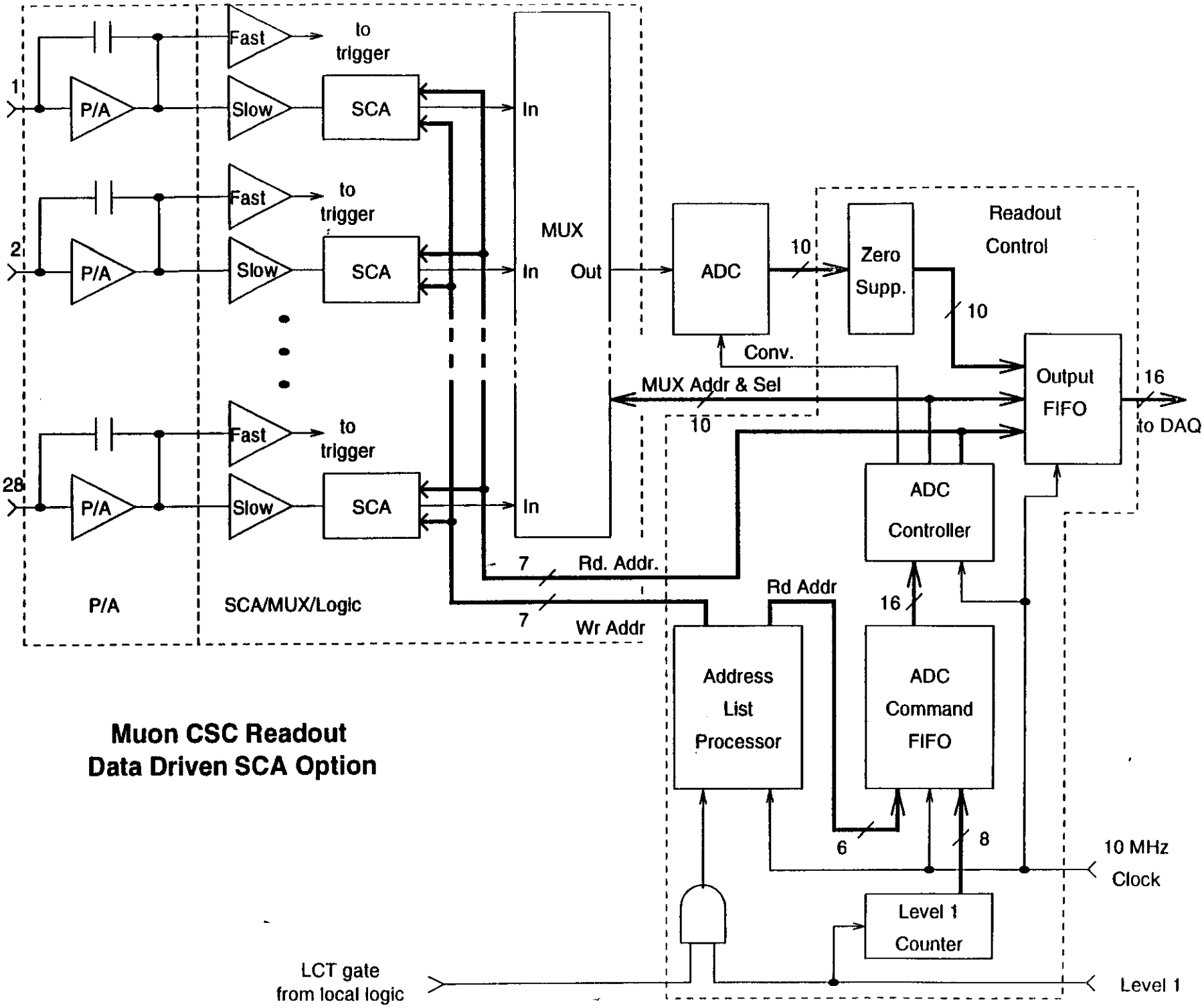

Muon CSC Readout
Data Driven SCA Option

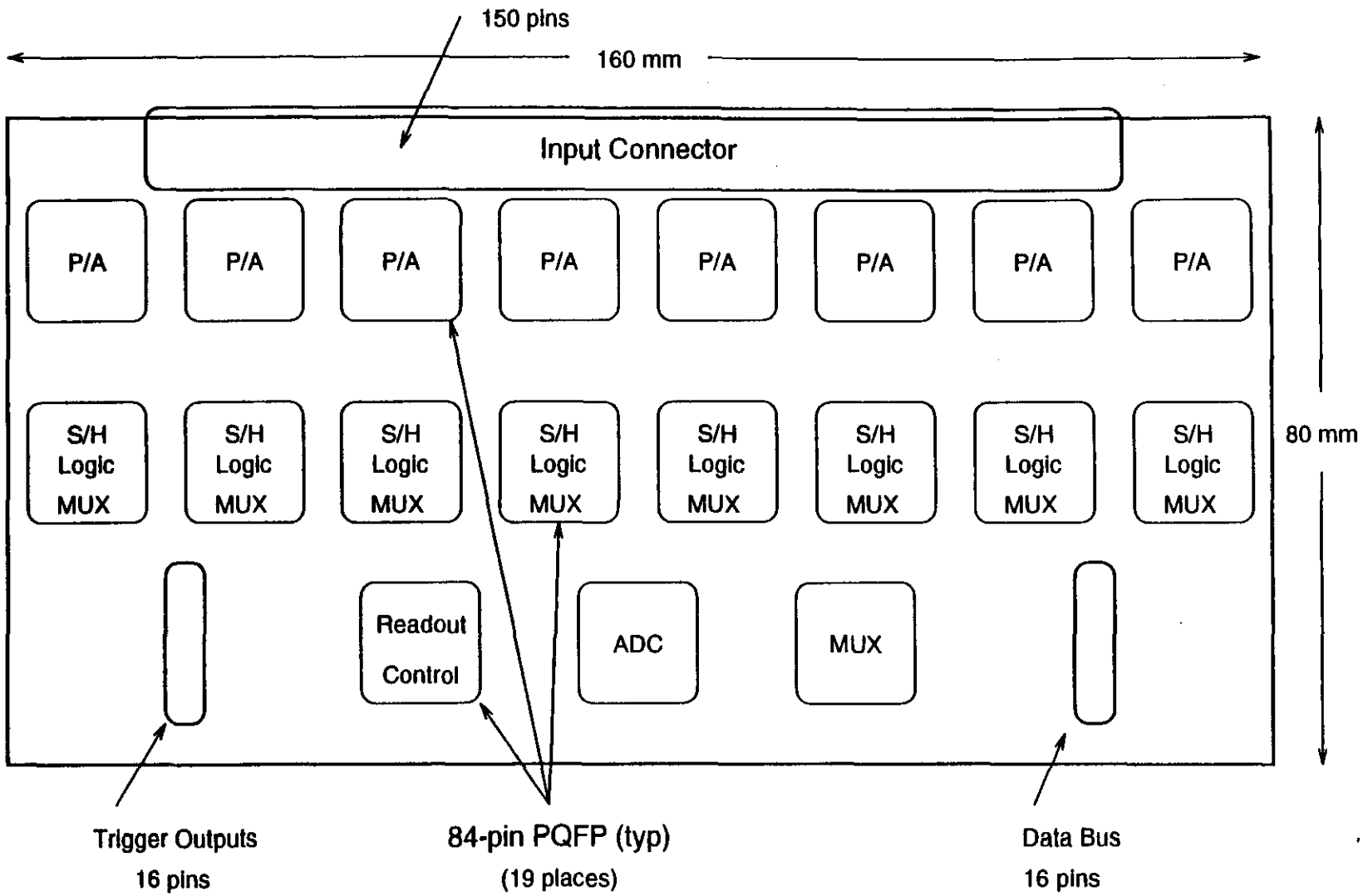

CSC Chamber Board Layout
128 Channel Version

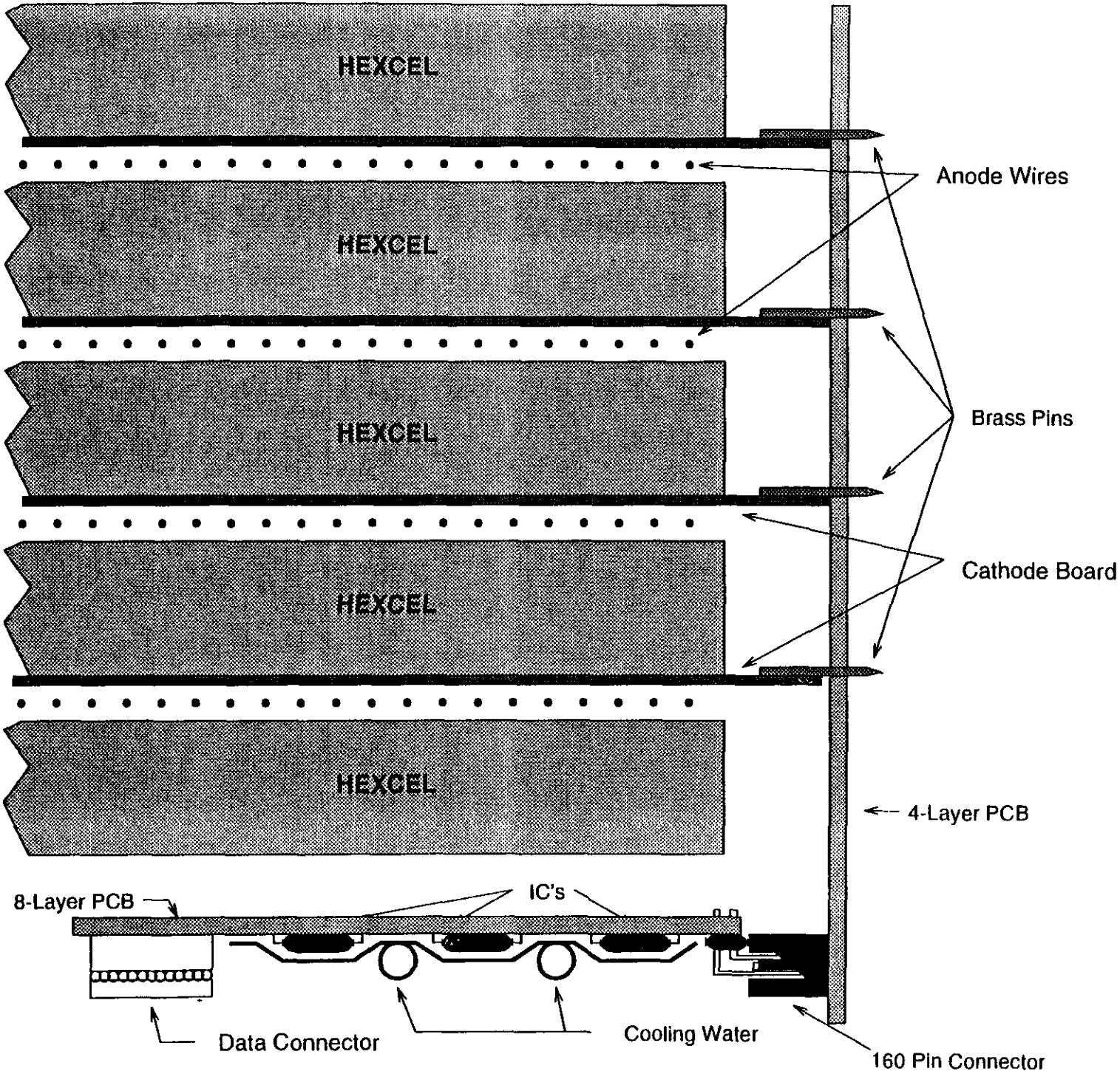
HEXCEL
HEXCEL
HEXCEL
HEXCEL
HEXCEL
Anode Wires
Brass Pins
Cathode Board
4-Layer PCB
8-Layer PCB
IC's
Data Connector
Cooling Water
160 Pin Connector

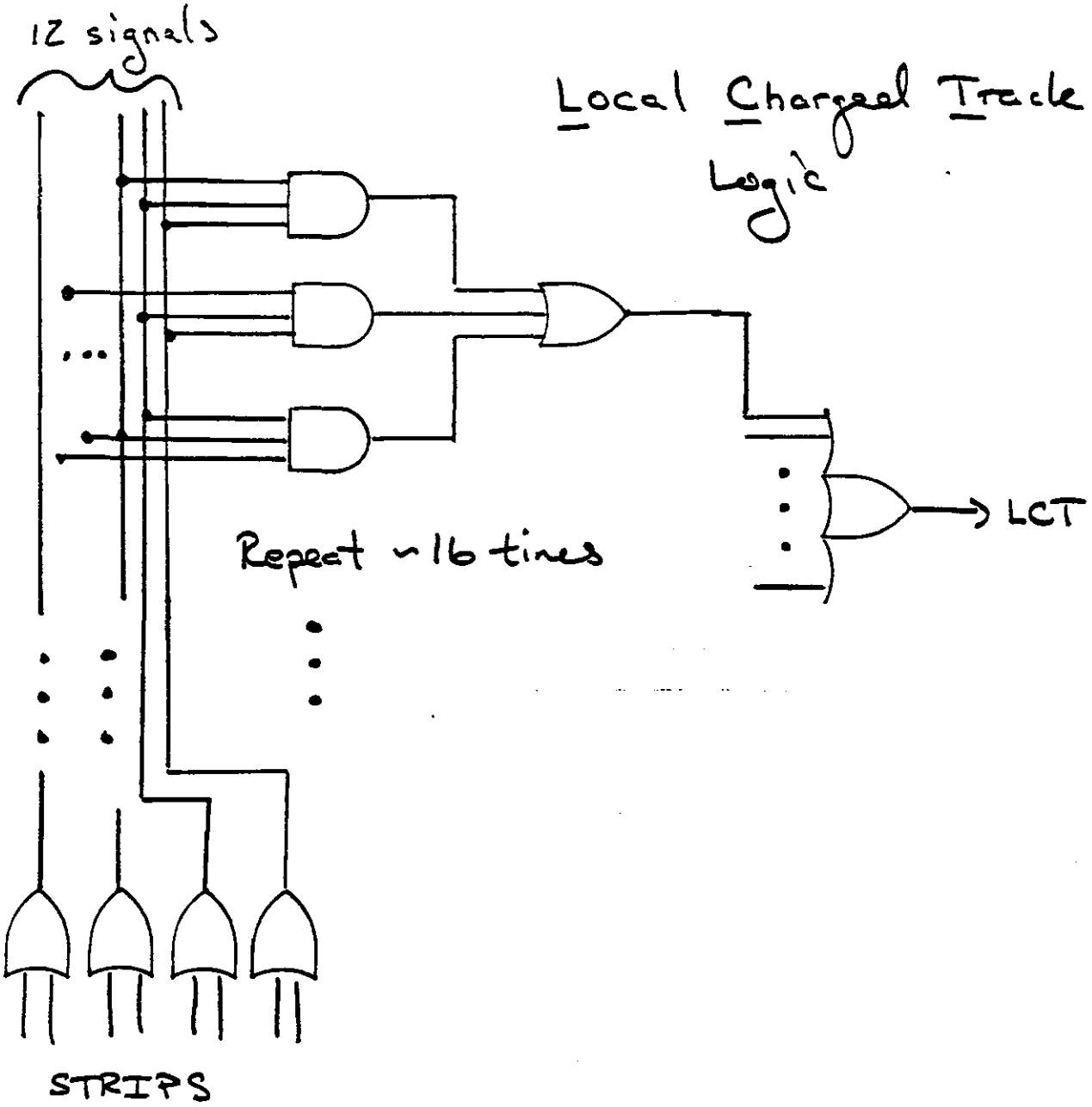
12 signals
Local Charged Track Logic
Repeat ~16 times
LCT
STRIPS

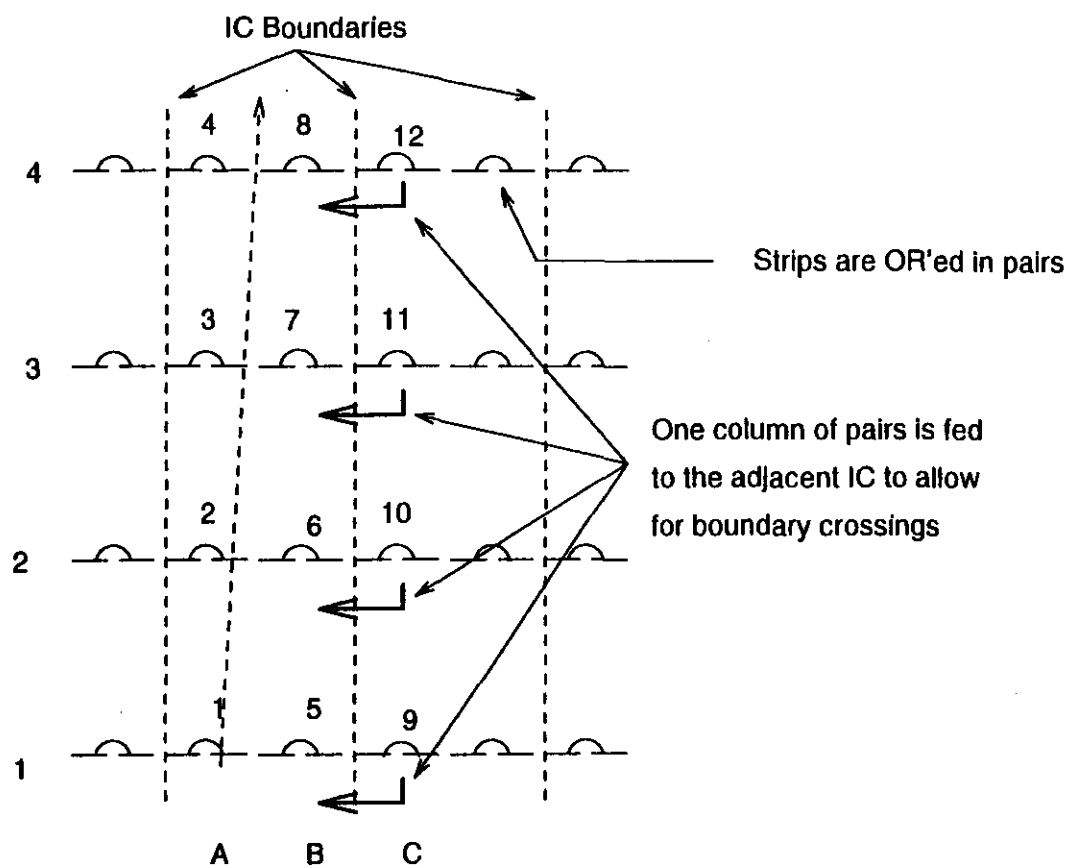

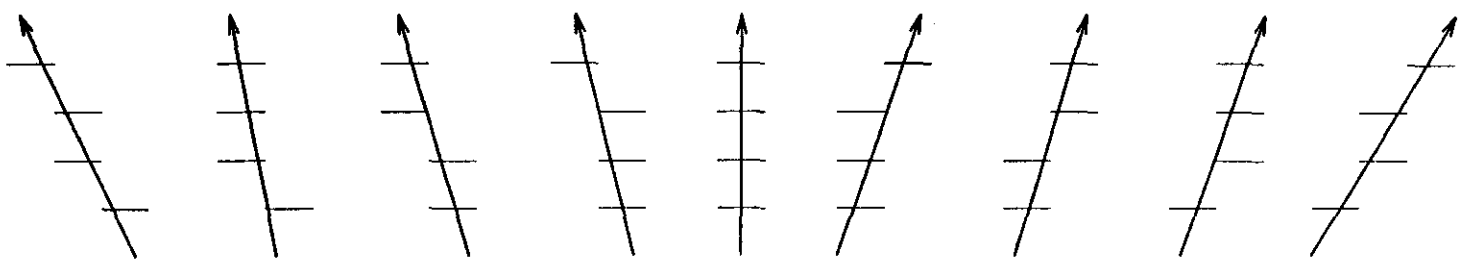

Possible Tower Combinations

Towers	Combinations			
A1 A2 A3 A4				
1 2 3 4	1 2 3	1 2 4	1 3 4	2 3 4
A1 A2 A3 B4				
1 2 3 8		1 2 8	1 3 8	2 3 8
A1 A2 B3 B4				
1 2 7 8	1 2 7		1 7 8	2 7 8
A1 B2 B3 B4				
1 6 7 8	1 6 7	1 6 8		6 7 8
A1 B2 B3 C4				
1 6 7 12		1 6 12	1 7 12	6 7 12
B1 A2 A3 *				
5 2 3	5 2 3			
B1 A2 A3 A4				
5 2 3 4		5 2 4	5 3 4	
B1 B2 A3 A4				
5 6 3 4	5 6 3	5 6 4		6 3 4
B1 B2 B3 A4				
5 6 7 4	5 6 7		5 7 4	6 7 4
B1 B2 B3 B4				
5 6 7 8		5 6 8	5 7 8	
B1 B2 B3 C4				
5 6 7 12		5 6 12	5 7 12	
B1 B2 C3 C4				
5 6 11 12	5 6 11		5 11 12	6 11 12
B1 C2 C3 C4				
5 10 11 12	5 10 11	5 11 12		10 11 12
B1 C2 C3 *				
5 10 11				
C1 B2 B3 A4				
9 6 7 4	9 6 7	9 6 4	9 7 4	
C1 B2 B3 B4				
9 6 7 8		9 6 8	9 7 8	
C1 C2 B3 B4				
9 10 7 8	9 10 7	9 10 8		10 7 8
C1 C2 C3 B4				
9 10 11 8	9 10 11		9 11 8	10 11 8

Total of 46 3-Input AND's

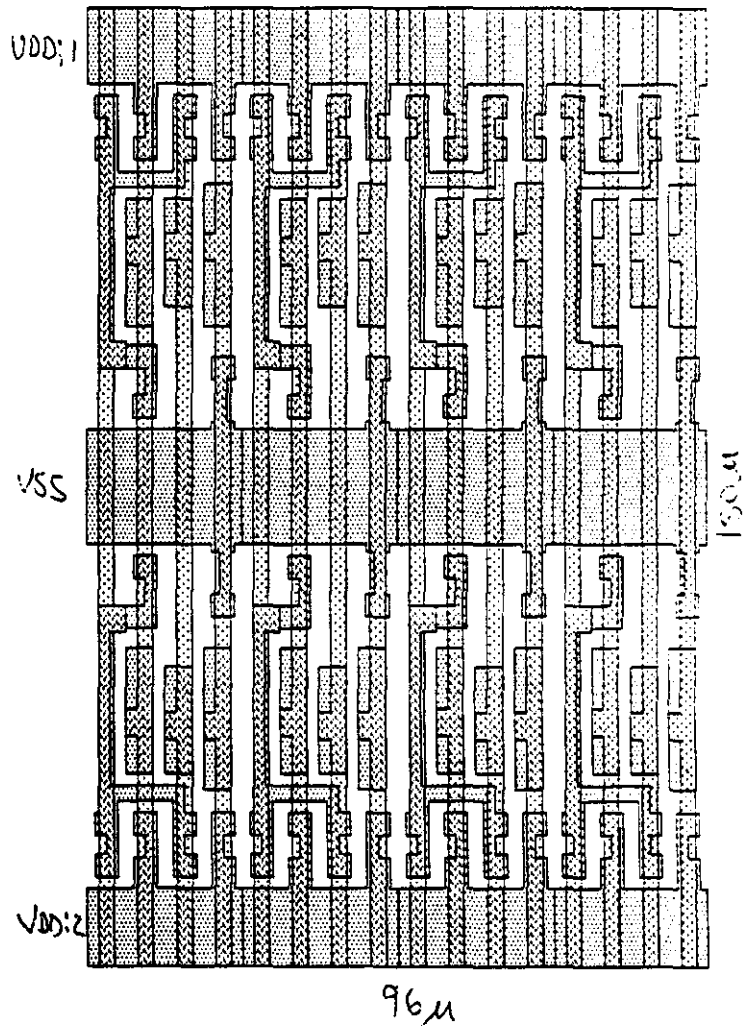

overall length = 16(96 + 18)
= 1824μ (1.8mm)
overall height = 150 + 50
= 200μ

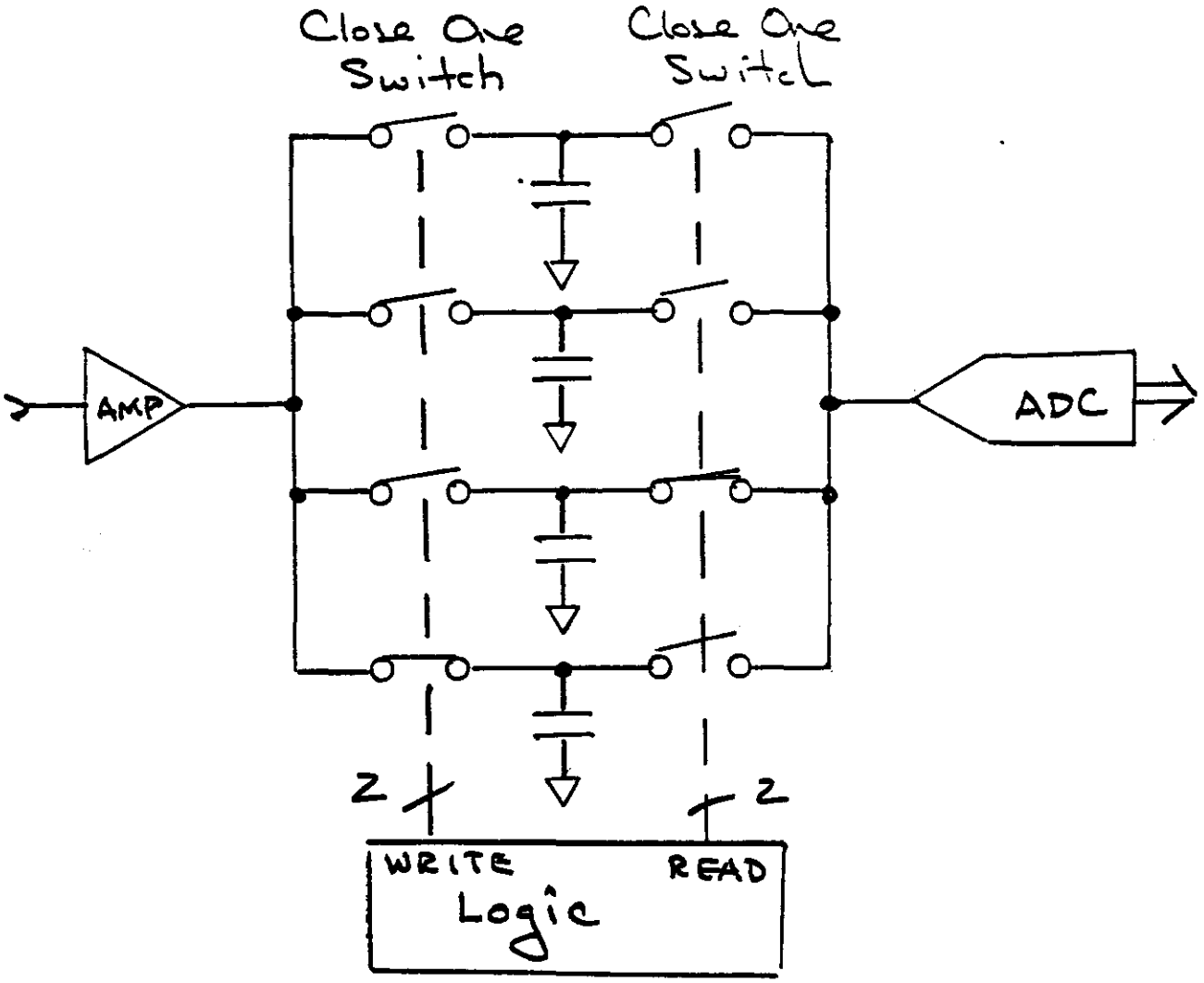

Quad Track + Hold Concept

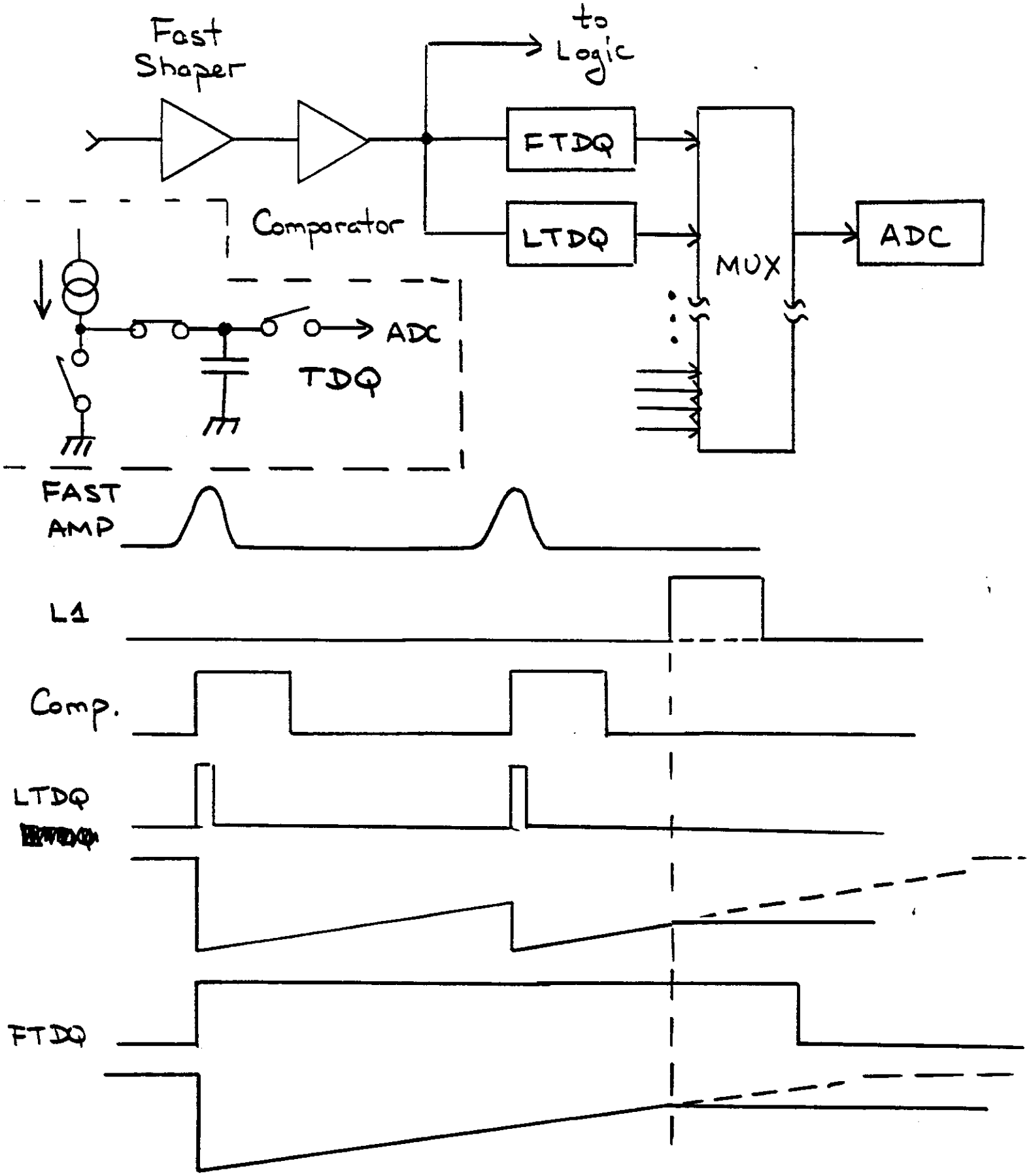
Fast
Shaper
to
Logic
FTDQ
LTDQ
MUX
ADC
Comparator
ADC
TDQ
FAST
AMP
L1
Comp.
LTDQ
FTDQ

Timing Discriminator Concept

a la Turko + Smith

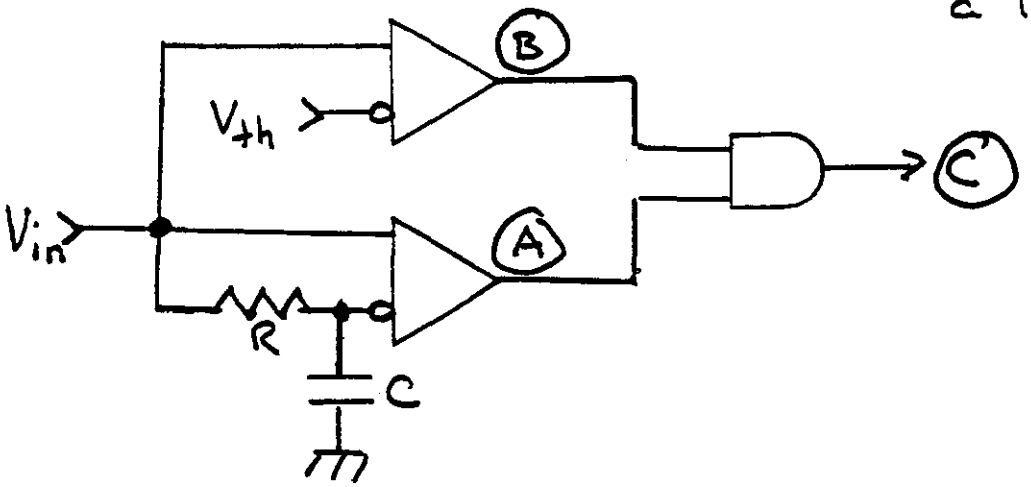

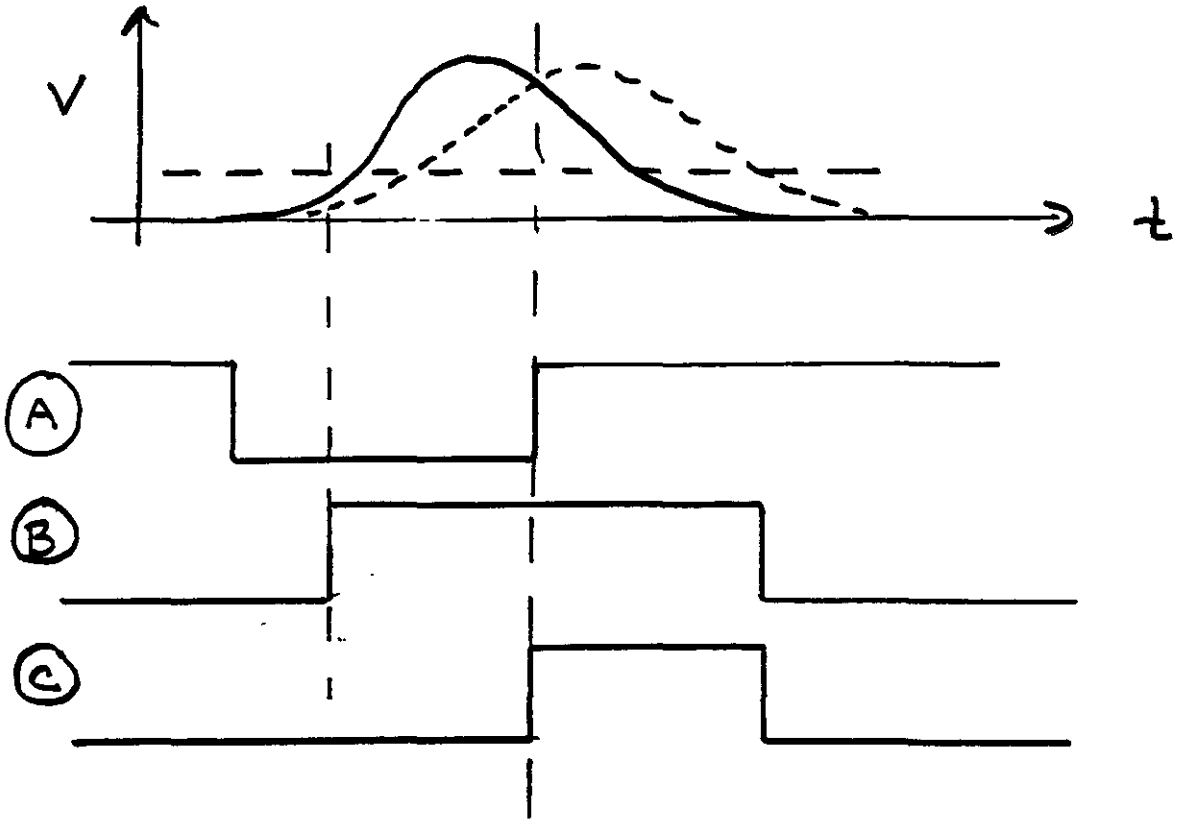

Input not shown

$V_p = 0.1\ V$

107

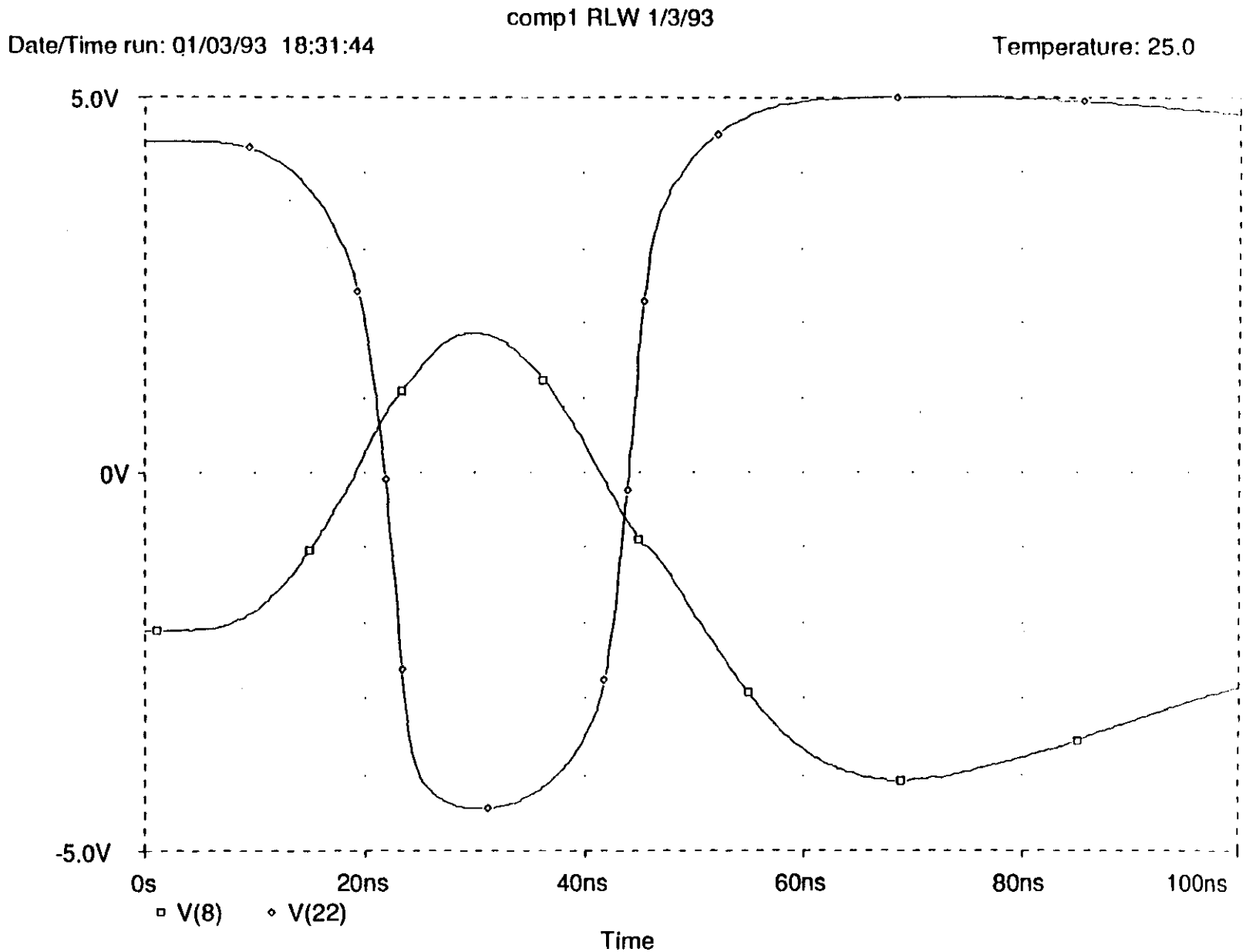

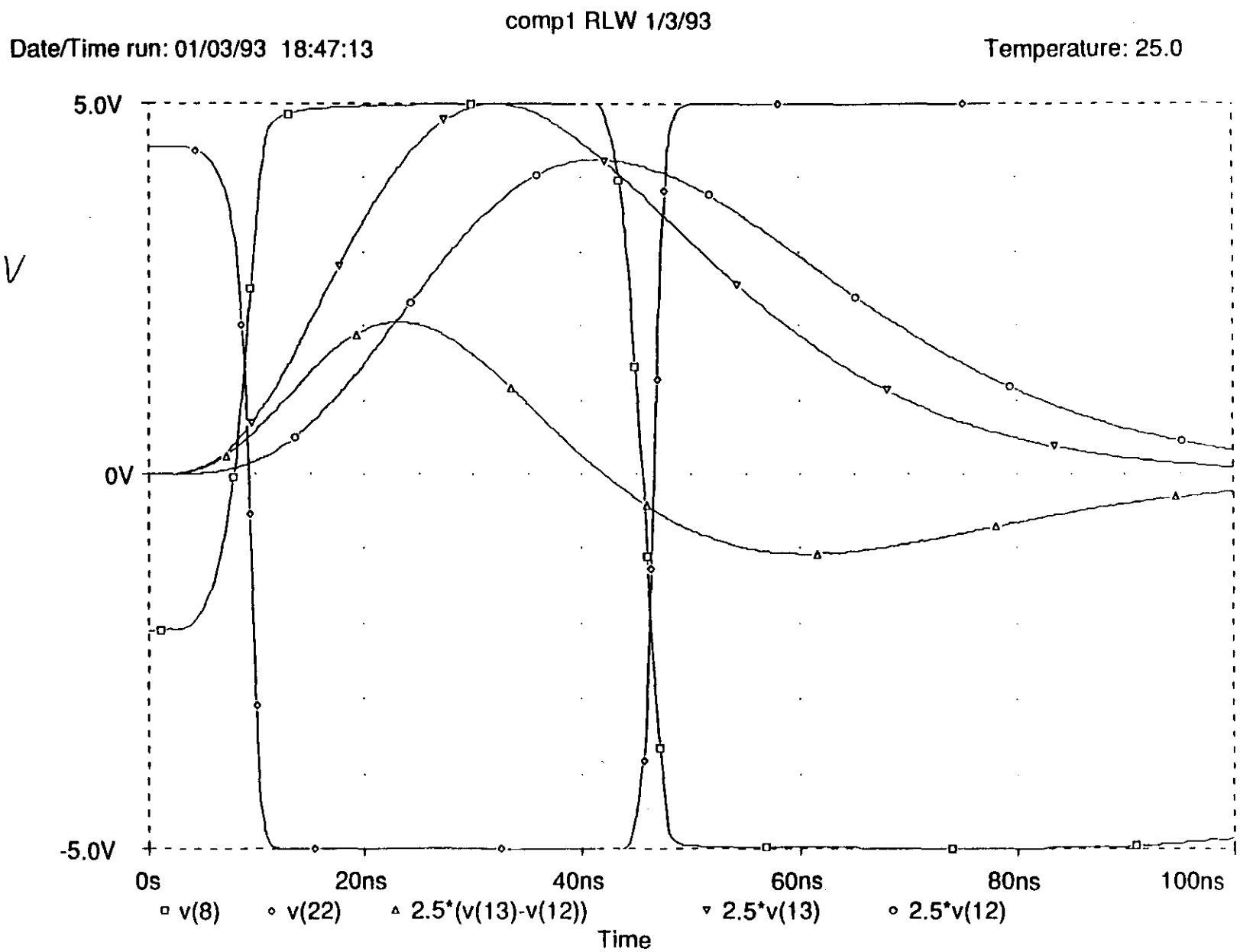
comp1 RLW 1/3/93
Date/Time run: 01/03/93 18:47:13
Temperature: 25.0
5.0V
0V
-5.0V
0s
20ns
40ns
60ns
80ns
100ns
v(8)
v(22)
2.5*(v(13)-v(12))
2.5*v(13)
2.5*v(12)
Time

$V_{IL} = 2.0\ V$

.5V in

Fast Timer Circuit

Date/Time run: 01/03/93 18:34:41

Temperature: 25.0

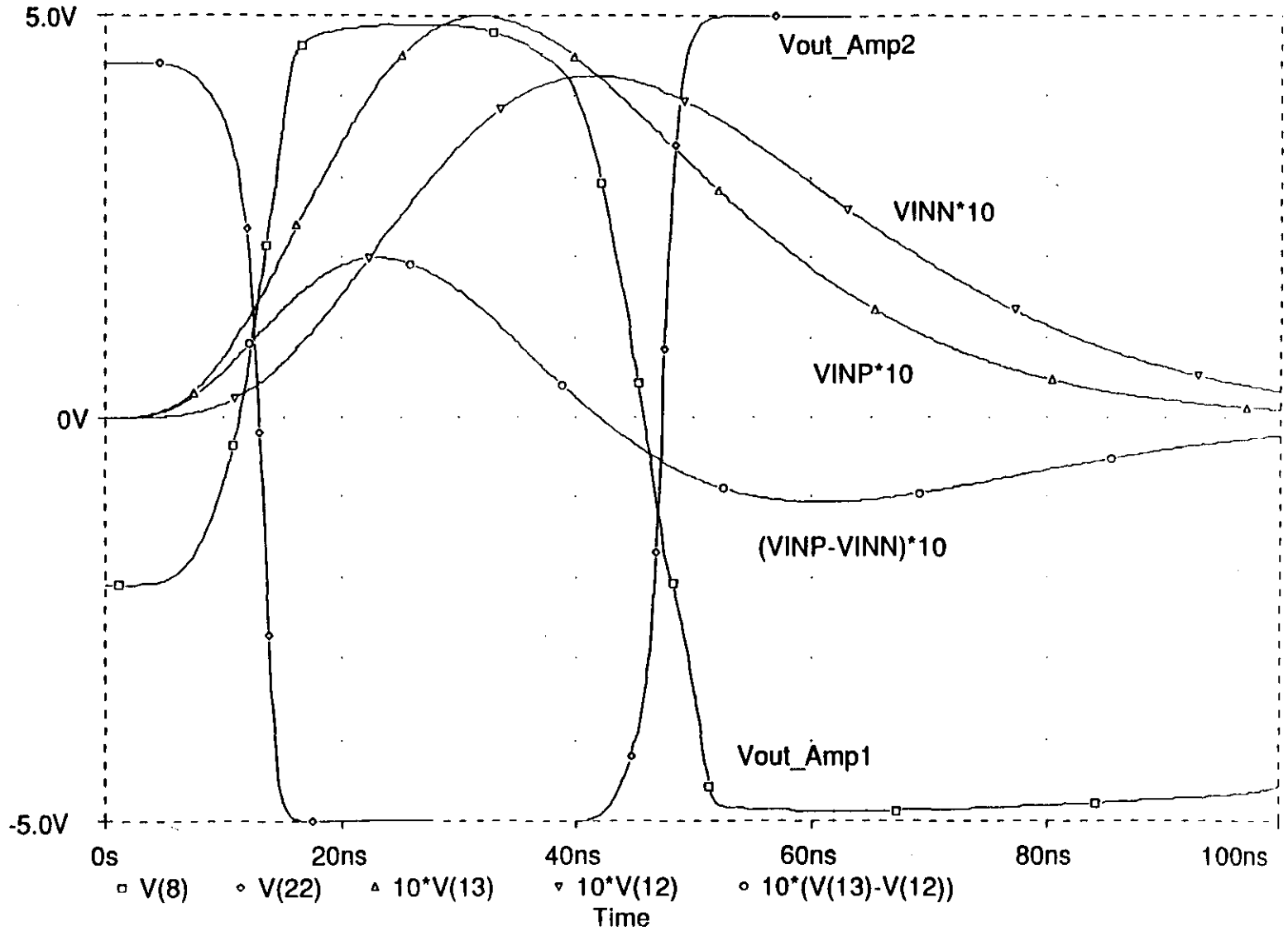

Comp 2

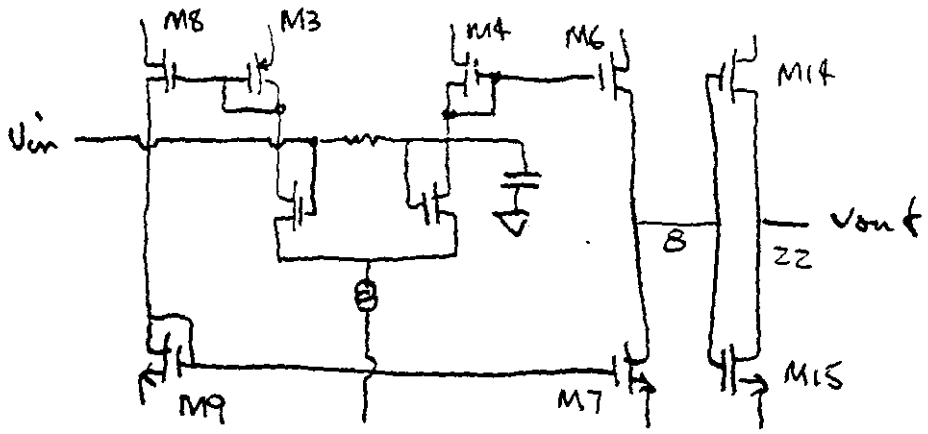

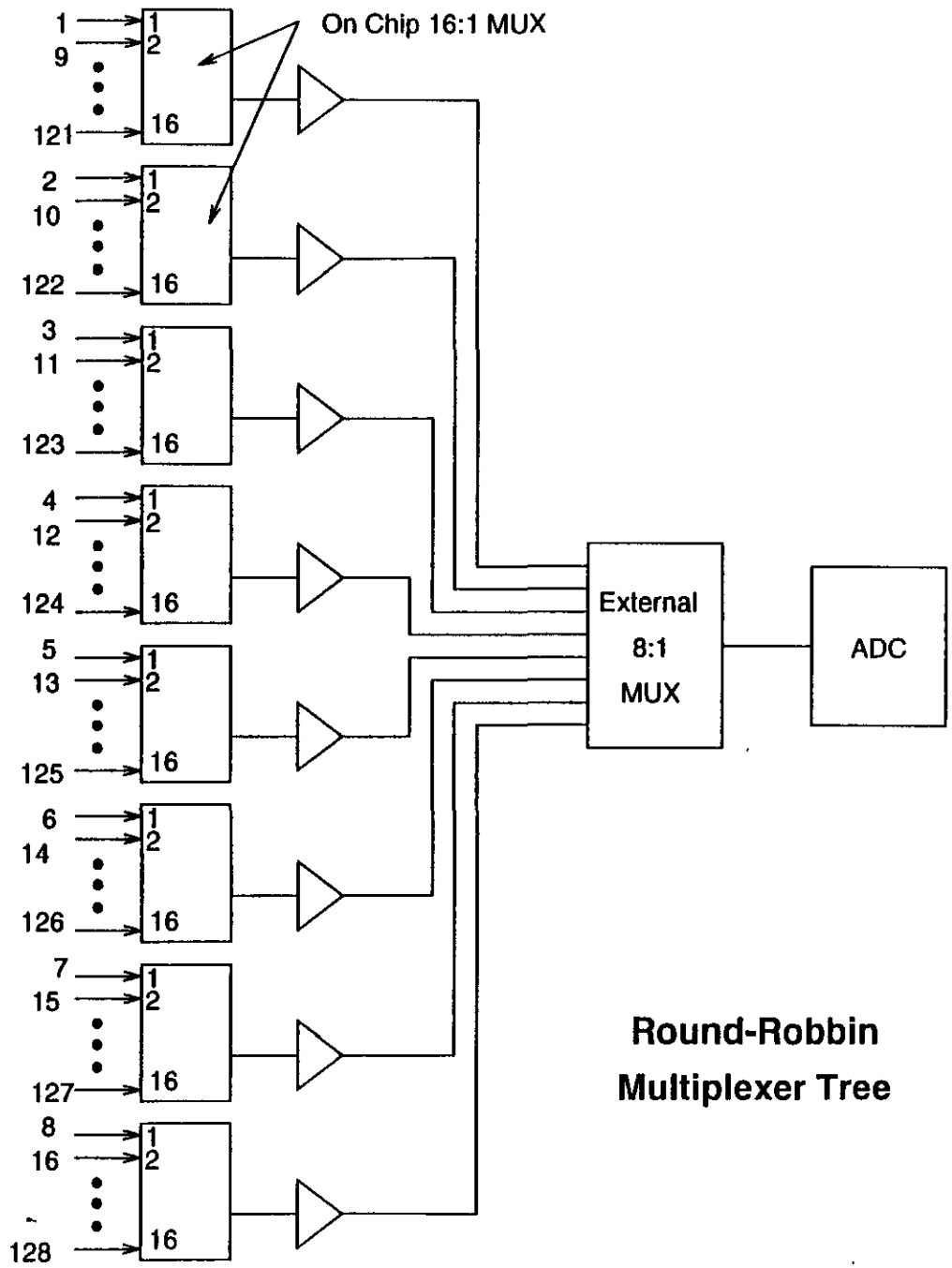

Round-Robbin Multiplexer Tree

gem

γeμ

Presentation by:

F. Nimblett

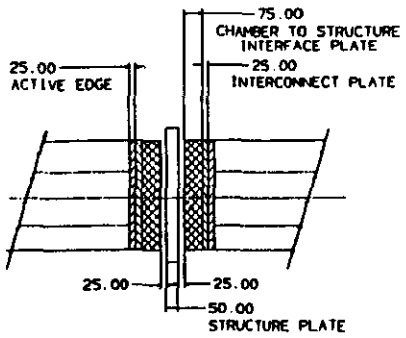

MIDDLE CHAMBERS

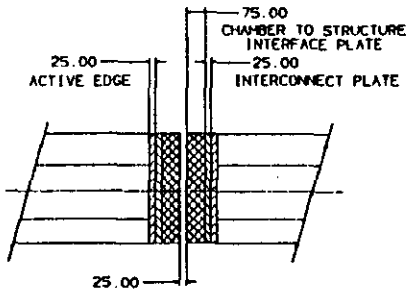

INNER AND OUTER CHAMBERS

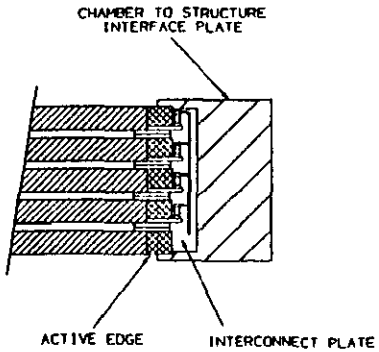

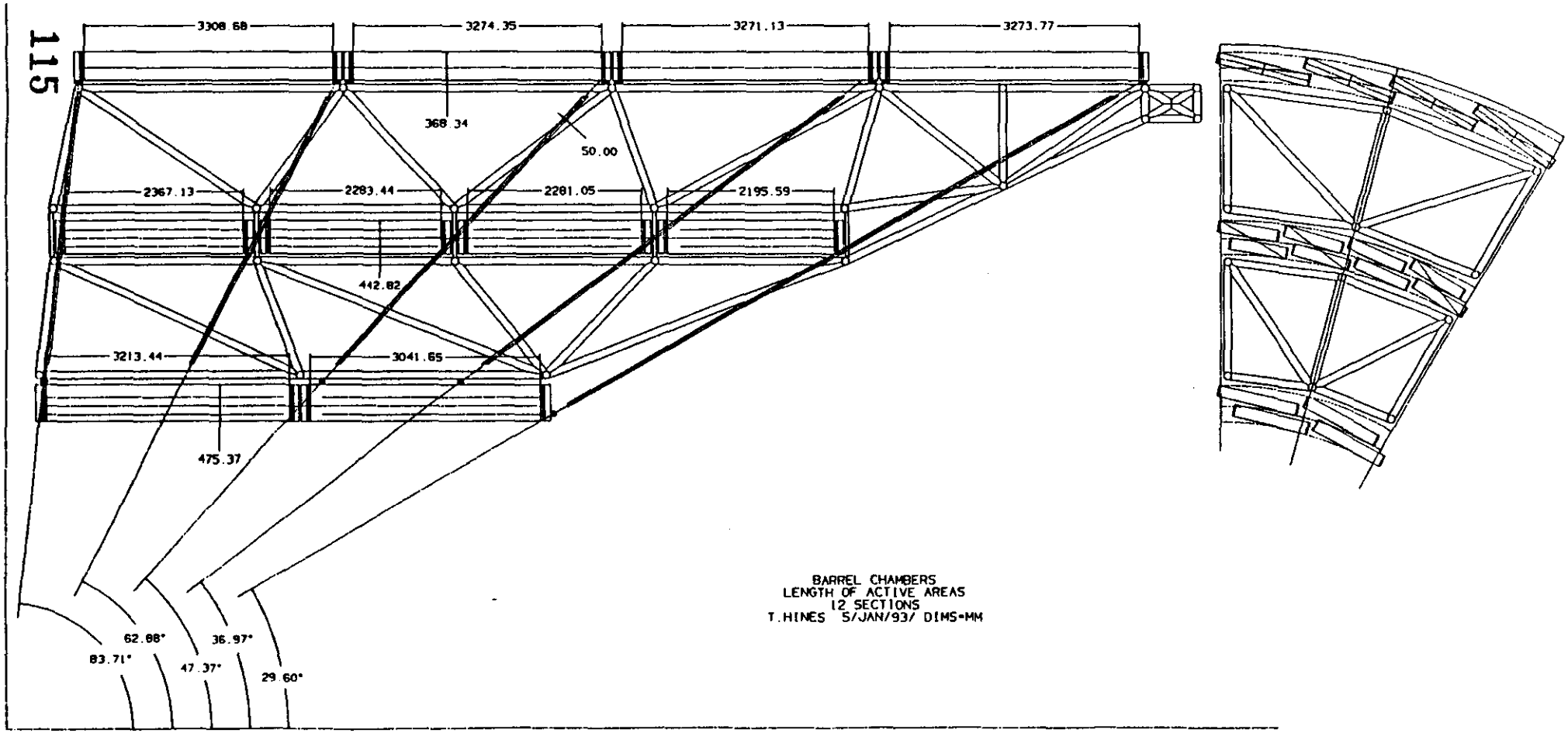

BARREL CHAMBERS
LENGTH OF ACTIVE AREAS
12 SECTIONS
T.HINES 5/JAN/93/ DIMS=MM

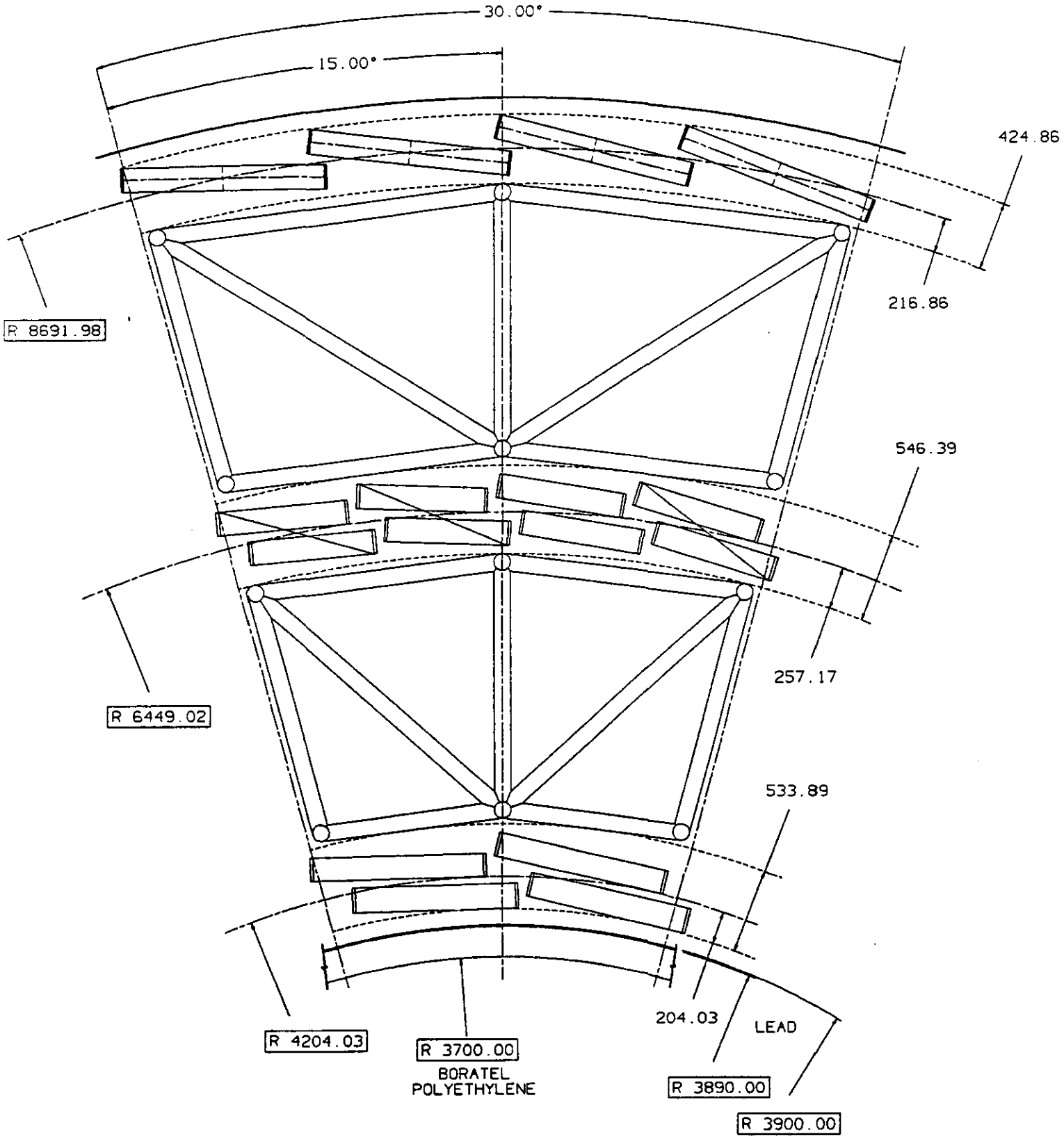

6° BARREL MODULE
12 SECTORS-4000MM MIN R
SUPPORT
T.HINES 5/JAN/93

DIMS=MM

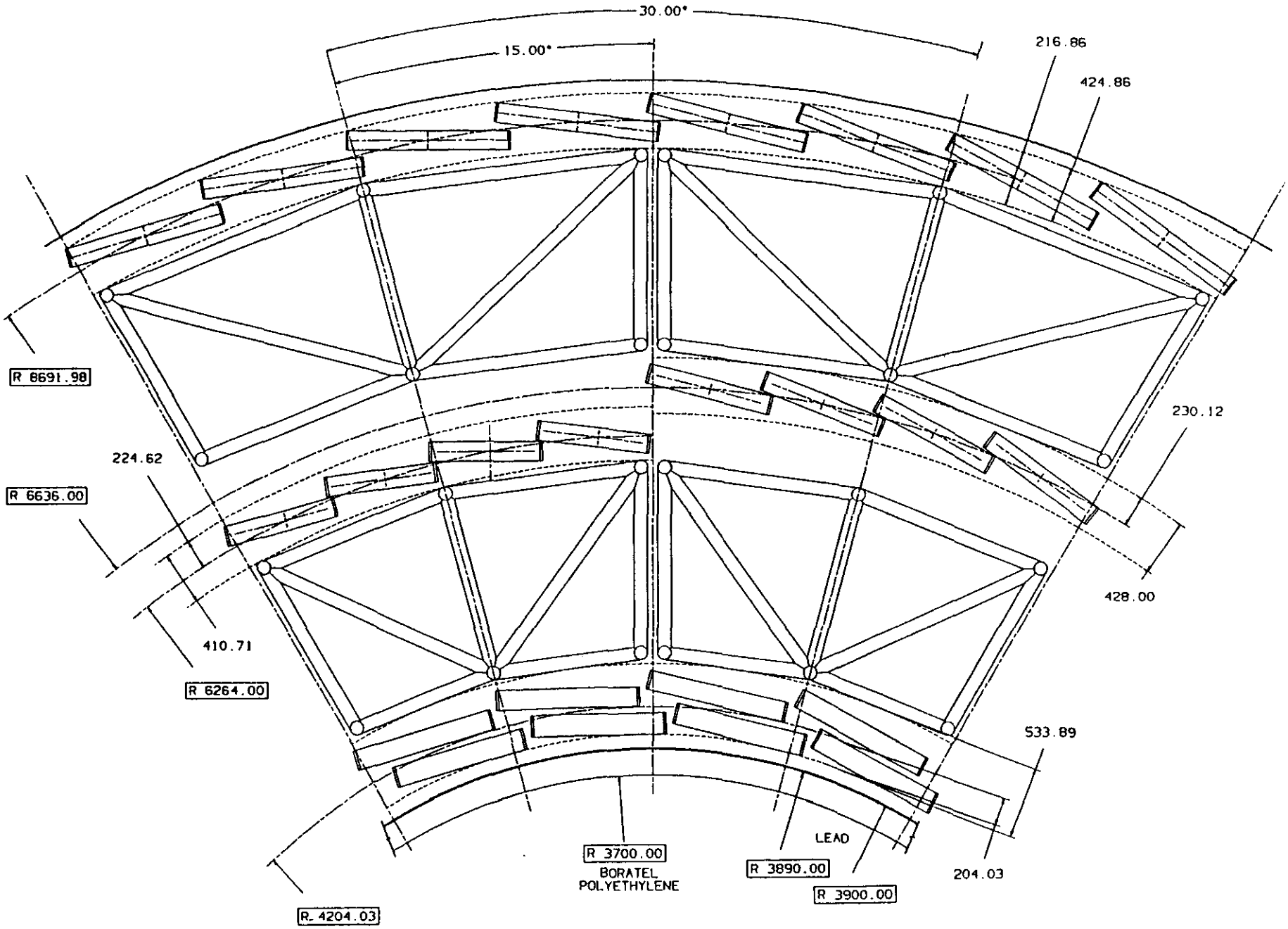

6° BARREL MODULE
12 SECTORS-4000MM MIN R
SUPPORT
T.HINES 5/JAN/93

DIMS=MM

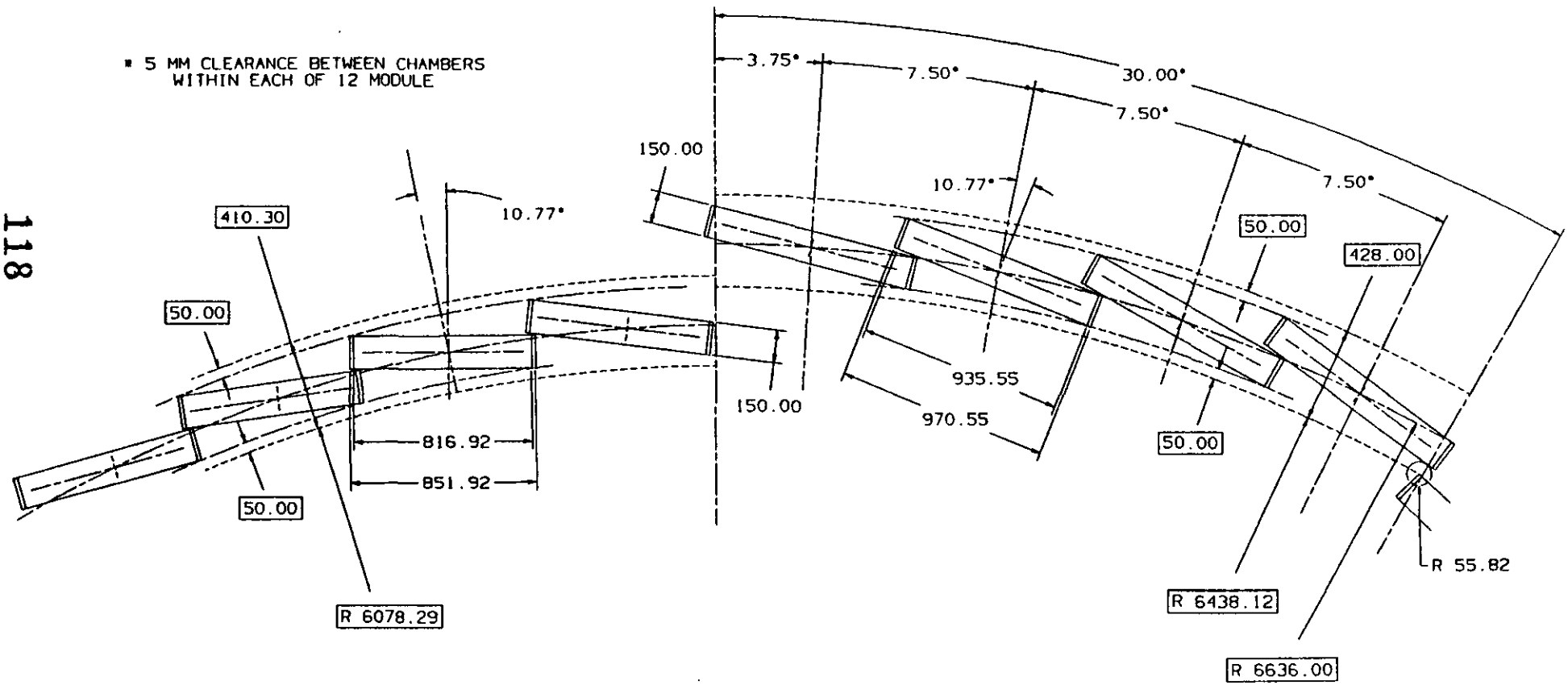

11.44142°-10.77469°
MIDCHAMBERS
12 SECTORS-4000MM MIN R
T.HINES 5/JAN/93

DIMS=MM

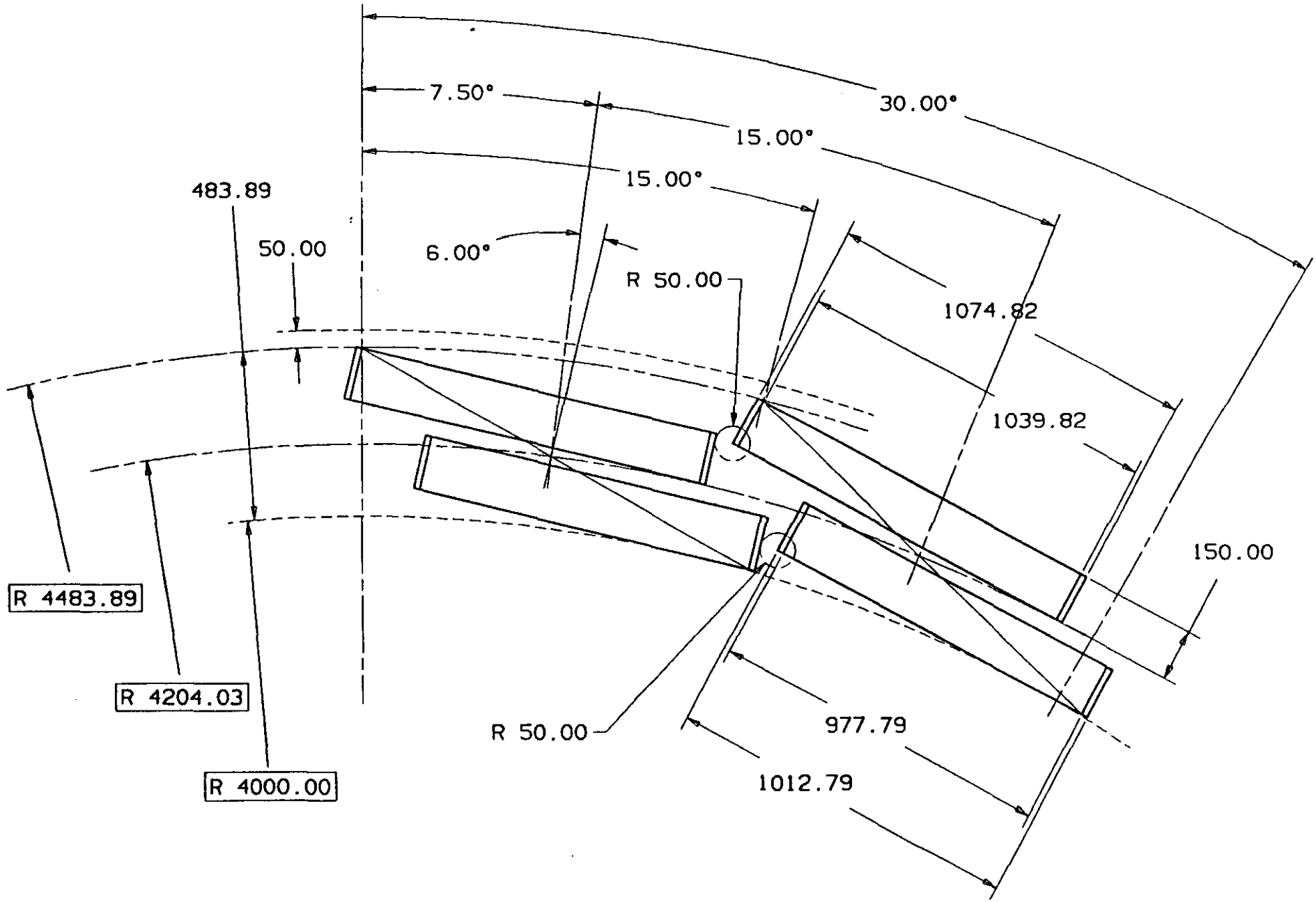

6° INNER CHAMBERS
12 SECTORS-4000MM MIN R
T.HINES 5/JAN/93

DIMS=MM

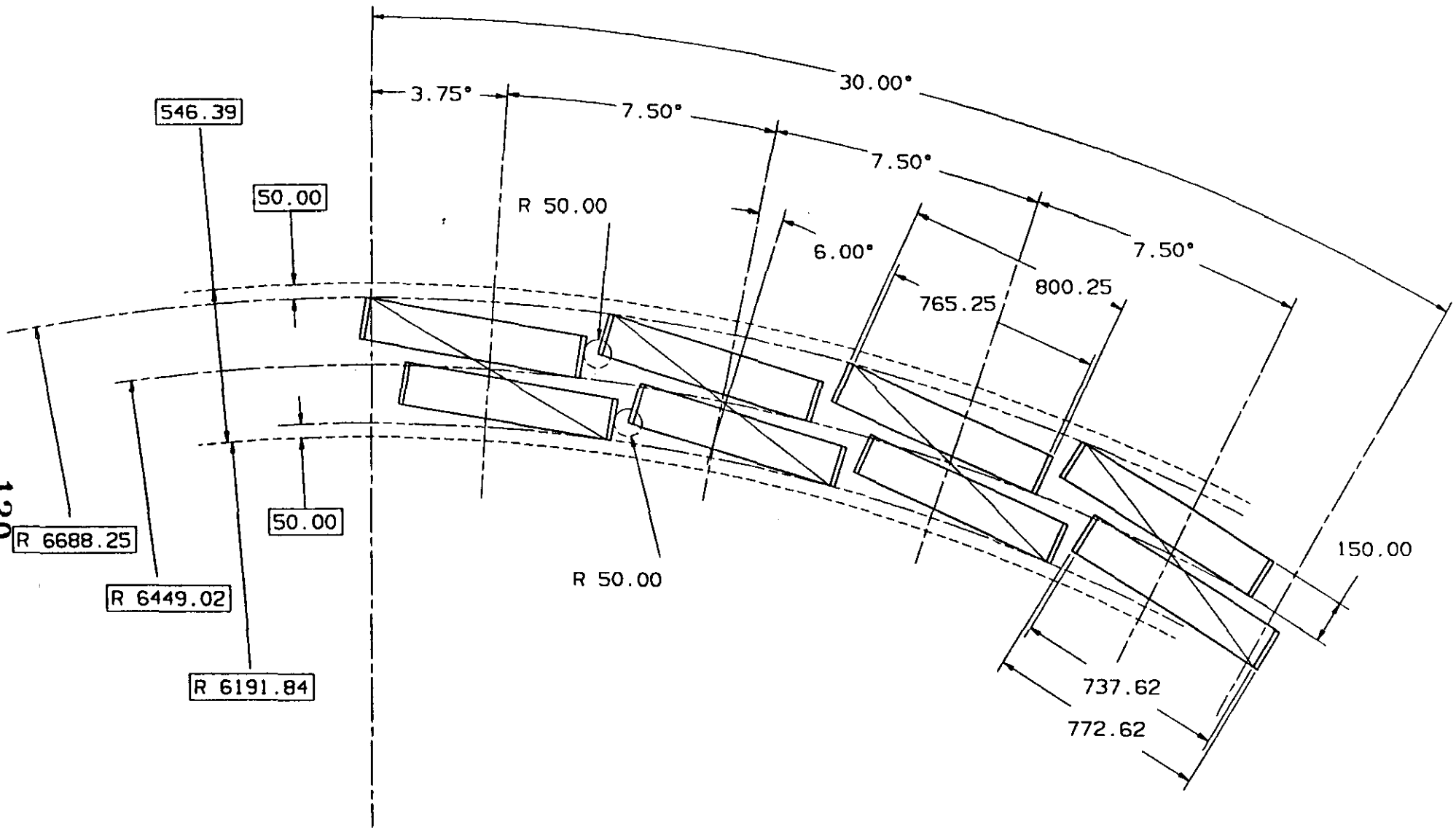

6° MID-CHAMBERS
12 SECTORS-4000MM MIN R
T.HINES 5/JAN/93

DIMS=MM

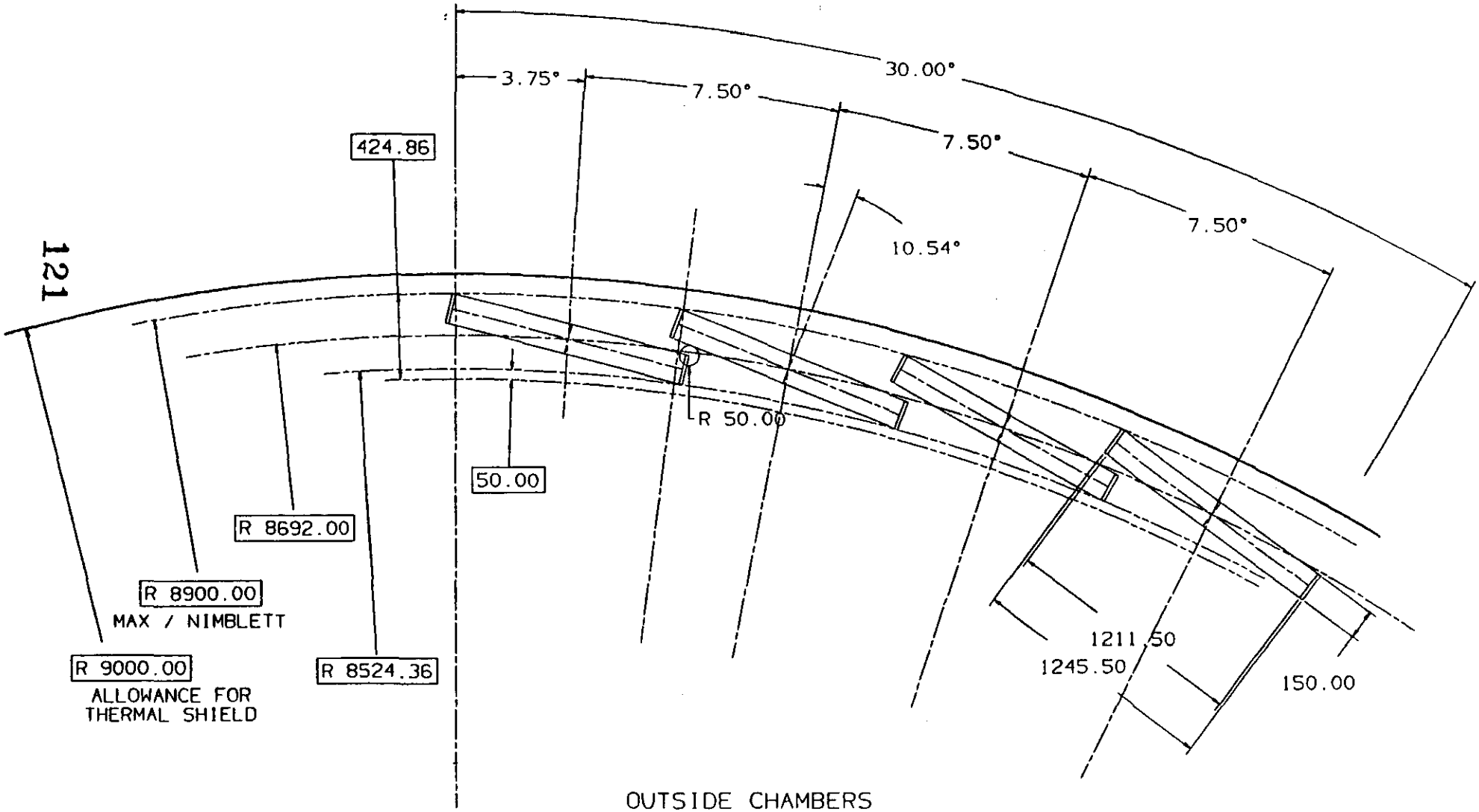

OUTSIDE CHAMBERS
12 SECTORS
T.HINES 5/JAN/93
DIMS=MM

active coverage 9.75° to 27.71°

module thickness(4 gaps) = 0.15 m
intermodule space = 0.10 m

neutron flux (Hz/cm^2) = 10,000
neutron efficiency = 0.005

Nomenclature:

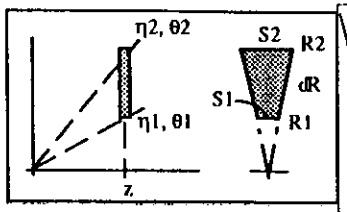

Layout:

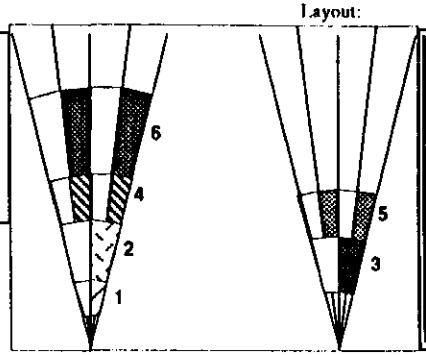

Version "g"

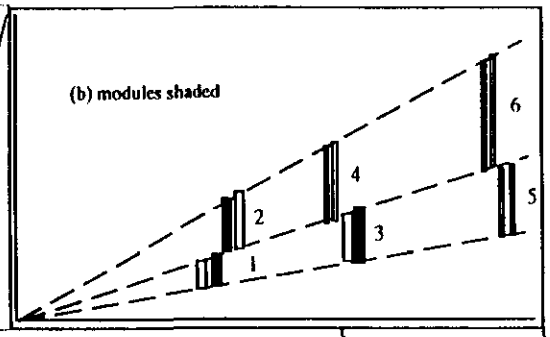

Note: modules (a) occupy even-numbered sectors
modules (b) occupy odd-numbered sectors
Nsctrs/2 are type (a) and Nsctrs/2 are type (b)

Caveat: this weight and cost model is very crude and for comparison purposes at best.

Total ch counts: single strip occ.

	ngaps	zfr	zba	zav	Dz's	n1	θ1	n2	θ2	Nsctrs	R1	R2	dR	S2	area	total area	str wid	# strips	wire gp	# r-ch	# str ch	# r ch	ch. pt.	neut.	wt/mod	cost for this
		m	m	m			deg		deg		m	m	m	m	m^2	m^2	mm	/pl/sctr	cm	/pl/sctr			/sec	/sec	Kg	module type
Inner modules																										
1a)	8	6.00	6.30	6.15		2.46	9.75	1.90	17.01	24	1.06	1.88	0.83	0.49	0.31	60.26	5.00	77	5.0	17	14,727	3,169	188	2,063	47	295,458
1b)	8	6.40	6.70	6.55		2.46	9.75	1.90	17.01	24	1.13	2.00	0.88	0.52	0.36	68.35	5.00	82	5.0	18	15,685	3,376	200	2,198	50	302,384
2a)	8	7.20	7.50	7.35		1.90	17.01	1.40	27.71	24	2.25	3.86	1.61	1.01	1.27	244.47	5.00	159	5.0	32	30,618	6,185	44	4,027	119	449,430
2b)	8	6.80	7.10	6.95		1.90	17.01	1.40	27.71	24	2.13	3.65	1.52	0.95	1.14	218.59	5.00	151	5.0	30	28,952	5,849	41	3,808	109	428,028
Middle modules																										
3a)	8	10.85	11.15	11.00	4.85	2.46	9.75	1.90	17.01	24	1.89	3.37	1.48	0.88	1.00	96.38	5.00	137	5.0	30	26,341	5,669	76	3,691	100	406,779
3b)	8	11.25	11.55	*11.40*	4.85	2.46	9.75	1.90	17.01	24	1.96	3.49	1.53	0.91	1.08	103.52	5.00	142	5.0	31	27,299	5,875	78	3,825	105	418,620
4a)	4	10.60	10.75	10.68	3.33	1.90	17.01	1.40	27.71	48	3.27	5.61	2.34	0.73	1.35	260.07	5.00	116	5.0	47	22,282	8,983	14	5,848	72	471,695
4b)	4	10.35	10.50	10.43	3.48	1.90	17.01	1.40	27.71	48	3.19	5.47	2.28	0.72	1.29	248.03	5.00	113	5.0	46	21,760	8,773	14	5,711	69	461,418
Outer modules																										
5a)	4	15.95	16.10	16.03	5.03	2.46	9.75	1.90	17.01	48	2.75	4.90	2.15	0.64	1.07	206.32	5.00	100	5.0	43	19,228	8,258	37	5,377	61	426,061
5b)	4	16.20	16.35	16.28	4.88	2.46	9.75	1.90	17.01	48	2.80	4.98	2.18	0.65	1.11	212.81	5.00	102	5.0	44	19,528	8,387	37	5,460	62	431,629
6a)	4	15.70	15.85	15.78	5.10	1.90	17.01	1.40	27.71	48	4.83	8.28	3.46	1.08	2.96	567.93	5.00	171	5.0	69	32,927	13,275	7	8,643	133	732,112
6b)	4	15.45	15.60	15.53	5.10	1.90	17.01	1.40	27.71	48	4.75	8.15	3.40	1.07	2.86	550.07	5.00	169	5.0	68	32,406	13,065	7	8,506	130	717,090
																				Total =>	291,752	90,863			38,000	$5,540,705
																									tot.wt.	subtot. cost

AV3b *11.41*

total area of strip cathodes (m^2)	2837
total volume of chambers (m^3)	14.2
Total number of modules	432

Endcap CSC Layout -- Baseline II Version "g"

active coverage 9.75° to 27.71°

FFS Space=	0.15 m	FFSgap
module thickness(4 gaps) =	0.15 m	modth
intermodule space =	0.10 m	modgap
intergroup space=	0.10 m	grpgap

STRUCTURE

Numb	1/2Angle	1/2Rad	
48	3.75	0.0654	ang48
24	7.50	0.1309	ang24

neutron flux (Hz/cm^2) = 10,000

neutron efficiency = 0.005

5.70	Z_max_cal
0.20	BorPoly
0.10	StyClr

Directions looking from IP

0.035	left — thickness (left)
0.035	right — thickness (right)
0.050	top — thickness (top)
0.050	bot — thickness (bottom)

Nomenclature:

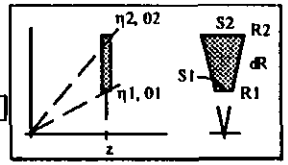

Layout:

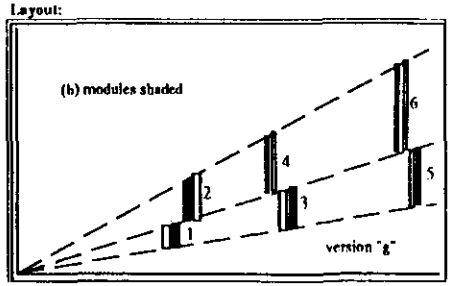

Note: modules (a) occupy even-numbered sectors
modules (b) occupy odd-numbered sectors
Nsctrs/2 are type (a) and Nsctrs/2 are type (b)

	ngaps	zfr m	zbn m	zav m	n1	01 deg	01Mav deg	Coverage 01MIN deg	Coverage 01MAX deg	n2	02 deg	02Mav deg	Coverage 02MIN deg	Coverage 02MAX deg	Nsctrs	R1 m	R1Cosphi m	R2 m	R2Cosphi m	dRMid m	dR m	dRCosphi m	S1 m	S2 m	area m^2	total area m^2
Inner modules																										
1a)	8	6	6.3	6.15	2.46	9.7664082	9.68444416	9.458078	9.921801	1.9	17.013183	16.87593886	17.273013	16.496214	24	1.0585766	1.0495203	1.8817911	1.8656922	1.4576062	0.8232	0.81617184	0.2763	0.4912	0.3132	60.14259
1b)	8	6.4	6.7	6.55	2.46	9.7664082	9.68444416	9.4716	9.906976	1.9	17.013183	16.87593886	17.248246	16.518926	24	1.1274271	1.1177818	2.0041841	1.987038	1.5524099	0.8768	0.86925618	0.2943	0.5232	0.3553	68.22044
2b)	8	6.8	7.1	6.95	1.9	17.013183	16.8759389	16.53907	17.22639	1.4	27.705174	27.50303581	28.01829	27.004986	24	2.126577	2.1083838	3.6496322	3.618409	2.8633964	1.5231	1.51002524	0.5551	0.9527	1.1385	218.5878
2a)	8	7.2	7.5	7.35	1.9	17.013183	16.8759389	16.55707	17.20695	1.4	27.705174	27.50303581	27.989793	27.031662	24	2.2489699	2.2297296	3.8596829	3.8266628	3.0281962	1.6107	1.59693316	0.5871	1.0076	1.2733	244.4731
Middle modules																										
3a)	8	10.85	11.15	11	2.46	9.7664082	9.68444416	9.556579	9.815743	1.9	17.013183	16.87593886	17.095728	16.661571	24	1.893389	1.8771908	3.3658053	3.3370104	2.6071006	1.4724	1.45981954	0.4943	0.8787	1.0021	96.20271
3b)	8	11.25	11.55	11.4	2.46	9.7664082	9.68444416	9.561009	9.811077	1.9	17.013183	16.87593886	17.087922	16.669003	24	1.9622395	1.9454523	3.4881982	3.4583562	2.7019042	1.526	1.51290389	0.5122	0.9106	1.0763	103.3265
4b)	4	10.35	10.5	10.425	1.906168	16.910085	16.8759389	16.76218	16.99121	1.405713	27.553369	27.50303581	27.672836	27.335147	48	3.1693616	3.1625757	5.4392594	5.4276136	4.2950946	2.2699	2.26503785	0.4146	0.7115	1.2753	244.8549
4a)	4	10.6	10.75	10.675	1.906168	16.910085	16.8759389	16.76483	16.98849	1.405713	27.553369	27.50303581	27.668837	27.339057	48	3.2453654	3.2384169	5.5696973	5.5577722	4.3980945	2.3243	2.31935531	0.4245	0.7286	1.3372	256.7394
Outer modules																										
5a)	4	15.95	16.1	16.025	2.466356	9.704829	9.68444416	9.640179	9.729114	1.906168	16.910085	16.87593886	16.950753	16.801764	48	2.7405935	2.7347257	4.8718484	4.8614174	3.7980715	2.1313	2.12669165	0.3585	0.6373	1.0588	203.2957
5b)	4	16.2	16.35	16.275	2.466356	9.704829	9.68444416	9.640856	9.728425	1.906168	16.910085	16.87593886	16.949598	16.802898	48	2.7833485	2.7773891	4.9478522	4.9372585	3.8573238	2.1645	2.15986937	0.3641	0.6472	1.0921	209.6883
6b)	4	15.45	15.6	15.525	1.906168	16.910085	16.8759389	16.79939	16.95317	1.405713	27.553369	27.50303581	27.616844	27.39009	48	4.7198406	4.7097351	8.1001921	8.082849	6.396292	3.3804	3.37311392	0.6174	1.0596	2.8283	543.0251
6a)	4	15.7	15.85	15.775	1.906168	16.910085	16.8759389	16.80059	16.95194	1.405713	27.553369	27.50303581	27.615033	27.391873	48	4.7958445	4.7855762	8.23063	8.2130076	6.4992919	3.4348	3.42743138	0.6273	1.0766	2.9201	560.6546
	3bavg	11.41																								

total area of strip cathodes (m^2)	2809
total volume of chambers (m^3)	14.0
Total number of modules	432

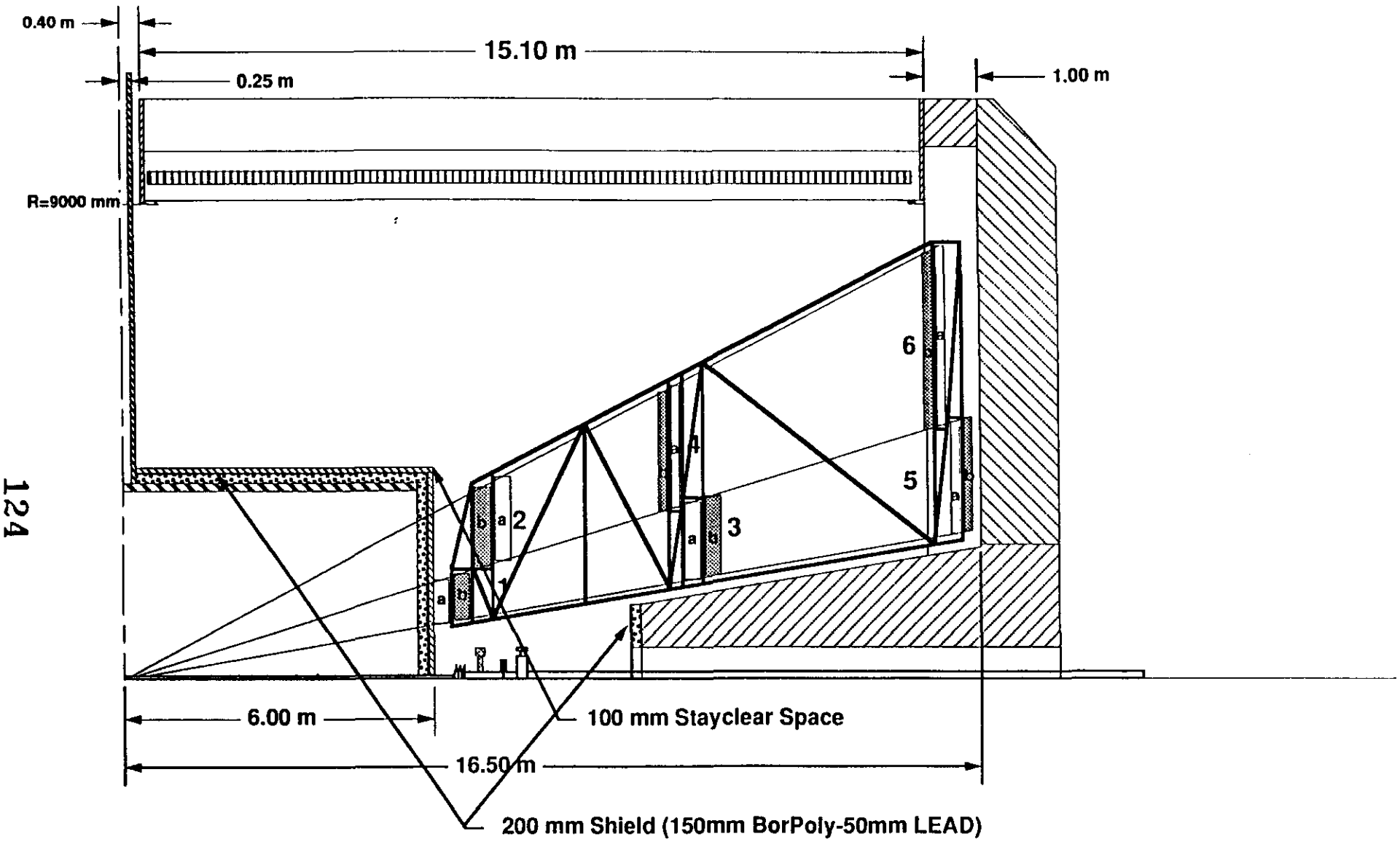

GEM Endcap Muon System Layout (version "g")

Frank Nimblett
06 January '93

active coverage 9.75° to 27.71°

module thickness(4 gaps) = 0.15 m
intermodule space = 0.10 m

neutron flux (Hz/cm^2) = 10,000
neutron efficiency = 0.005

Nomenclature:

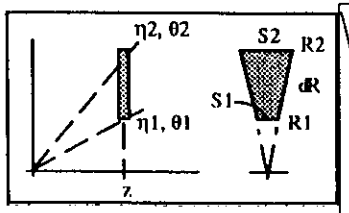

Layout:

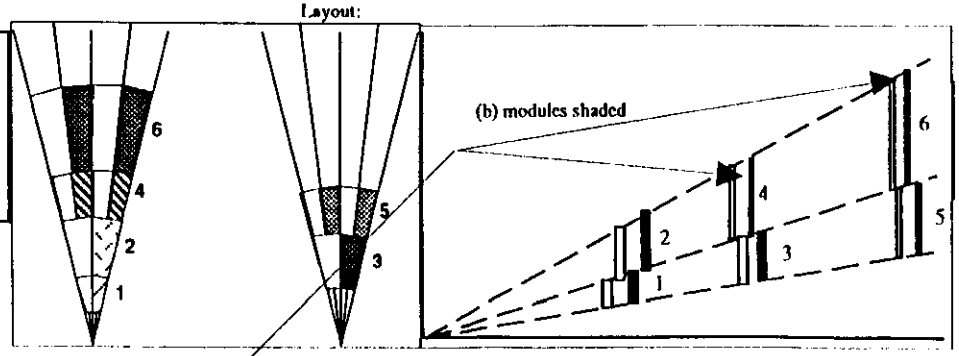

Note: modules (a) occupy even-numbered sectors
modules (b) occupy odd-numbered sectors
Nsctrs/2 are type (a) and Nsctrs/2 are type (b)

Separation with intervening structure makes it difficult to tie these pairs (a&b) of chambers together!!!

	ngaps	zfr	zba	zav	Dz's	η1	θ1	η2	θ2	Nsctrs	R1	R2	dR	S2	area	total area	str wid	# strips	wire gp	# r-ch	# str ch	# r ch	ch. pt.	neut.	wt/mod	cost for this
		m	m	m			deg		deg		m	m	m	m	m^2	m^2	mm	/pl/sctr	cm	/pl/sctr			/sec	/sec	Kg	module type
Inner modules																										
1a)	8	6.00	6.30	6.15		2.46	9.75	1.90	17.01	24	1.06	1.88	0.83	0.49	0.31	60.26	5.00	77	5.0	17	14,727	3,169	188	2,063	47	295,458
1b)	8	6.80	7.10	6.95		2.46	9.75	1.90	17.01	24	1.19	2.13	0.93	0.56	0.40	76.95	5.00	87	5.0	19	16,643	3,582	212	2,332	54	309,716
2a)	8	6.40	6.70	6.55		1.90	17.01	1.40	27.71	24	2.00	3.44	1.44	0.90	1.01	194.15	5.00	142	5.0	29	27,285	5,512	39	3,588	100	407,778
2b)	8	7.20	7.50	7.35		1.90	17.01	1.40	27.71	24	2.25	3.86	1.61	1.01	1.27	244.47	5.00	159	5.0	32	30,618	6,185	44	4,027	119	449,430
Middle modules																										
3a)	8	10.80	11.10	10.95	4.80	2.46	9.75	1.90	17.01	24	1.88	3.35	1.47	0.87	0.99	95.51	5.00	137	5.0	29	26,221	5,643	75	3,674	99	405,327
3b)	8	11.45	11.75	11.60	4.65	2.46	9.75	1.90	17.01	24	1.99	3.55	1.56	0.93	1.12	107.18	5.00	145	5.0	31	27,778	5,978	80	3,892	108	424,693
4a)	4	10.55	10.70	10.63	4.08	1.90	17.01	1.40	27.71	48	3.25	5.58	2.33	0.73	1.34	257.64	5.00	116	5.0	47	22,178	8,941	14	5,821	71	469,621
4b)	4	11.20	11.35	11.28	3.93	1.90	17.01	1.40	27.71	48	3.45	5.92	2.47	0.77	1.51	290.13	5.00	123	5.0	49	23,534	9,488	15	6,177	78	497,307
Outer modules																										
5a)	4	15.70	15.85	15.78	4.83	2.46	9.75	1.90	17.01	48	2.71	4.83	2.12	0.63	1.04	199.93	5.00	99	5.0	42	18,928	8,130	36	5,293	59	420,574
5b)	4	16.20	16.35	16.28	4.68	2.46	9.75	1.90	17.01	48	2.80	4.98	2.18	0.65	1.11	212.81	5.00	102	5.0	44	19,528	8,387	37	5,460	62	431,629
6a)	4	15.45	15.60	15.53	4.90	1.90	17.01	1.40	27.71	48	4.75	8.15	3.40	1.07	2.86	550.07	5.00	169	5.0	68	32,406	13,065	7	8,506	130	717,090
6b)	4	15.95	16.10	16.03	4.75	1.90	17.01	1.40	27.71	48	4.90	8.42	3.51	1.10	3.05	586.08	5.00	174	5.0	70	33,449	13,485	7	8,779	137	747,367
		AV3b	11.61																							
																				Total =>	293,295	91,565			38,417	$5,575,991
																									tot.wt.	subtot. cost

Total ch counts: single strip occ.

total area of strip cathodes (m^2) 2875
total volume of chambers (m^3) 14.4
Total number of modules 432

Endcap CSC Layout -- Baseline II Version "h"

active coverage 9.75° to 27.71°

FFS Space=	0.15 m	FFSgap	
module thickness(4 gaps) =	0.15 m	modth	
intermodule space =	0.10 m	modgap	
intergroup space=	0.10 m	grpgap	STRUCTURE

Numb	1/2Angle	1/2Rad	
48	3.75	0.0654	ang48
24	7.50	0.1309	ang24

neutron flux (Hz/cm^2) = 10,000

neutron efficiency = 0.005

5.70	Z_max_cal
0.20	BorPoly
0.10	StyClr

Directions looking from IP

0.035 tleft	thickness (left)
0.035 tright	thickness (right)
0.050 ttop	thickness (top)
0.050 tbot	thickness (bottom)

Nomenclature:

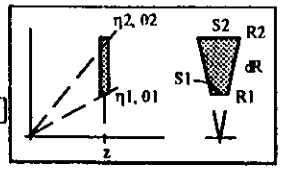

Layout:

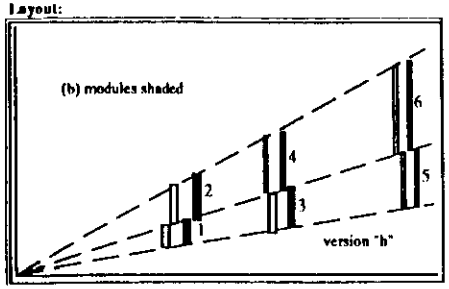

Note: modules (a) occupy even-numbered sectors
modules (b) occupy odd-numbered sectors
Nsctrs/2 are type (a) and Nsctrs/2 are type (b)

	ngaps	zfr m	zbo m	zav m	η1	01 deg	01Mav deg	Coverage 01MIN deg	Coverage 01MAX deg	η2	02 deg	02Mav deg	Coverage 02MIN deg	Coverage 02MAX deg	Nsctrs	R1 m	R1Cosphi m	R2 m	R2Cosphi m	dRMid m	dR m	dRCosphi m	S1 m	S2 m	area m^2	total area m^2
Inner modules																										
1a)	8	6	6.3	6.15	2.46	9.7664082	9.68444416	9.458078	9.921801	1.9	17.013183	16.87593886	17.273013	16.496214	24	1.0585766	1.0495203	1.8817911	1.8656922	1.4576062	0.8232	0.81617184	0.2763	0.4912	0.3132	60.14259
1b)	8	6.8	7.1	6.95	2.46	9.7664082	9.68444416	9.483599	9.893894	1.9	17.013183	16.87593886	17.226387	16.539075	24	1.1962776	1.1860433	2.126577	2.1083838	1.6472135	0.9303	0.92234053	0.3123	0.5551	0.4	76.80713
2b)	8	7.2	7.5	7.35	1.9	17.013183	16.8759389	16.55707	17.20695	1.4	27.705174	27.50303581	27.989793	27.031662	24	2.2489699	2.2297296	3.8596829	3.8266628	3.0281962	1.6107	1.59693316	0.5871	1.0076	1.2733	244.4731
2a)	8	6.4	6.7	6.55	1.9	17.013183	16.8759389	16.51893	17.24825	1.4	27.705174	27.50303581	28.050332	26.975111	24	2.0041841	1.997038	3.4395814	3.4101553	2.6985966	1.4354	1.42311731	0.5232	0.8979	1.0112	194.1507
Middle modules																										
3a)	8	10.8	11.1	10.95	2.46	9.7664082	9.68444416	9.556003	9.816351	1.9	17.013183	16.87593886	17.096745	16.660604	24	1.8847827	1.8686581	3.3505062	3.3218421	2.5952501	1.4657	1.453184	0.492	0.8747	0.993	95.33012
3b)	8	11.45	11.75	11.6	2.46	9.7664082	9.68444416	9.563111	9.808866	1.9	17.013183	16.87593886	17.084224	16.672529	24	1.9966648	1.979583	3.5493947	3.5190291	2.7493061	1.5527	1.53944606	0.5212	0.9266	1.1144	106.9838
4b)	4	11.2	11.35	11.275	1.906168	16.910085	16.8759389	16.7707	16.98246	1.405713	27.553369	27.50303581	27.659968	27.347738	48	3.4277747	3.4204356	5.8827482	5.8701528	4.6452942	2.455	2.4497172	0.4484	0.7695	1.4917	286.4111
4a)	4	10.55	10.7	10.625	1.906168	16.910085	16.8759389	16.76431	16.98902	1.405713	27.553369	27.50303581	27.669622	27.33829	48	3.2301647	3.2232486	5.5436097	5.5317405	4.3774945	2.3134	2.30849182	0.4225	0.7251	1.3247	254.3399
Outer modules																										
5a)	4	15.7	15.85	15.775	2.466356	9.704829	9.68444416	9.639481	9.729825	1.906168	16.910085	16.87593886	16.951943	16.800593	48	2.6978386	2.6920623	4.7958445	4.7855762	3.7388192	2.098	2.09351394	0.3529	0.6273	1.0261	197.0021
5b)	4	16.2	16.35	16.275	2.466356	9.704829	9.68444416	9.640856	9.728425	1.906168	16.910085	16.87593886	16.949598	16.802898	48	2.7833485	2.7773891	4.9478522	4.9372585	3.8573238	2.1645	2.15986937	0.3641	0.6472	1.0921	209.6883
6b)	4	15.95	16.1	16.025	1.906168	16.910085	16.8759389	16.80176	16.95075	1.405713	27.553369	27.50303581	27.61328	27.393601	48	4.8718484	4.8614174	8.3610679	8.3431662	6.6022918	3.4892	3.48174883	0.6373	1.0937	3.0134	578.5658
6a)	4	15.45	15.6	15.525	1.906168	16.910085	16.8759389	16.79939	16.95317	1.405713	27.553369	27.50303581	27.616844	27.39009	48	4.7198406	4.7097351	8.1001921	8.082849	6.396292	3.3804	3.37311392	0.6174	1.0596	2.8283	543.0251

3bavg 11.61

total area of strip cathodes (m^2)	2847
total volume of chambers (m^3)	14.2
Total number of modules	432

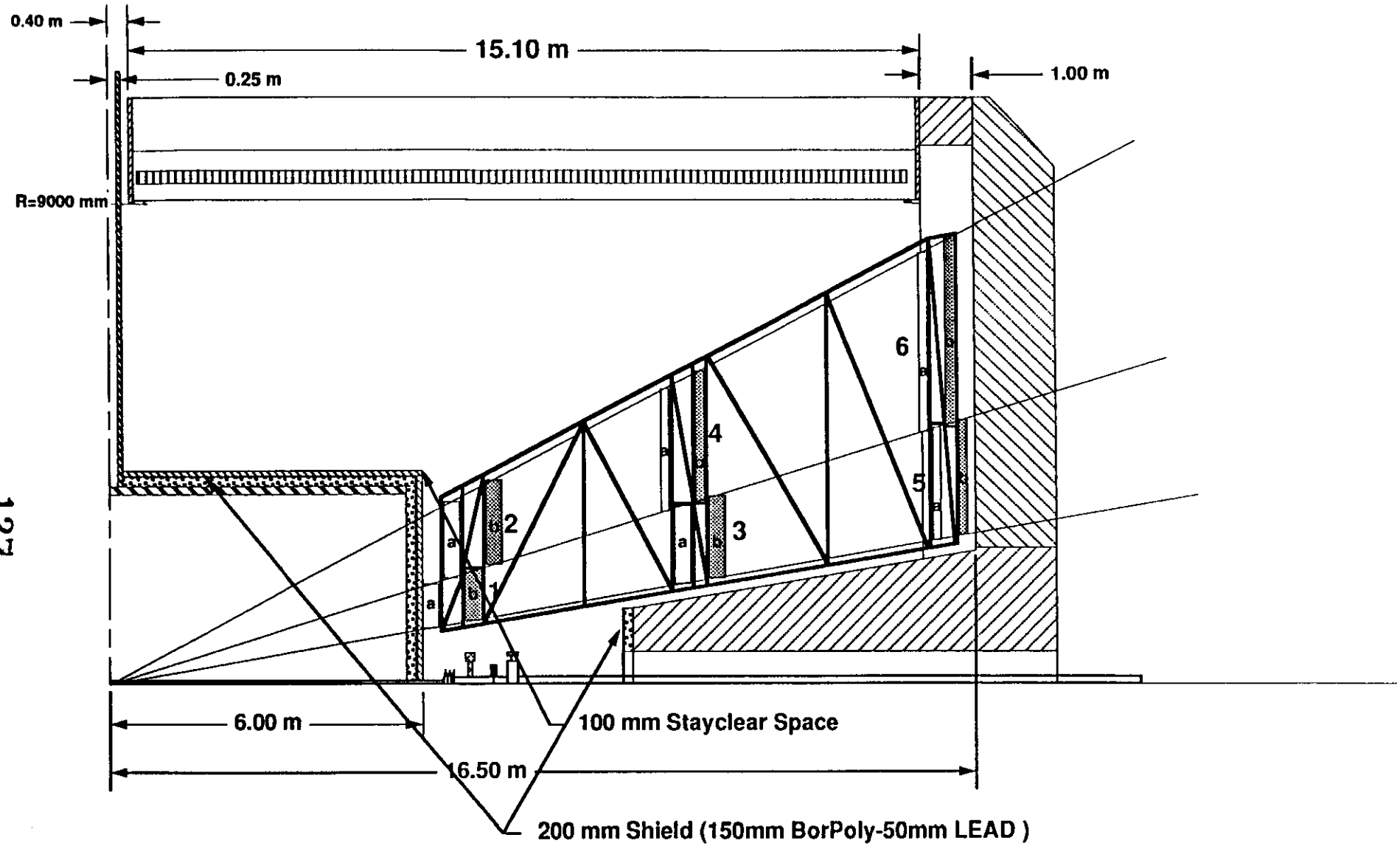

GEM Endcap Muon System Layout (version "h")

Frank Nimblett
06 January '93

gem

γeμ

Presentation by:

A. Korytov

Jan 5, 1993
A.Korytov
M.I.T.

P_T-TRIGGER IN THE END-CAP MUON SYSTEM: RADIAL VS. RECTANGULAR CHAMBER LAYOUTS.

Mechanical inconvenience of radial layout for a drift tube design for the End-Cap Muon System gave a motivation to re-examine what should be actually measured in the End-Caps to provide p_T trigger.

For simplicity sake, the calculation are done in assumption of an axial magnetic field. This provides fast analytical estimations and is not too far from a real situation (except a region at small θ-angles in vicinity of the iron field concentrator, where a radial component is of about the same magnitude as axial). The actual field components were calculated by J. Sullivan and could be found elsewhere [1].

Fig.1 shows two views of an end-cap sector with a muon track in it. The value of s is a measure of p_T and could be calculated as follows:

$$s \sim \frac{B \cdot L_3^2}{p_T}, \quad \text{where} \quad L_3 = z_3 \cdot \tan\theta / \cos\varphi. \tag{1}$$

The effect of cosφ can be neglected at trigger level ($\cos 11^\circ = 0.98$). Also, to simplify calculations, tanθ will be further replaced by θ (this is accurate at 2% level for angles smaller than 30°). Given that, one gets for s :

$$s \sim \frac{\theta^2}{p_T}. \tag{2}$$

1. Radial Strips.

In case of radial strips, the measured value is an angle Δφ:

$$\Delta\varphi \sim s / L_2 \sim s / r_2 \sim s / (z_2 \cdot \tan\theta) \sim s / \theta \sim \frac{\theta}{p_T} = A \cdot \frac{\theta}{p_T}. \tag{3}$$

This expression makes it clear that Δφ is not a direct measure of p_T and for a constant p_T Δφ is different for different θ-angles. This obviously results in that Δφ alone can not provide a trigger with a sharp turn-on curve if the chamber has a wide range of θ-angles. In the current design $\theta_{max}/\theta_{min} \sim 2$ within one chamber. If the Δφ-trigger is tuned to be 100% efficient for p_T=20 GeV/c (what means all tracks with $\Delta\varphi < \Delta\varphi_o = A * \theta_{max}/p_{TRIGGER}$ are accepted), the tracks with p_T=10 GeV/c at $\theta = \theta_{min}$ will be also accepted.

Assuming that the particle rate $dN/d\eta$ is flat (for any given p_T), one immediately obtains:

$$\frac{1}{N}\cdot\frac{dN}{d\theta}\sim\frac{Const(p_T)}{\theta} \tag{4}$$

This distribution may be used to estimated the chamber efficiency (tuned for a particular $p_{TRIGGER}$) to accept tracks of lower p_T: the trigger ($\Delta\varphi<\Delta\varphi_o=A\theta_{max}/p_{TRIGGER}$) accepts tracks with lower p_T in the angle range from θ_{min} up to $\theta_{max}*(p_T/p_{TRIGGER})$. The result is:

$$\varepsilon = 1-\frac{\ln(p_{TRIGGER}\ /\ p_T)}{\ln 2}, \quad (\text{valid when } 1 < p_{TRIGGER}\ /\ p_T < 2). \tag{5}$$

2. Straight Strips/Tubes.

In the case of a rectangular chamber with straight strips or drift tubes, the measured difference $dx\sim s$ could be treated as a measure of p_T ($\cos\varphi$ factor is again neglected):

$$dx = A\cdot\frac{\theta^2}{p_T}\ . \tag{6}$$

<u>The dependence on θ is even stronger</u> as compared to radial strips and tracks with a p_T as low as 1/4 of $p_{TRIGGER}$ may be accepted at $\theta=\theta_{min}$ (assuming $\theta_{max}/\theta_{min}\sim 2$).

Again, taking into account angle distribution of particles, one can easily obtain the chamber efficiency as follows:

$$\varepsilon = 1-\frac{1}{2}\cdot\frac{\ln(p_{TRIGGER}\ /\ p_T)}{\ln 2}, \quad (\text{valid when } 1 < p_{TRIGGER}\ /\ p_T < 4) \tag{7}$$

Another important remark should be mentioned: for tracks of infinitely high momentum any tube hit in SL3 is <u>uniquely</u> correlated with a corresponding tube in SL2 (independently of θ and φ) – fig.2. Thus, in this context, $\Delta\varphi$ and dx are equivalent (in case of radial strips, the strip No. in SL2 is the same as the No. of a strip hit in SL3, whilst with straight strips/tubes these numbers are different --- this is the only difference).

3. Drift Tubes with θ information.

The drift tubes have an excellent feature: time difference from both ends of a wire provides information about localization of a track along a wire with an accuracy determined by a TDC bin width only. Fig.3 [2] shows the accuracy achieved in the LSDT's [3] with 1 ns bin width TDC's (LeCroy 2277). Expected sigma of a distribution is 17.3 cm in a good agreement with the measured values (sigma=17.3 cm, RMS=18.2 cm). However, it is not the resolution that is so good about drift tubes. The real merit is that this information is available from the same tubes which give a p_T measurement (trigger). This information is therefore available immediately without any problem of combinatorial combinations (ghosts) which appear in a system with independent measurements of both coordinates. If a radial coordinate along the chamber (r) is measured independently of a coordinate across it and one would like to use r for p_T trigger, then an extraction of θ information would require a pattern recognition in time scale of L1-trigger. This does not seem to be feasible.

On the other hand, in the drift technology this information is easily available and certainly may be used in trigger. Also, I.Pless noted [3] that RPC's can provide correlated measurements of both coordinates (however, confusion could occur if two tracks are separated by less than 1 m).

The expression (6) may be re-written as:

$$p_T = A \cdot \frac{\theta^2}{dx} \quad \text{and} \quad \theta \sim r / z_3 \,, \quad \text{if } r \text{ is calculated in SL 3.} \tag{8}$$

This can be converted into p_T resolution:

$$\frac{\delta p_T}{p_T} = 2\frac{\delta r}{r} \tag{9}$$

where δr ~20cm/sqrt(4) = 10 cm (4 planes in SL3), and r varies from about 4m up to 8 m so that the resolution would also vary along the chamber. It should be noted here, that 10 cm accuracy gives momentum resolution of 5% or better. This essentially means that the momentum resolution (at rigger level) will be determined by strip width and multiple scattering al low momenta, rather than by radial measurements.

4. Summary and discussion.

The trigger turn-on curves for all three possibilities discussed above are presented in fig.4. These curves (expressions (5), (7) and similar function obtained for the expression (9)) are calculations with the only effect taken into account: θ-dependence of the chosen trigger schemes. All other contributions (cosφ dependence, effects of finite strip/tube sizes, multiple scattering in the calorimeter and muon chambers, the realistic B-field) were neglected.

One can see that radial strips are definitely better for trigger purposes when no information along a strip is available.

However, even radial strips apparently have intrinsic insufficiency to provide sharp turn-on trigger.

It is of certain interest, to verify this simple model with a realistic MC made for the case of radial strips by C.Yanagisawa [5] -- fig.5. From a corresponding curve in fig.4 one can conclude that if the trigger is 100% turned on for particular p_T, then it should get 100% turned off for any transverse momentum two times smaller than that chosen p_T (assuming $\theta_{max}/\theta_{min}\sim 2$). A comparison of curves for 10, 20 and 40 GeV/c in fig.5 reveals exactly the same.

Thus, this analytical analysis gives an idea why these curves go this way and not another.

From fig.4. one can see that the availability of information about a hit position along a tube gives significant improvement of the trigger.

Non-zero efficiency at lower p_T can result in dramatic consequences since the p_T-spectrum is very steep. Fig.6 shows an example of p_T-distribution (provided by R.McNeil). For p_T>3 GeV/c the spectrum can be reasonably approximated as:

$$\frac{1}{N}\frac{dN}{dp_T} \propto \frac{1}{p_T^{4.15}} \qquad (10)$$

The efficiencies shown in fig.4, being converted with distribution (10), result in p_T-distributions of tracks which would be accepted by the different trigger schemes as shown in fig.7. One can see that a lot of tracks with considerably lower p_T would be accepted if no radial information is used.

Quantitatively, the depth of a 'tail' going towards low momenta in relative units could be define, for example, as follows:

$$\frac{N_{good}}{N_{good}+N_{junk}}, \tag{11}$$

where

$$N_{good}=\int_{1}^{+\infty}\varepsilon(p_T)\cdot\frac{dN}{dp_T}\cdot dp_T \tag{12}$$

$$N_{junk}=\int_{0}^{1}\varepsilon(p_T)\cdot\frac{dN}{dp_T}\cdot dp_T. \tag{13}$$

The following table gives numbers (eq.11) for the trigger schemes discussed above:

Radial Strips (no r information)	27.7%
Straight Strips/Tubes (no r information)	5.6%
Straight Drift Tubes ($\delta r \sim 10$ cm in SL3)	73.7%

One can clearly see the importance of information along strips/tubes.

Acknowledgments.

The fast and simple analysis presented above has appeared as a consiquence of multiple and very fruitful discussions with C.Bromberg, G.Mitselmakher, L.Osborne, L.Rosenson, F.Taylor and many other members of the GEM Muon Group.

References:

1. GEM Magnet TDR.

2. "Performance of a LSDT large scale prototype", to be published.

3. R.Sumner et al., "LSDT's for the GEM Muon System", GEM TN-92-203.

4. I.Pless, Muon Meeting at Tuscon, 3/8/1992.

5. C.Yanagasawa, Muon Meeting at SSC Lab, 4/29/1992.

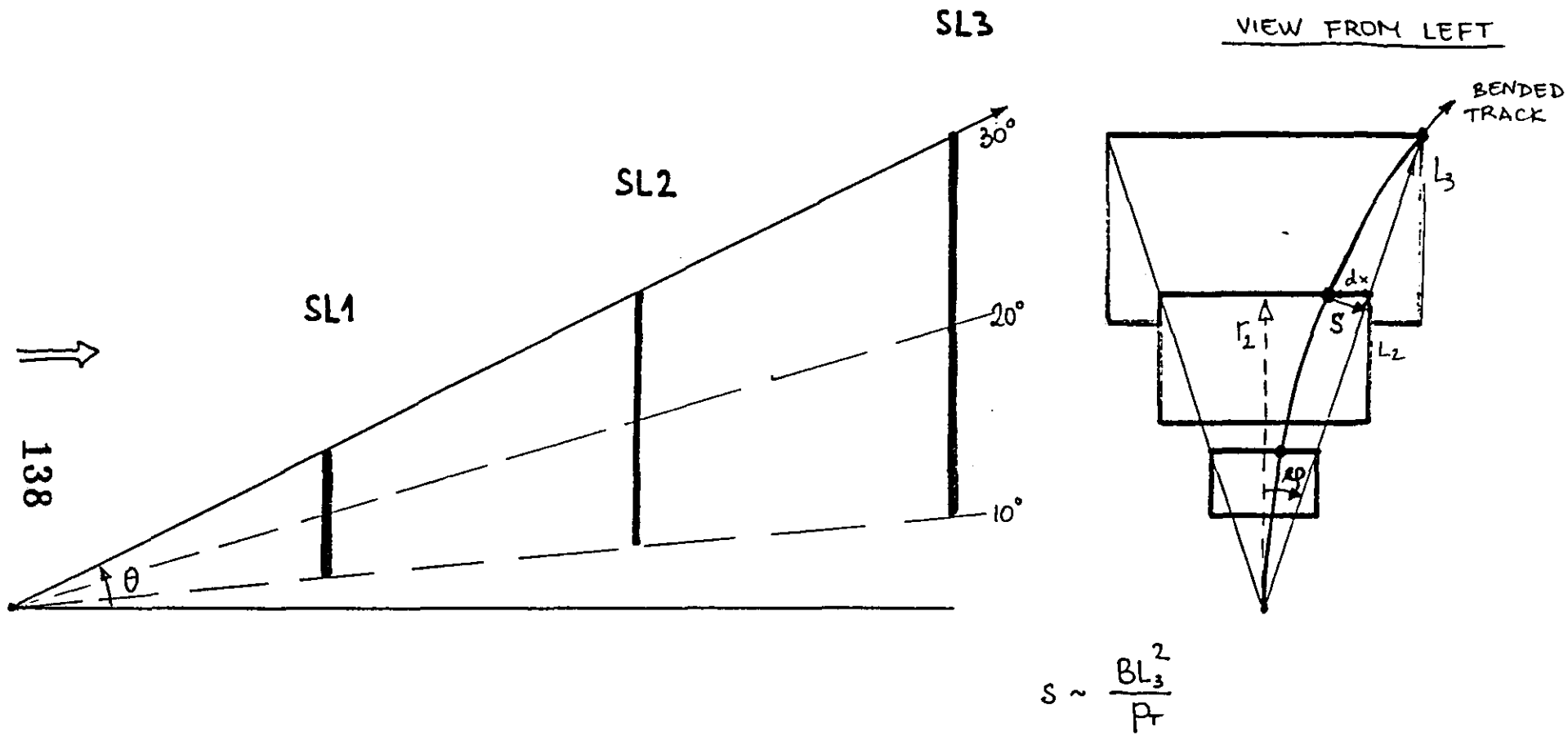

Fig.1. Two views of an end-cap sector with a muon track in it.

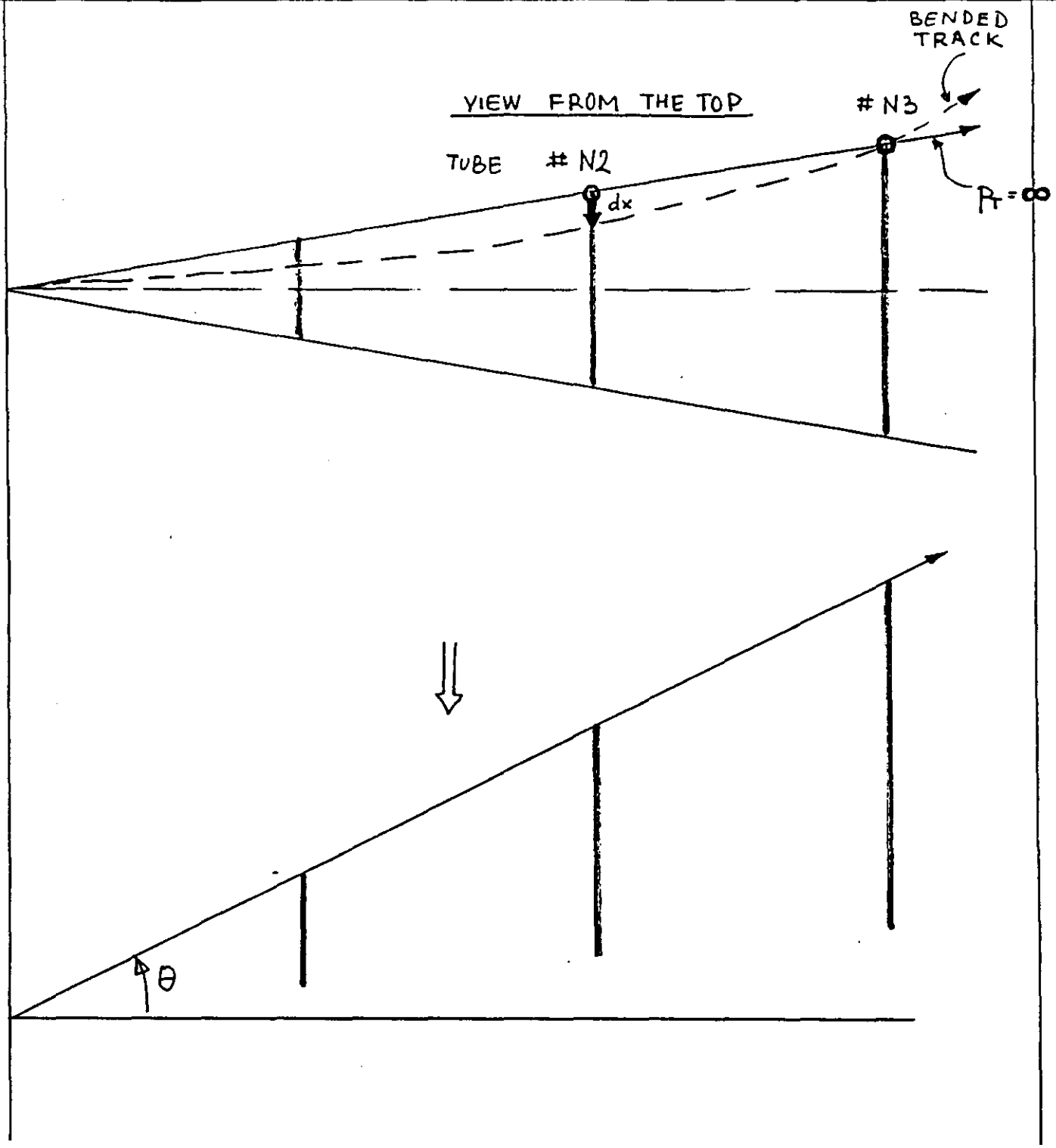

Fig.2. Two views of an end-cap sector with two muon tracks. One of infinitely high momentum looks like a straight line. If this track hits a tube N3 in SL3, no matter where it hits it along the tube it has to hit the tube N2 in SL2. For each N3 there is only one N2.
A deviation dx from N2 is a measure of bending.

PRELIMINARY 9/18/92

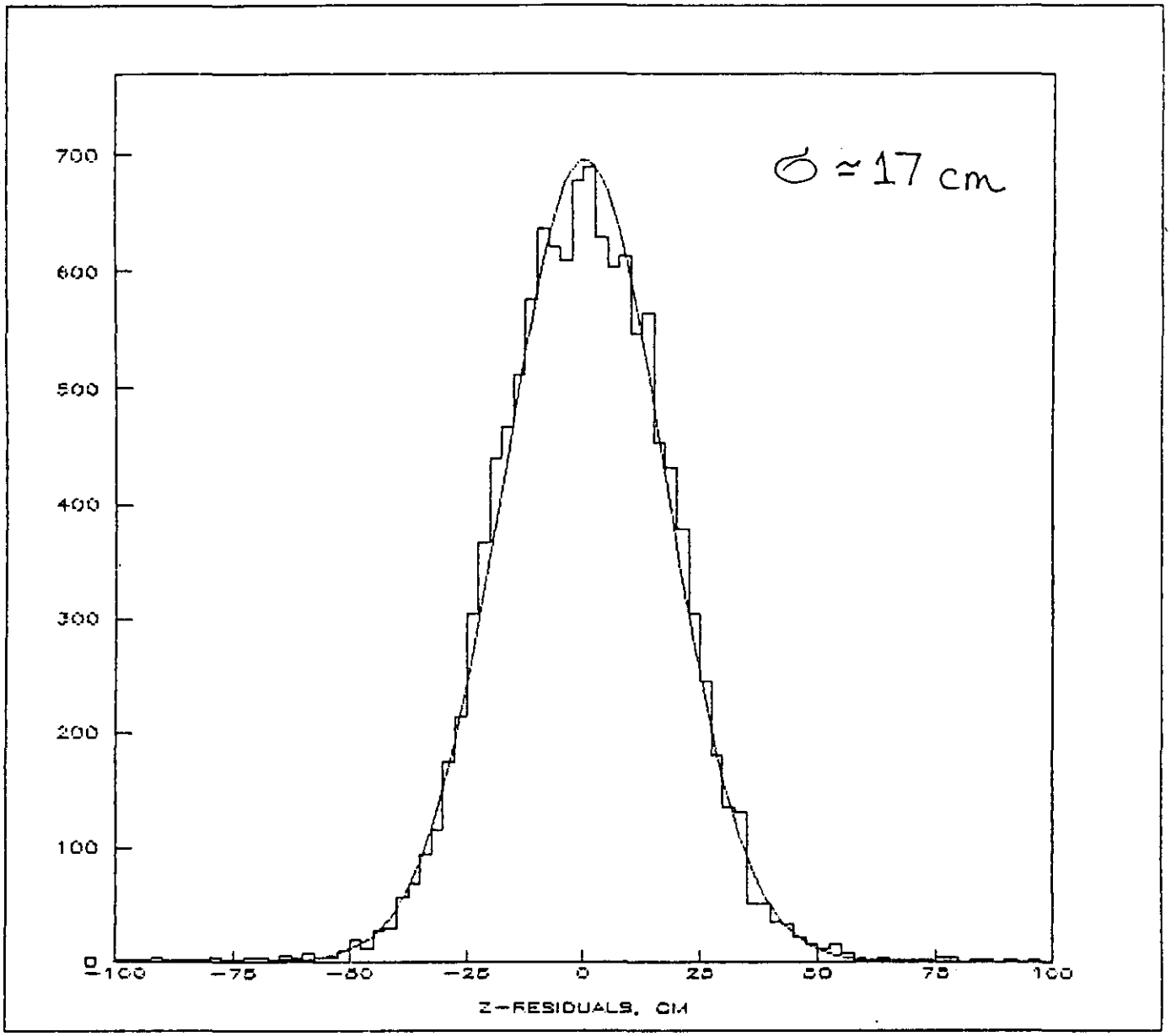

Fig.3. Resolution along a wire in LSDT's as measured by time difference (sigma=17.3 cm, RMS=18.2 cm).

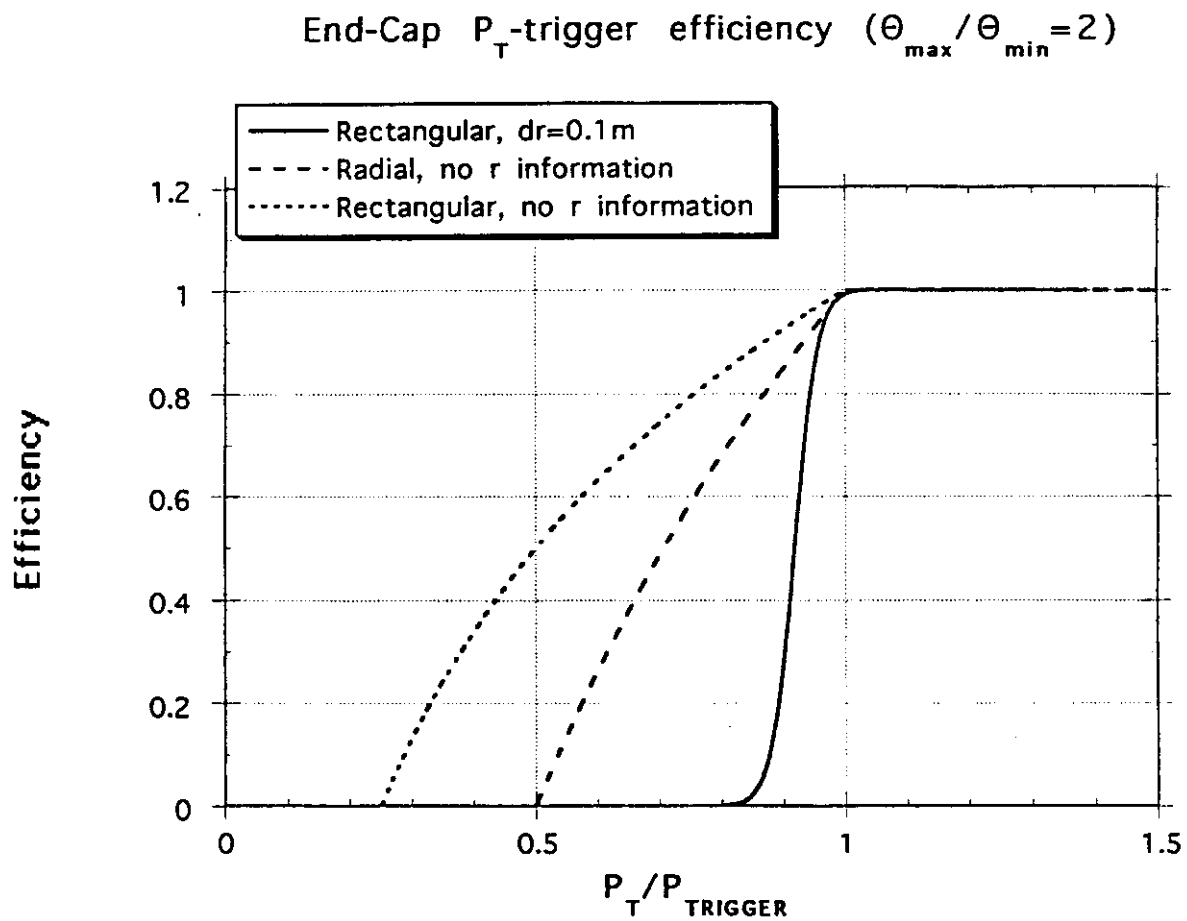

Fig.4. Turn-on curves of a p_T trigger for different chambers (trigger is tuned to have efficiency 99% or higher for $p_T > p_{T0}$).

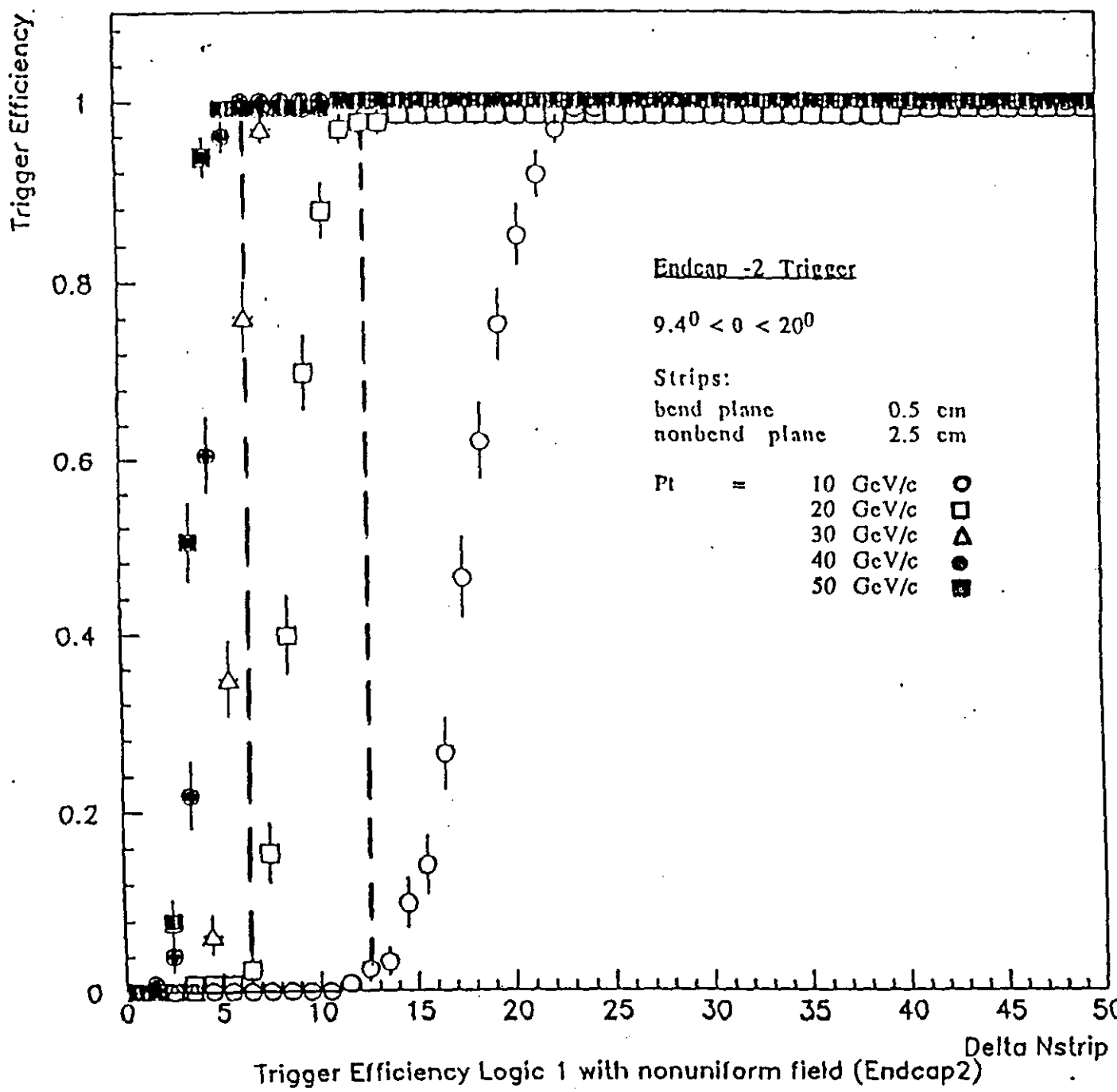

Fig.5. MC Calculations for radial strips. (C.Yanagisawa [5])

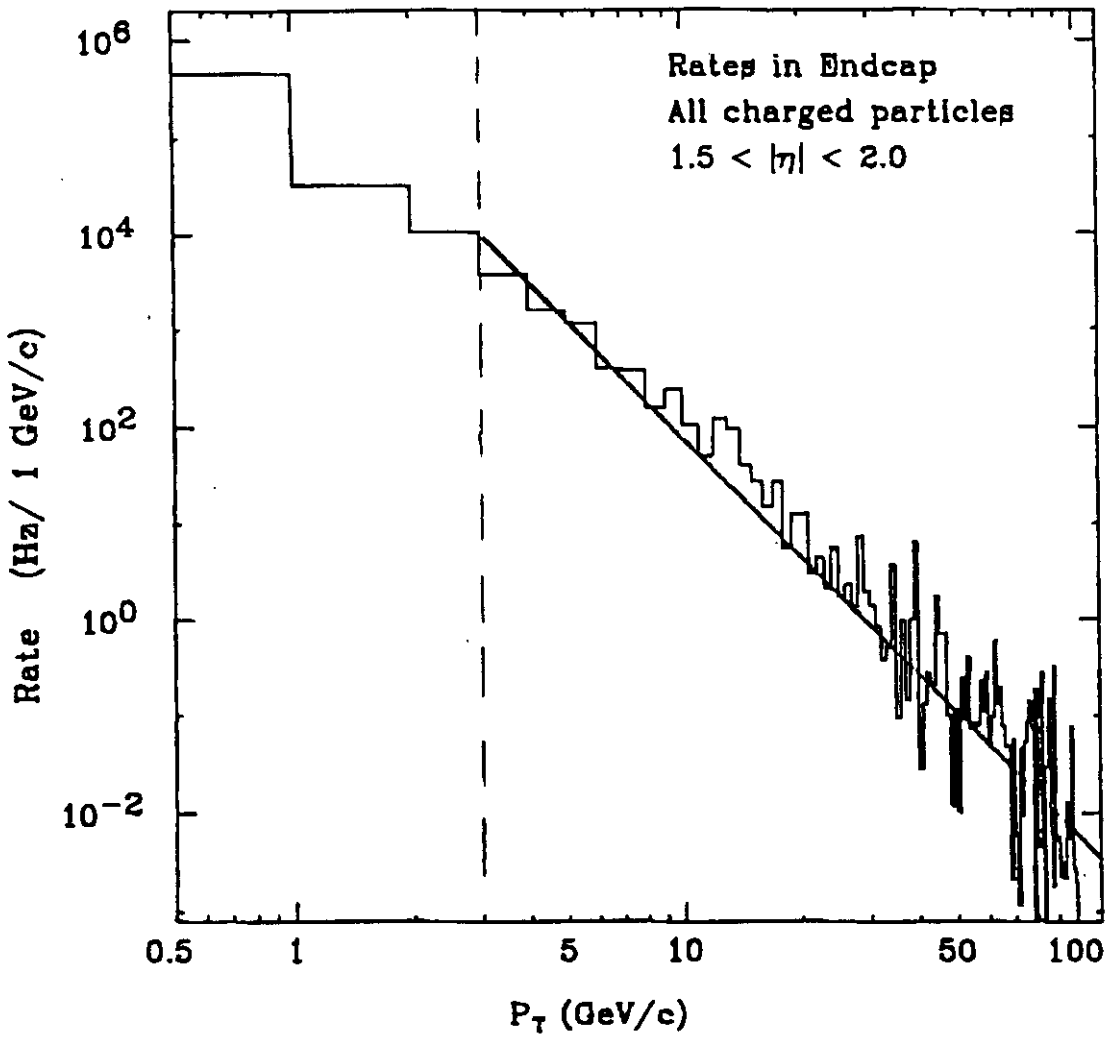

Fig. 6 p_T-Spectrum of particles beyond the calorimeter in the forward region (provided by R. McNeil).

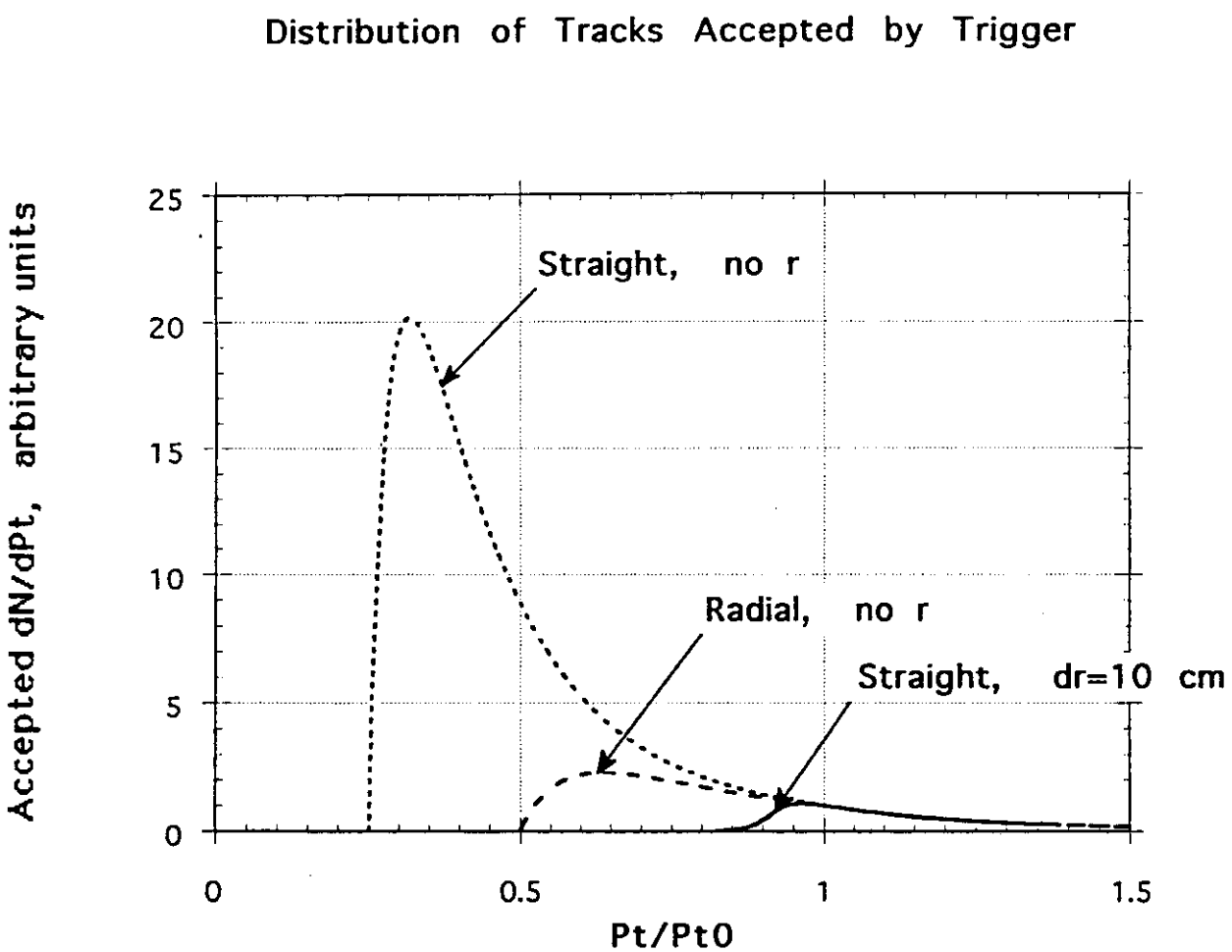

Fig.7. Distribution of tracks accepted by the triggers (tuned to have efficiency 99% or higher for $p_T > p_{T0}$).

gem

γeμ

Presentation by:

V. Chernyatin

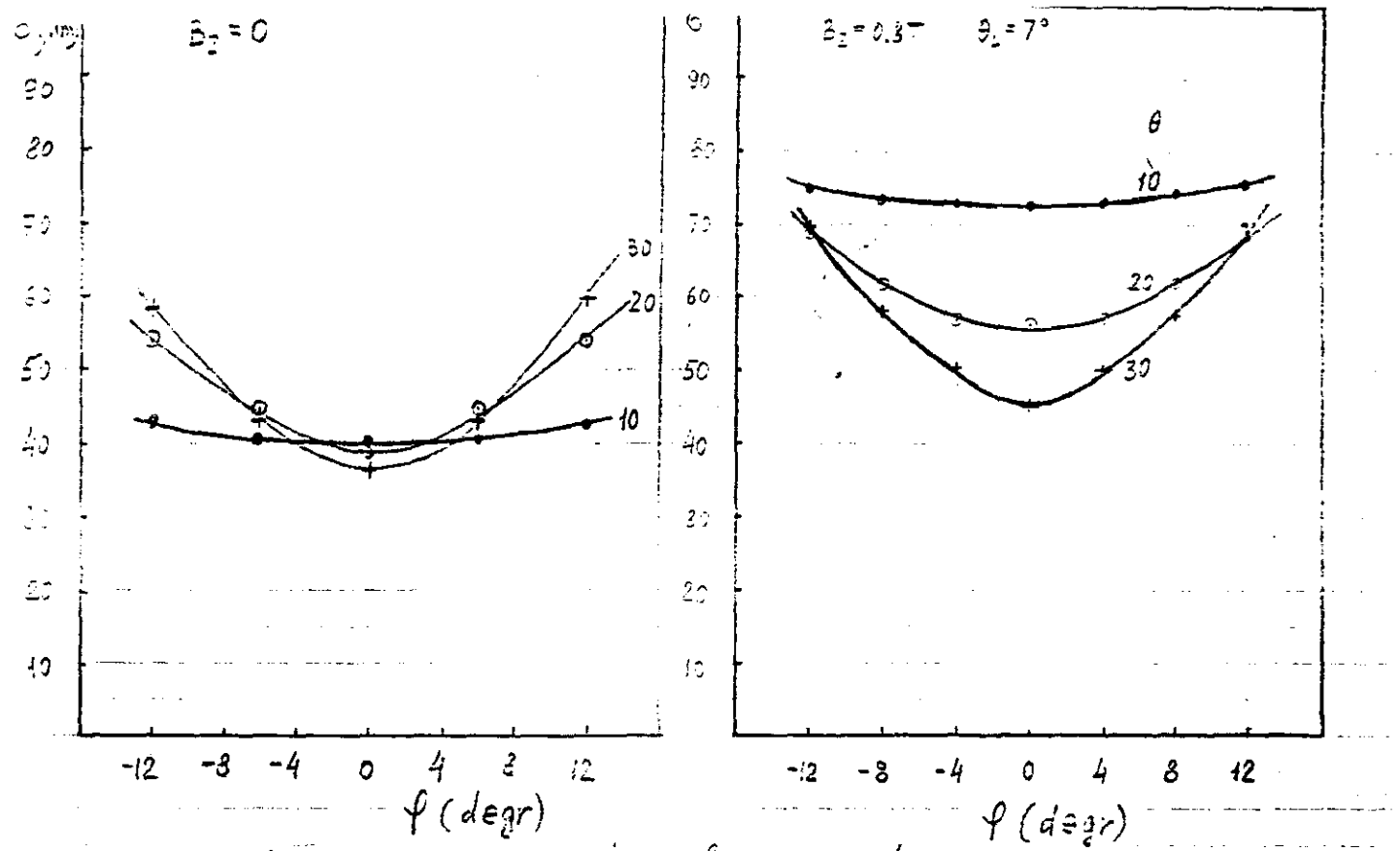

endcap rectangular geometry

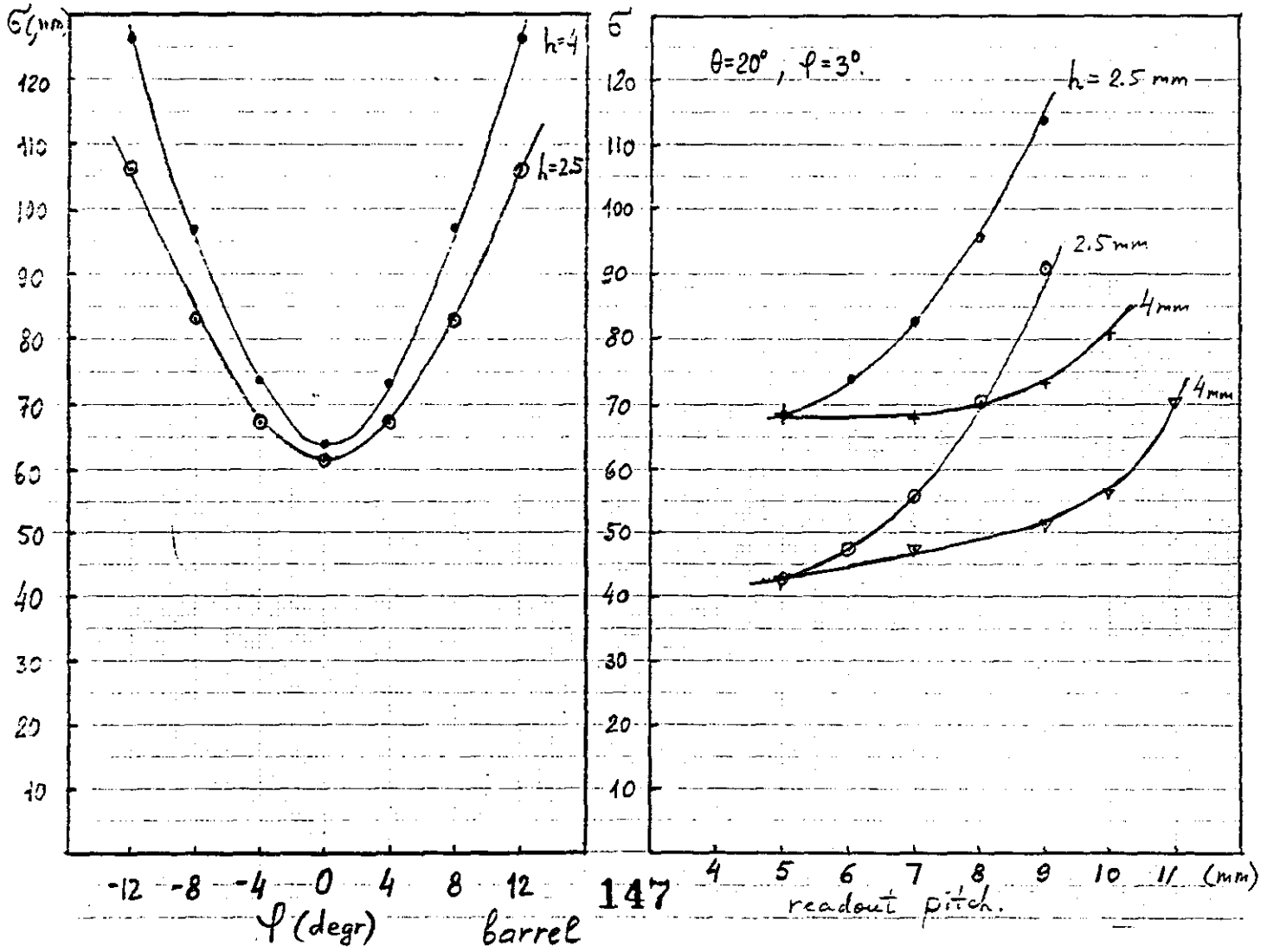

barrel readout pitch.

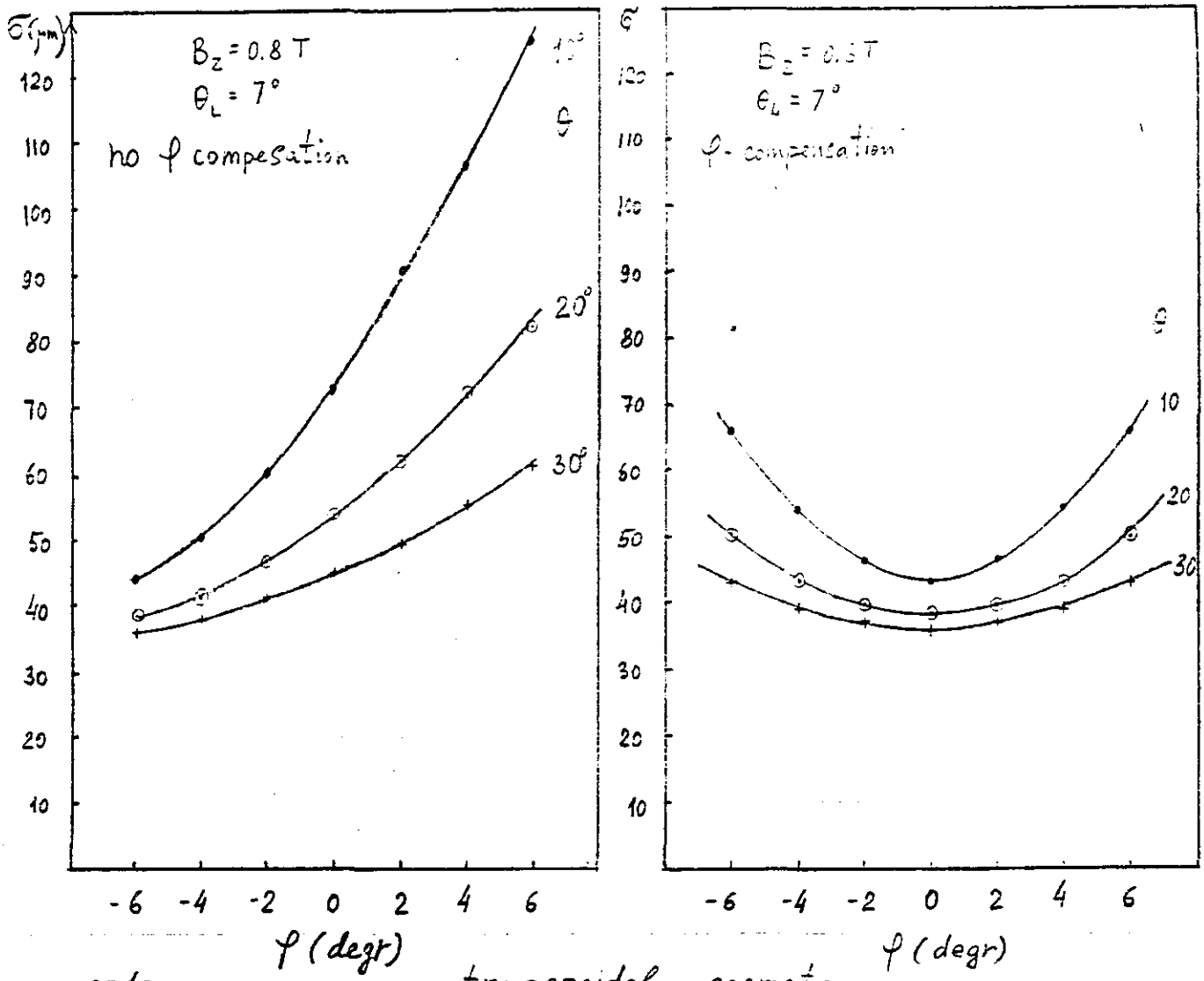

endcap trapezoidal geometry

gem

γeμ

Scott Whitaker
6 Jan 1993

Trapezoidal vs Rectangular CSC Endcap Chambers

Some brief comments on the pro's and con's of rectangular or trapezoidal chambers for the endcap muon system:

• We could make rectangular chambers with the cathodes etched to have radial strips -- these chambers would then have "ears" sticking out at low theta that served no use. The advantages of this might be easier fixturing and chamber assembly; there would be little cost savings on the cathodes, and greater costs for materials. Channel counts would be the same to a good approximation.

• Another concept for rectangular chambers would be to make regular cartesian chambers -- wires and strips orthogonal. This could give savings in cathode fabrication costs, if vendors believe parallel strips are less costly to etch. The strip channel count would go up, and the radial channel count stays about the same. The chamber weights go up, and costs of materials etc also rise; assembly costs might be lower, however, as for the case above. The Lorentz angle effects are still important in either concept. Occupancy in strips is unchanged in rectangular chambers, but occupancy in radial channels goes up due to the wires being longer.

I have adapted the spreadsheet developed for trapezoidal chambers to look at the impact of going with option-2 rectangular chambers -- wires and strips orthogonal. The spreadsheets for the II.h design and for rectangular chambers are attached. The total chamber area and volume rise by 27% compared to the trapezoidal design II.h. The number of strip channels also rises by 27%; the strips are 5 mm wide everywhere, rather than tapering in the trapezoidal design with an average width of 5 mm.

My spreadsheet also includes a crude cost and weight model. According to this model, total chamber weight increases by 18%. The cost is guesstimated on the basis of costs per area, costs per unit of perimeter, and labor costs. Holding labor constant at 200 hours per module, the simple model gives an increase of 12% in the cost of chamber fabrication. This is probably bogus, since there would be advantages in fixturing and assembly that would offset the increased material costs.

• Triggering with radial strips is more direct than triggering with chambers that have parallel strips, which would require determination of the radial position to convert the strip position to an azimuthal measurement. The triggering issue with cartesian chambers needs extensive study in order to establish the feasibility and credibility of this approach.

• Measurement of the polar angle now contributes to measurement of the azimuthal angle and to the determination of the transverse momentum. We need to do some simulations to see if the radial position measurement is sufficiently fine to avoid degradation of the Pt measurement. A back-of-envelop calculation says it is, but the effects of occupancy and pileup need to be included.

My opinion: With respect to triggering and momentum resolution, there are some clear complications and potential disadvantages for rectangular chambers compared to trapezoidal chambers. Rectangular chambers will be larger, will weigh more, and will likely have more strip channels than trapezoidal chambers. Rectangular chambers would probably be easier and cheaper to build, considering both the fabrication of the components and the precise assembly of the chambers. Serious chamber design work should be started to assess the relative merits and costs of the chamber concepts; serious simulations and calculations should be done to study triggering and performance. I think we should stick with trapezoidal chambers for the TDR unless sufficient work on rectangular chambers is done to resolve performance concerns.

Endcap CSC Layout -- Rectangular chambers

SW 5-Jan-1993

active coverage 9.75° to 27.71°

module thickness(4 gaps) = 0.15 m
intermodule space = 0.10 m

neutron flux (Hz/cm^2) = 10,000
neutron efficiency = 0.005

Nomenclature:

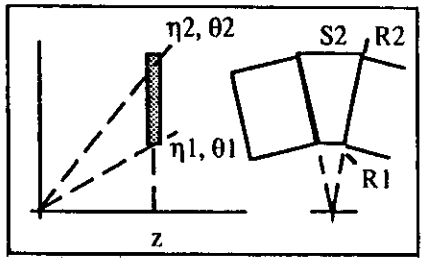

Layout:

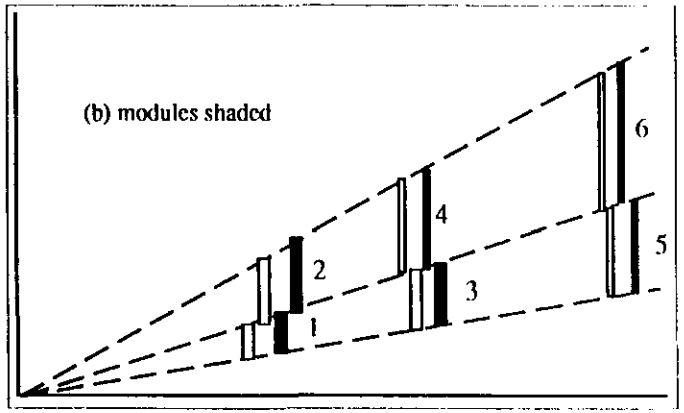

Note: modules (a) occupy even-numbered sectors
modules (b) occupy odd-numbered sectors
Nsctrs/2 arc type (a) and Nsctrs/2 arc type (b)

	ngaps	zfr	zba	zav	Dz's	η1	θ1	η2	θ2	Nsctrs	R1	R2	S2	area	str wid	# strips	wire gp	# r-ch	Total ch counts: # str ch	# r ch	single strip occ. ch. pt.	neut.
		m	m	m			deg		deg		m	m	m	m^2	mm	/pl/sctr	cm	/pl/sctr			/sec	/sec
Inner modules																						
1a)	8	5.95	6.25	6.10		2.46	9.75	1.90	17.01	24	1.05	1.87	0.49	0.40	5.00	97	5.0	16	18,710	3,144	186	2,047
1b)	8	6.75	7.05	6.90		2.46	9.75	1.90	17.01	24	1.19	2.11	0.55	0.51	5.00	110	5.0	19	21,164	3,556	211	2,315
2a)	8	6.35	6.65	6.50		1.90	17.01	1.40	27.71	24	1.99	3.41	0.89	1.26	5.00	178	5.0	28	34,217	5,470	39	3,561
2b)	8	7.15	7.45	7.30		1.90	17.01	1.40	27.71	24	2.23	3.83	1.00	1.59	5.00	200	5.0	32	38,428	6,143	43	3,999
Middle modules																						
3a)	8	10.70	11.00	10.85	4.75	2.46	9.75	1.90	17.01	24	1.86	3.32	0.87	1.25	5.00	173	5.0	29	33,280	5,592	74	3,640
3b)	8	11.35	11.65	11.50	4.60	2.46	9.75	1.90	17.01	24	1.98	3.52	0.92	1.41	5.00	184	5.0	31	35,274	5,926	79	3,858
4a)	4	10.55	10.70	10.63	4.13	1.90	17.01	1.40	27.71	48	3.25	5.58	0.73	1.70	5.00	146	5.0	47	28,025	8,941	14	5,821
4b)	4	11.10	11.25	11.18	3.88	1.90	17.01	1.40	27.71	48	3.42	5.87	0.77	1.88	5.00	154	5.0	49	29,476	9,404	15	6,122
Outer modules																						
5a)	4	15.70	15.85	15.78	4.93	2.46	9.75	1.90	17.01	48	2.71	4.83	0.63	1.33	5.00	126	5.0	42	24,245	8,130	36	5,293
5b)	4	16.20	16.35	16.28	4.78	2.46	9.75	1.90	17.01	48	2.80	4.98	0.65	1.42	5.00	130	5.0	44	25,014	8,387	37	5,460
6a)	4	15.45	15.60	15.53	4.90	1.90	17.01	1.40	27.71	48	4.75	8.15	1.07	3.62	5.00	213	5.0	68	40,950	13,065	7	8,506
6b)	4	15.95	16.10	16.03	4.85	1.90	17.01	1.40	27.71	48	4.90	8.42	1.10	3.86	5.00	220	5.0	70	42,269	13,485	7	8,779
																		Total =>	371,053	91,242		

total area of strip cathodes (m^2)	3625
total volume of chambers (m^3)	18.1
Total number of modules	432

Rectangular chambers

CSC MATERIALS AND COSTS

Caveat: this weight and cost model is very crude and for comparison purposes at best.

Costs NOT included:
EDIA
Electronics (incl cables, cooling)
Installation
Alignment hardware
Gas system, plumbing
and much, much more!

component	unit	cost ($)	weight	units	
hexcel	m^2	108	1.80	Kg/m^2	Hexcel HRH-10-1/4-2.0
circuit bds	m^2	20	2.03	Kg/m^2	.047 in, rho = 1.7
copper, plain	m^2	10	0.16	Kg/m^2	1/2 oz/ft^2
copper, strip cathodes	m^2	500	0.16	Kg/m^2	"
wires	m	0.288	0.0000136	Kg/m	30 mu dia W
Al sides	m	20	1.07	Kg/m	50 cm *1/32 in
frames, closeouts	m	10	0.64	Kg/m	G10 2.5cm *1.5cm
electronics	each		5	Kg	wild guess
subtotals:					
module area (4 gaps)	m^2	2800	31	Kg/m^2	
module area (8 gaps)	m^2	5432	56	Kg/m^2	
module peri(4 gaps)	m	70	4	Kg/m	
module peri(4 gaps)	m	130	8	Kg/m	

Labor Rates:	$/hr	hr/module
labor_a	25	100
labor_b	25	100

wt/mod Kg	cost for this module type	total/module	Cost Breakdown -- costs for one module: hexcel	cir bds	plain Cu	strip cath	wire	Al sides	frames	labor.a	labor.b
53	308,529	12,855	384	142	40	1,582	368	104	235	5,000	5,000
61	326,474	13,603	492	182	51	2,024	470	118	266	5,000	5,000
116	446,577	18,607	1,223	453	126	5,034	1,170	185	417	5,000	5,000
139	498,559	20,773	1,543	571	159	6,349	1,475	208	468	5,000	5,000
116	445,521	18,563	1,216	450	125	5,005	1,163	186	418	5,000	5,000
127	469,963	19,582	1,366	506	141	5,622	1,307	197	443	5,000	5,000
83	526,041	10,959	916	339	102	3,391	783	122	306	2,500	2,500
90	555,302	11,569	1,013	375	113	3,752	866	129	322	2,500	2,500
70	467,302	9,735	720	267	80	2,668	616	110	275	2,500	2,500
73	481,336	10,028	767	284	85	2,839	656	113	284	2,500	2,500
155	836,860	17,435	1,955	724	217	7,241	1,672	179	447	2,500	2,500
163	874,925	18,228	2,083	771	231	7,715	1,781	185	461	2,500	2,500
		181,938	13,678	5,066	1,469	53,221	12,327	1,836	4,341	45,000	45,000
45,185 tot.wt.	$6,237,391 subtot. cost										
		fractions (unwt'd ave)	**0.075**	**0.028**	**0.008**	**0.293**	**0.068**	**0.010**	**0.024**	**0.247**	**0.247**